A New Equation of State for Argon Covering the Fluid Region for Temperatures From the Melting Line to 700 K at Pressures up to 1000 MPa

Ch. Tegeler, R. Span, and W. Wagner[a]

Lehrstuhl für Thermodynamik, Ruhr-Universität Bochum, D-44780 Bochum, Germany

This work reviews the available data on thermodynamic properties of argon and presents a new equation of state in the form of a fundamental equation explicit in the Helmholtz energy. The functional form of the residual part of the Helmholtz energy was developed by using state-of-the-art linear optimization strategies and a new nonlinear regression analysis. The new equation of state contains 41 coefficients, which were fitted to selected data of the following properties: (a) thermal properties of the single phase $(p\rho T)$ and (b) of the liquid–vapor saturation curve (p_s, ρ', ρ'') including the Maxwell criterion, (c) speed of sound w, isochoric heat capacity c_v, second and third thermal virial coefficients B and C and second acoustic virial coefficient β_a. For the density, the estimated uncertainty of the new equation of state is less than $\pm 0.02\%$ for pressures up to 12 MPa and temperatures up to 340 K with the exception of the critical region and less than $\pm 0.03\%$ for pressures up to 30 MPa and temperatures between 235 and 520 K. In the region with densities up to half the critical density and for temperatures between 90 and 450 K the estimated uncertainty of calculated speeds of sound is in general less than $\pm 0.02\%$. The new formulation shows reasonable extrapolation behavior up to very high pressures and temperatures. Independent equations for the vapor pressure, for the pressure on the sublimation and melting curve and for the saturated liquid and saturated vapor densities are also included. Tables for the thermodynamic properties of argon from 84 to 700 K for pressures up to 1000 MPa are given. © *1999 American Institute of Physics and American Chemical Society.* [S0047-2689(99)00203-2]

Contents

[a]Author to whom correspondence should be addressed; Electronic mail: wagner@thermo.ruhr-uni-bochum.de

List of Symbols

Symbol description

a,d,n,t	Adjustable parameters
B	Second virial coefficient
C	Third virial coefficient
c_p	Isobaric heat capacity
c_v	Isochoric heat capacity
A	Specific Helmholtz energy
g	Specific Gibbs energy
h	Specific enthalpy
i,j,k,l,m	Serial numbers
I,J,K,L	Maximum value of the serial numbers i,j,k,l
M	Number of data, molar mass
p	Pressure
R	Specific gas constant
s	Specific entropy
T	Thermodynamic temperature, ITS-90
u	Specific internal energy
v	Specific volume
w	Speed of sound
x,y	Independent variables
y,z	Any thermodynamic property

Greek

α	Dimensionless Helmholtz energy $(\alpha=A/RT)$
α,β,δ	Critical exponents
$\beta,\gamma,\epsilon,\eta$	Adjustable parameters
β_a	Second acoustic virial coefficient
γ_a	Third acoustic virial coefficient
$\gamma_1,\gamma_2,\gamma_3$	Linearization factors
δ	Reduced density $(\delta=\rho/\rho_c)$
δ_a	Fourth acoustic virial coefficient
δ_T	Isothermal throttling coefficient
Δ	Difference in any quantity
∂	Partial differential
κ^0	Isentropic coefficient of the ideal gas $(\kappa^0=c_p^0/c_v^0)$
μ	Joule–Thomson coefficient
ρ	Density
σ	Variance, Uncertainty
τ	Inverse reduced temperature $(\tau=T_c/T)$
χ^2	Weighted sum of squares

Superscripts

o	Ideal-gas property
r	Residual
p	Preliminary value
$'$	Saturated liquid state
$''$	Saturated vapor state

Denotes a vector

Subscripts

b	At the normal boiling point $(p_s=0.101\,325\,\text{MPa})$
c	At the critical point
calc	Calculated
corr	Corrected
exp	Experimental
i,j,k,l,m	Indices
m	Denotes the melting pressure
s	Denotes states at saturation
sub	Denotes the sublimation pressure
σ	Along the saturated liquid line
t	At the triple point
tr	Contribution of translation
0	In the reference state
OH	In the initial state of Hugoniot–curve measurements
90	Temperatures according to the ITS-90
68	Temperatures according to the IPTS-68
48	Temperatures according to the IPTS-48 or ITS-48

Physical Constants for Argon

M	Molar mass $M=(39.948\pm0.001)$ g mol^{-1}, see Coplen (1997)
R_m	Universal gas constant $R_m=(8.314\,51\pm0.000\,210[1])$ J mol^{-1}K^{-1}, see Cohen and Taylor (1986)[1]
R	Specific gas constant $R=(0.208\,133\,3\pm0.000\,007\,4)$ kJ kg^{-1}K^{-1}
T_c	Critical temperature $T_c=(150.687\pm0.015)$ K, see Sec. 2.2.
p_c	Critical pressure $p_c=(4.863\pm0.003)$ MPa, see Sec. 2.2.
ρ_c	Critical density $\rho_c=(535.6\pm1.0)$ kg m^{-3}, see Sec. 2.2.
T_t	Triple-point temperature $T_t=83.805\,8$ K, see Sec. 2.1.
p_t	Triple-point pressure $p_t=(68.891\pm0.002)$ kPa, see Sec.2.1.
T_0	Reference temperature $T_0=298.15$ K
p_0	Reference pressure $p_0=0.101\,325$ MPa
h_0^o	Reference enthalpy in the ideal-gas state at T_0 $h_0^o=0$ kJ kg^{-1}
s_0^o	Reference entropy in the ideal-gas state at T_0, p_0 $s_0^o=0$ kJ (kg K^{-1})

---

[1]Cohen and Taylor give a standard deviation of $\pm0.000\,070$ J mol^{-1} K^{-1}.

TABLE 1. Selected equations of state for argon

Authors	Year	Temperature range/K	Pressure range/MPa	Structure of the equation	Number of coefficients	Data used in the correlation
Gosman et al.	1969	84–300	0–101	Modified BWR[a,b]	16	$p\rho T$
Bender	1970	90–1073	0–50	Extended BWR	20	$p\rho T, p_s, \rho', \rho''$
Vasserman and Rabinovich	1970	85–180	0–50	Polynomial	7	$p\rho T$
Vasserman et al.	1971	153–423	0–180[c]	Polynomial	28	$p\rho T$
		423–1223	0–90	Polynomial	10	$p\rho T$
Stewart et al.	1981	84–1224	0–1000	Extended BWR[d]	32	$p\rho T, \rho', \rho'', c_v, w$
Stewart et al.	1982	84–1200	0–1000	Optimized[e]	34	$p\rho T, \rho', \rho'', c_v, w$
Jacobsen et al.	1986	84–1200	0–1000	Optimized[e]	28	$p\rho T, p_s, \rho', \rho'', w, w', w''$
Stewart and Jacobsen	1989	84–1200	0–1000	Optimized[e]	28	$p\rho T, p_s, \rho', \rho'', w, w', w''$
Tiesinga et al.	1994	148–180	4.36–17.2[f]	Crossover equation	18	$p\rho T, c_v$

[a]Benedict–Webb–Rubin (Benedict et al., 1940).
[b]Modified by Strobridge (1962).
[c]The equation is valid for densities up to $1000\,\mathrm{kg\,m^{-3}}$.
[d]Developed by Jacobsen (1972) for nitrogen.
[e]Mathematical structure optimized for the representation of the selected data by the regression analysis of Wagner (1974).
[f]The equation is valid for densities between 300 and $800\,\mathrm{kg\,m^{-3}}$. The additional constraint $\bar{\chi}^{-1} \leqslant 2.2$ restricts this range only for temperatures above 170 K to densities between 330 and $745\,\mathrm{kg\,m^{-3}}$ at the highest temperature ($T = 180\,\mathrm{K}$).

1. Introduction

1.1. Background

Since the discovery of argon in 1893, this substance has been the subject of numerous experimental and theoretical investigations. Due to the widespread use of argon in both scientific and industrial applications, there is special interest in its thermodynamic properties. The chemically inert behavior and the low market price resulting from its large occurrence in air (about 0.934% by volume) predestine argon for the generation of protective atmospheres in industrial applications, e.g., as an inert-gas shield for arc welding and cutting or as a blanket for the production of titanium and other reactive elements.

From a thermodynamic point of view the great importance of argon lies in its molecular simplicity. Since the molecule is monoatomic, nonpolar and completely spherical, argon is commonly used as a reference fluid to establish and test molecular approaches for the prediction of thermodynamic properties and for the calibration of new apparatuses for thermodynamic measurements.

For all these applications knowledge of the thermodynamic properties of argon is an important precondition. Therefore, in 1972 the International Union of Pure and Applied Chemistry (IUPAC) published a monograph [Angus et al., (1972)] which presented extensive tables of its thermal and caloric properties. Since then, along with the increasing demands on accuracy, the experimental techniques have been improved, but only a few experimental investigations on the thermodynamic behavior of argon have been carried out in the subsequent 2 decades. Although argon is generally considered as a reference fluid with well known properties, the quality of the thermodynamic data of argon has remained poor compared with other reference fluids such as methane.

Nowadays this situation has remarkably improved because highly accurate experimental information has become available for large parts of the fluid region during the last few years.

In addition to the increased quality of the experimental data, correlation techniques have significantly improved during the last decade. Sophisticated multiproperty fitting procedures [Schmidt and Wagner (1985); Setzmann and Wagner, (1991)] and new optimization procedures [Setzmann and Wagner (1989)] have resulted in a new basis for the development of empirical equations of state.

1.2. Prior Equations of State

Numerous correlations for the thermodynamic properties of argon can be found in the literature, but most of them cover only small parts of the fluid region and do not meet present demands on accuracy. In many cases their parameters were fitted to data of only one author. Table 1 summarizes the most important equations of state for argon which have been published since 1969. Up to the time when Angus et al. (1972) prepared the IUPAC tables for argon, no equation of state had existed which had been valid in the whole fluid region covered by experimental data. To cover the whole range, the tables were therefore constructed by using different equations with complementary ranges of validity. Angus et al. selected the equations developed by Gosman et al. (1969) at the National Bureau of Standards (NBS) and by Vassermann and Rabinovich (1970) and Vassermann et al. (1971) at the Odessa Institute of Marine Engineers (OIIMF). Gosman et al. used the mathematical structure originally developed by Benedict et al. (1940) and modified by Strobridge (1962) [modified Benedict, Webb, and Rubin (BWR) equation] for their pressure-explicit equation of state

and fitted the parameters to $p\rho T$ data of different authors. At the OIIMF the range covered by experimental data was divided into three regions, which were described by different polynomial equations. To establish these equations, a reference $p\rho T$ data set was produced from the available $p\rho T$ data using graphical methods. Although no caloric data were used at either the NBS or the OIIMF, Angus *et al.* derived values for the enthalpy, internal energy, entropy and the heat capacities from the equations. Since the equations do not allow the calculation of the liquid–vapor phase equilibrium, saturation properties had to be calculated with the aid of the vapor-pressure equations given by the NBS and the OIIMF. The equation developed by Bender (1970) was the first equation of state for argon which could be used for the direct calculation of phase equilibrium data, but it is valid only for pressures up to 50 MPa.

The most recent wide-range equations of state for argon were developed by Stewart and co-workers. Their latest equation was published by Jacobsen *et al.* (1986), and since its second publication by Stewart and Jacobsen (1989) has been widely accepted as an international reference for argon. However, when data for the thermodynamic properties of argon are needed, the IUPAC tables from 1972 are still often referred to.

In 1994, Tiesinga *et al.* published a scaled equation of state for the description of the thermodynamic properties of argon in the critical region, which has the form of the crossover equation developed by Luettmer-Strathmann *et al.* (1992). The equation yields the theoretically expected limiting behavior at the critical point, but it is restricted to the enlarged critical region and because of its complex mathematical structure it is not very convenient for practical applications.

Thus, each of the existing equations of state has at least one of the following disadvantages:

(i)   State-of-the-art data for the thermodynamic properties of argon are not represented within their uncertainty.

(ii) The range of validity is restricted to a narrow temperature or pressure range.

(iii) Unreasonable behavior is observed in regions with a poor data situation.

(iv) Data in the enlarged critical region are not represented within their uncertainty.

(v)   The temperature values used do not correspond to the current International Temperature Scale of 1990 (ITS-90).

It is the purpose of this article to present an equation of state for argon which overcomes the disadvantages of the existing correlations. The new equation describes the thermodynamic surface of argon in the range covered by reliable experimental data within the uncertainties of the best data. This development became possible using existing state-of-the-art fitting and optimization procedures and finally by the development of a new nonlinear optimization algorithm.

2. Phase Equilibria of Argon

An accurate description of phase equilibria by auxiliary equations is an important precondition for the development of a wide-range equation of state and it is also helpful for users who are only interested in phase equilibria. Therefore, all available experimental information on the triple point, the critical point, the normal boiling point, the melting pressure, the sublimation pressure, the vapor pressure, the densities of the saturated liquid and saturated vapor, and on caloric properties on the liquid–vapor phase boundary have been reviewed. Simple correlation equations have been developed for the temperature dependency of the thermal properties.

In order to condense the description of the data situation, the characteristic information on the single data sets is summarized in tables for the corresponding property. The data sets have been divided into three groups. The assignment considers the critically assessed uncertainty of the data, size of the data set and covered temperature range. In addition, attention is paid to the data situation for the respective property. Group 1 contains the data sets used for the development of the corresponding correlation equation. Group 2 contains data sets suitable for comparisons. Compared with group 1 data, the quality of these data deteriorates at least under one of the three aspects mentioned above. Group 3 contains very small data sets and data sets with rather high uncertainty. Further consideration of these data is not reasonable on the level of accuracy aspired to here. Nevertheless, this does not signify a devaluation of these data sets—the whole ranking is influenced more by the quality in relation to the best available reference data than by an absolute level of uncertainty; for other purposes group 3 data sets may be very useful.

Since the correlation equations and all temperature values in this paper correspond to the ITS-90 temperature scale [Preston-Thomas (1990)], the temperature values of the available data, based on older temperature scales, were converted to ITS-90. The conversion from the IPTS-68 temperature scale to ITS-90 temperatures was carried out based on the equations given by Rusby (1991) for $T < 903.15$ K and Rusby *et al.* (1994) for $903.15\,\text{K} \leq T \leq 1337.15$ K. The number of digits of the converted values was increased by one digit in order to guarantee numerically consistent reconversion. Data corresponding to the IPTS-48 temperature scale were converted to IPTS-68 according to the procedure given by Bedford and Kirby (1969). The conversion of temperature values on other scales is discussed separately.

The algorithm used for the conversion from the IPTS-68 to the ITS-90 scale causes an additional uncertainty of ± 1.5 mK for temperatures below 273.15 K and ± 1 mK for temperatures above 273.15 K. This additional uncertainty is *not* considered in the uncertainties given in the tables of this section, since these uncertainties were mainly used for consistency tests between data of different authors. In this case, the uncertainty in the absolute temperature, which is influenced by the uncertainty of the conversion, is less important. The comparison between two very similar temperature values is not influenced by the uncertainty of the conversion if

TABLE 2. Available data for the triple point of argon

Authors	Year	T_t/K	p_t/kPa
Crommelin	1913	83.85[a]	68.748
Holst & Hamburger	1916	83.81[a]	69.51
Born	1922	83.97[b]	68.284
Eucken & Hauck	1928	83.55[a]	
Clusius	1936	83.85±0.05[a]	68.86
Frank & Clusius	1939		68.90±0.03
Clusius & Weigand	1940	83.79±0.02[b]	68.90±0.03
Clusius & Staveley	1941		68.9078±0.0021
Clark et al.("London results")[c]	1951	83.77[b]	68.75
Freeman & Halsey	1956	83.77±0.03	68.541±0.007
Michels et al.	1957	83.796±0.003	
		83.800±0.001	
Heastie	1957	83.80±0.03[b]	68.768±0.007
Pool et al.	1958	83.805±0.006[b]	68.904±0.005
Flubacher et al.	1961	83.813	68.909±0.003
Michels & Prins	1962	83.80±0.02	69.408±0.007
			69.337±0.007
Thomaes et al.	1962		68.908±0.005
Clusius et al.	1963	^{40}Ar: 83.805[b]	68.896
		^{36}Ar: 83.756[b]	68.864
Lovejoy	1963	83.8069	
Fender & Halsey	1965	83.795±0.015	68.86±0.08
Duncan & Staveley	1966		68.877±0.001
Davies et al.	1967		68.877±0.003
Ancsin & Phillips	1969	83.8083	
Lee et al.	1970	^{40}Ar: 83.809	68.897±0.005
		^{36}Ar: 83.746	68.862±0.003
Chen et al.	1971	83.814±0.001	68.9475±0.0080
Furukawa et al.	1972	83.8078±0.005	
Ancsin	1973	83.8056	
Wagner	1973	83.812±0.005	68.95±0.01
Kemp et al.	1976	83.8054±0.0002	
Furukawa	1978	83.80840	
		83.80837	
Kemp & Kemp	1978	83.8054±0.0001	
Khnykov et al.	1978	83.8054±0.0009	
Pavese	1978	83.8086±0.000 15	
		83.8090±0.000 15	
Shiratori	1979	83.8042	
Pavese	1981		68.890±0.0015
Bonhoure & Pello	1983		68.8900±0.0007
Pavese et al.	1984	83.80593±0.000 59	
Kang et al.	1988	83.8086±0.0006	69.02±2.32
Krishan et al.	1989	83.80677±0.001 00	
Defining fixed point of the ITS90	**1990**	**83.8058**	
Bandyopadhyay et al.	1991		68.8908±0.0010
Gilgen	1993		68.893±0.035[d]

[a]Since the calibration of the thermometer is unknown, this temperature was not converted to ITS-90.

[b]The authors determined the temperature by measuring the vapor pressure of oxygen; we redetermined the temperature value by evaluating the correlation of Wagner et al. (1976) for the measured vapor pressure of oxygen.

[c]In this article, experimental results of two laboratories are given. The results of Clark et al. are called "London results," the results of Michels et al. are called "Amsterdam results." Values for the triple-point parameters are given only by Clark et al.

[d]Gilgen (1993) obtained this value by extrapolating his correlation for the vapor pressure to T_t= 83.8058 K; the error resulting from the extrapolation is negligible, because the experimental value with the lowest temperature is very close to the triple point (T= 84 K).

TABLE 3. Available data for the critical point of argon. Uncertainties are given where the original articles contain such estimates

Authors	Year	Method to determine critical-point parameter	T_c/K	p_c/MPa	ρ_c/kg m^{-3}
Olszwesski	1895	a	152.15[j]	5.13	
Ramsay & Travers	1901	a	155.6[j]	5.36	
Crommelin	1910	a	150.71[j]	4.8632	
Crommelin	1911	b			509
Mathias et al.	1912	c			530.78
Michels et al.	1958	d	150.88[k]	4.898	535.8
McCain & Ziegler	1967	a	150.66±0.02	4.856±0.005	
Grigor & Steele	1968	c	150.6±0.1	4.86±0.02	529.5±1
Teague & Pings	1968	a	150.718±0.015	4.882±0.003	
Terry et al.	1969	e			527
Bale et al.	1970	f	150.68±0.02		
			150.61±0.05		
Levelt Sengers	1970b	g	150.77±0.02	4.877	535.7±0.4
Voronel et al.	1973	c	150.6772±0.01		531.0±1.0
		h	150.6787±0.01		
Shavandrin et al.	1976	c	150.66±0.01		534.5±0.5
Koval'chuk	1977	c	150.67±0.01		535.1±0.4
Gilgen et al.	1994b	i	150.687±0.015	4.863±0.003	535.6±1.0

[a]Disappearance and reappearance of the meniscus.
[b]Evaluation of vapor pressure and $p\rho T$ measurements in the critical region with the relation $(\partial p/\partial T)_{\rho=\rho_c}=(dp_s/dT)_{T=T_c}$.
[c]Evaluation of density measurements on the saturated liquid and saturated vapor line.
[d]Graphical evaluation of density measurements on the saturated liquid and saturated vapor line.
[e]Extrapolation of a correlation for the saturated liquid density.
[f]Evaluation of refractive index measurements; T_c from fitting a power-law equation to experimental values.
[g]New evaluation of the data of Michels et al. (1958); critical parameters from fitting a power-law equation to the data.
[h]Evaluation of measurements of the isochoric heat capacity in the critical region.
[i]Evaluation of density measurements on the saturated liquid and saturated vapor line for the determination of T_c and ρ_c; p_c determined by evaluation of the vapor-pressure equation for $T=T_c$.
[j]Since the calibration of the thermometer is unknown, this temperature was not converted to ITS-90.
[k]Including a temperature correction given by Levelt (1970a).

both temperatures are converted with the same procedure.

2.1. Triple Point

As Table 2 shows, temperature and pressure of the triple point of argon have been measured by numerous authors. On the present temperature scale ITS-90 the triple-point temperature of argon was adopted as a defining fixed point with a value of 83.8058 K. Due to its better reproducibility, it replaces the normal boiling-point temperature of oxygen, which had been used to define the preceding temperature scale IPTS-68.

The most precise measurements on the triple-point pressure of argon were taken by Pavese (1981), Bonhoure and Pello (1983) and Bandyopadhyay et al. (1991), which confirm each other within their very small uncertainties of ±0.7–±1.5 Pa.

Therefore, the following values for the temperature and pressure of the triple point were selected:

$$T_t = 83.8058\,\text{K}, \qquad (2.1)$$

$$p_t = (68.891 \pm 0.002)\,\text{kPa}. \qquad (2.2)$$

2.2. Critical Point

Table 3 gives a survey of values for the critical parameters of argon found in the literature. Most of the data for the critical temperature agree well within their uncertainty. The value for the critical temperature published by Michels et al. (1958), which was determined from their measurements of saturated vapor and saturated liquid densities in the critical region, lies about 0.2 K above the values given by other authors. Levelt (1970b) reanalyzed the measurements of Michels et al. (1958) but the resulting value for the critical temperature is still too high. Essentially, the differences in the critical pressures can be explained by the variation of the vapor pressure with the assumed critical temperature.

The critical parameters published by Gilgen et al. (1994b) were determined from their accurate measurements of vapor pressures and saturated-vapor and saturated-liquid densities. These data are also consistent with the most accurate density measurements in the homogeneous region, which were published by Gilgen et al. (1994a). Thus, in this work we accepted the critical parameters given by Gilgen et al. (1994b):

$$T_c = (150.687 \pm 0.015)\,\text{K}, \qquad (2.3)$$

TABLE 4. Available data for the normal boiling point of argon. Uncertainties are given where the original articles contain such estimates

Authors	Year	T_b/K
Olszwesski	1895	86.15[a]
Ramsay & Travers	1901	87.05[a]
Crommelin	1913	87.31[a]
Frank & Clusius	1939	87.29[b]
Clusius & Frank	1943	87.31±0.02[b]
Clark et al. ("London")	1951[c]	87.29[b]
("Amsterdam")		87.25
Freeman & Halsey	1956	87.30±0.03
Clusius et al.	1963	[40]Ar:87.30[b,d]
		[36]Ar:87.24[b,d]
Ancsin	1973	87.3026
Chen et al.	1975	87.3092±0.0070
Kemp et al.	1976	87.3021±0.0002
Pavese	1981	87.3032±0.0005

[a]Since the calibration of the thermometer is unknown, this temperature was not converted to ITS-90.
[b]The authors determined the temperature by measuring the vapor pressure of oxygen; we redetermined the temperature value by evaluating the vapor-pressure equation of Wagner et al. (1976) for the measured vapor pressure of oxygen.
[c]See footnote c of Table 2.
[d]The authors examined the isotopes [40]Ar and [36]Ar. Natural argon consists to 99.6% of [40]Ar.

$$p_c = (4.863 \pm 0.003) \text{ MPa}, \qquad (2.4)$$

$$p_c = (535.6 \pm 1.0) \text{ kg m}^{-3}. \qquad (2.5)$$

2.3. Normal Boiling Point

Table 4 lists a summary of reported values for the normal boiling-point temperature, which means the temperature at which argon boils under a pressure of 0.101 325 MPa. For this pressure the solution of the vapor-pressure equation, Eq. (2.9), yields a temperature of 87.3026 K. The most precise measurements were made by Kemp et al. (1976) and Pavese (1981), which confirm this value with a deviation of less than 1 mK. Thus, for the value of the normal boiling-point temperature we selected

$$T_b = (87.303 \pm 0.002) \text{ K}. \qquad (2.6)$$

2.4. Melting Pressure

Table 5 summarizes the 18 available data sets for the melting pressure of argon. Most data sets show either large systematic deviations from each other or a large scatter. Only the measurements of Crawford and Daniels (1968), (1969), Hardy et al. (1971) and Cheng et al. (1973) confirm each other within the uncertainties estimated by these authors. The data set of Hardy et al. (1971) comprises temperatures from the triple point to 273 K (pressures up to 1100 MPa) and thus it includes the temperature ranges examined by the two other groups. These data have an overall uncertainty of less than ±0.1% in pressure for temperatures above 110 K and are consistent with the selected value for the triple-point pres-

TABLE 5. Summary of the data sets for the melting pressure of argon. Uncertainties estimated by the authors are given for group 1 data only

Authors	Year	Number of data	Temperature range/K	ΔT (mK)	Δp (MPa)	Group
Simon et al.	1930	22	84–150			3
Bridgman	1934	6	84–193			2
Bridgman	1935	6[a]	84–193			3
Clusius & Weigand	1940	29	84–89			2
Robinson	1954	13	84–266			3
Lahr & Eversole	1962	15	137–360			3
Michels & Prins	1962	12	84–118			2
Crawford & Daniels	1968	11	95–201			2
Crawford & Daniels	1969	11[b]	95–201			2
Stishov et al.	1970	3	292–322			2
Hardy et al.	1971	85	84–273	2	0.1	1
Stishov & Fedosimov	1971	12	198–323			2
Cheng	1972	4	156–253	20	0.4	1
Cheng et al.	1973	4[c]	156–253	20	0.4	1
Lewis et al.	1974	8	92–211			2
Liebenberg et al.	1974	1	295			2
Finger et al.	1981	1	293			3
Zha et al.	1986	17	379–717			2

[a]Bridgman (1935) determined these values by reevaluation of his earlier measurements (Bridgman, 1934).
[b]These data are identical with the experimental results published by Crawford and Daniels (1968).
[c]These data are identical with the experimental values given by Cheng (1972).

O Hardy *et al.* (1971)   + Bridgman (1934)
∇ Michels & Prins (1962)   □ Crawford & Daniels (1968)
▷ Stishov *et al.* (1970)   ◁ Stishov & Fedosimov (1971)
■ Cheng *et al.* (1973)   ◇ Lewis *et al.* (1974)
▲ Liebenberg *et al.* (1974)

FIG. 1. Percentage deviations of experimental melting-pressure data from values calculated from the melting-pressure equation, Eq. (2.7).

sure. Therefore, we used Hardy *et al.*'s data to establish the new melting-pressure equation which is given by

$$\frac{p_m}{p_t}=1+a_1\left[\left(\frac{T}{T_t}\right)^{1.05}-1\right]+a_2\left[\left(\frac{T}{T_t}\right)^{1.275}-1\right],\quad (2.7)$$

with $T_t=83.8058$ K, $p_t=68.891$ kPa, $a_1=-7476.2665$ and $a_2=9959.0613$. Equation (2.7) is constrained to the triple-point pressure by its functional form. Data sets which differ from the measurements of Hardy *et al.* (1971) by not more than $\pm 2\%$ were placed in group 2. The data sets of group 3 show large systematic differences of up to $+10\%$. Figure 1 compares group 1 and group 2 data with values calculated from Eq. (2.7).

Zha *et al.* (1986) measured pressures on the melting curve up to very high temperatures and pressures (6000 MPa at 717 K). Figure 2 compares these data with the other data sets at lower temperatures and with values calculated from Eq. (2.7) (solid line). The dashed line represents an equation, which was fitted only to the data of Zha *et al.* (1986). It is obvious that these measurements are inconsistent with all

☑ Zha *et al.* (1986)
- - - Equation fitted to the data of Zha *et al.* (1986)
─── Eq. (2.7)
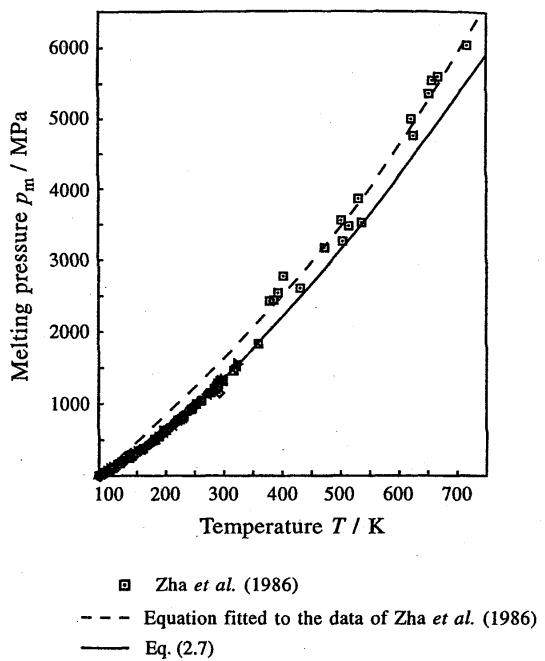
FIG. 2. Representation of the melting-pressure curve. The plotted curves correspond to values calculated from Eq. (2.7) and from an equation fitted to the experimental data of Zha *et al.* (1986). This figure illustrates the systematic offset of Zha *et al.*'s data.

other data sets. Therefore, Zha *et al.*'s data were rejected. Figure 2 also shows that Eq. (2.7) yields reasonable results even at very high temperatures.

2.5. Sublimation Pressure

For the pressure on the sublimation curve of argon ten publications are available, see Table 6. The group 1 data sets were used to establish the new correlation equation for the sublimation pressure:

TABLE 6. Summary of the data sets for the sublimation pressure of argon. Uncertainties estimated by the authors are given for group 1 data only

Authors	Year	Number of data	Temperature range/K	ΔT (mK)	Δp	Group
Ramsay & Travers	1901	7	77–84			3
Crommelin	1913	4	67–82			3
Crommelin	1914	8	68–84			3
Holst & Hamburger	1916	3	83.6–83.8			3
Born	1922	15	66–84			3
Clark *et al.*[a]	1951	7	70–82			3
Flubacher *et al.*	1961	25	66–84			2
Leming	1970	79	25–84	±2	1%–5%	1–2[b]
Chen *et al.*	1971	71	75–84	+1	7 Pa	1
Chen *et al.*	1978	39	75–84	±1	1 Pa	1

[a]See footnote c of Table 2; experimental values of the sublimation pressure were only given by Clark *et al.*
[b]Group 1 for $T\leqslant74$ K, group 2 for $T>74$ K (see text).
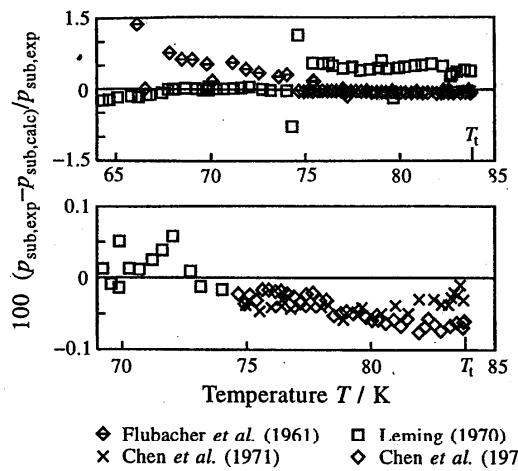
Fig. 3. Percentage deviations of experimental data for the sublimation pressure assigned to groups 1 and 2 (upper diagram) and group 1 (lower diagram) from values calculated from the sublimation-pressure equation, Eq. (2.8).

$$\ln\left(\frac{p_{sub}}{p_t}\right) = \frac{T_t}{T}\left[a_1\left(1 - \frac{T}{T_t}\right) + a_2\left(1 - \frac{T}{T_t}\right)^{2.7}\right], \quad (2.8)$$

with $T_t = 83.8058$ K, $p_t = 68.891$ kPa, $a_1 = -11.391\,604$ and $a_2 = -0.395\,134\,31$.

The upper diagram of Fig. 3 illustrates the deviation of the group 1 and group 2 data from values calculated from Eq. (2.8). At temperatures below 74 K the data set of Leming (1970) supports the measurements of Chen et al. (1971), (1978), while these data sets differ systematically at higher temperatures by about 0.5%. Here, the values of Chen et al. are considered as more reliable, since they are consistent with the well founded triple-point parameters. The data of Leming were placed in group 1 only for temperatures below 74 K.

The lower diagram in Fig. 3 shows the comparison of the group 1 data with values calculated from Eq. (2.8) in more detail. The values of Chen et al. (1971) and Chen et al. (1978) deviate systematically by about −0.05%. For the va-
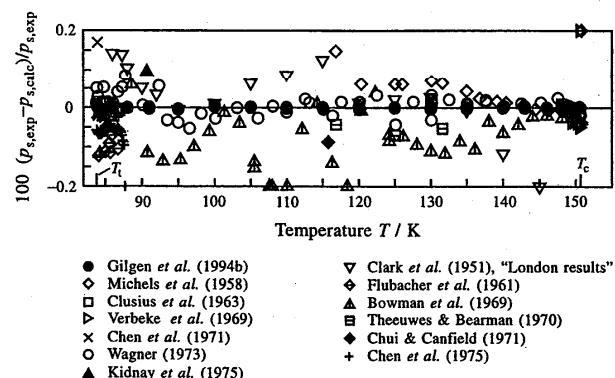
Fig. 4. Percentage deviations of experimental vapor-pressure data assigned to groups 1 and 2 from values calculated from the vapor-pressure equation, Eq. (2.9).

TABLE 7. Summary of the data sets for the vapor pressure of argon

Authors	Year	Number of data	Temperature range/K	Group
Olszwesski	1895	10	134–145	3
Ramsay & Travers	1901	15	86–156	3
Crommelin	1910	6	132–150.7	3
Crommelin	1911	4	133–148	3
Crommelin	1913	7	86–123	3
Holst & Hamburger	1916	5	84–90	3
Born	1922	13	84–90	3
Bourbo & Ischkin	1936	3	87–95	3
Clark et al.[a]	1951			
"London results"		16	86–145	2
"Amsterdam results"		23	91–150.0	3
Narinskii	1957	38	87–124	3
Michels et al.	1958	23	117–150.7	2
Flubacher et al.	1961	6	84–87	2
Clusius et al.	1963	14	84–87	2
Radovskii	1963	58	84–150.6	3
van Itterbeek et al.	1963	9	138–148	3
van Itterbeek et al.	1964	34	85–149	3
Blagoi et al.	1967	13	88–120	3
Davies et al.	1967	2	104–116	3
McCain & Ziegler	1967	21	114–150.6	3
Bowman et al.	1969	36	84–150.1	2
Streett & Staveley	1969	10	101–143	3
Verbeke et al.	1969	9	149.2–150.7	2
Leming	1970	2	84.1–84.5	3
Theeuwes & Bearman	1970	4	117–148	2
Chen et al.	1971	16	84–85	2
Chui & Canfield	1971	1	116	2
Wagner	1973	57	84–150.7	2
Kim	1974	3	129–145	3
Chen et al.	1975	43	84–88	2
Kidnay et al.	1975	1	91	2
Gilgen et al.	1994b	47	84–150.7	1[b]

[a]See footnote c of Table 2.
[b]Uncertainties are given in the text.

por pressures of Chen et al. (1971), (1975) an error of the same magnitude is observed (see Fig. 4). At temperatures below 70 K the data of Leming are represented to within ±8 Pa with the exception of two outliers; below 40 K the deviations range from +0.001 to +0.003 Pa.

2.6. Vapor Pressure

Table 7 summarizes the 32 available data sets for the vapor pressure of argon. The very accurate data of Gilgen et al. (1994b) describe the whole vapor-pressure curve from the triple point up to the critical point with an uncertainty which ranges from ±0.01% to ±0.04% for the lowest vapor pressures. A critical assessment of all data sets has shown that there are no other vapor-pressure data of comparable accuracy. Therefore, only the data of Gilgen et al. were assigned

TABLE 8. Summary of the data sets for the saturated liquid density of argon

Authors	Year	Number of data	Temperature range/K	Group
Baly & Donnan	1902	12	85–89	3
Crommelin	1911	4	132–148	3
Mathias et al.	1912	8	90–148	3
Michels et al.	1958	12	117–150.7	3
van Itterbeek & Verbeke	1960	2	86–90	2
Saji & Kobayashi	1964	5	84–87	3
Davies et al.	1967	1	116	2
Streett	1967	3	102–121	3
Goldman & Scrase	1969	36	87–145	2
Streett & Staveley	1969	10	101–143	3
Terry et al.	1969	16	86–118	3
Verbeke et al.	1969	27	88–150	3
Chui & Canfield	1971	1	116	2
Gladun	1971	13	88–149	3
Voronel et al.	1973	66	148–150.7	3
Pan et al.	1975	4	91–115	2
Shavandrin et al.	1976	20	101–150.6	3
Koval'chuk	1977	25	134–150.7	2
Anisimov et al.	1978	25[a]	134–150.7	2
Haynes	1978	6	100–120	2
Albuquerque	1980a	15	94–147	2–3[b]
Albuquerque	1980b	4	110–120	2
Gilgen et al.	1994b	27	84–150.7	1[c]

[a]These experimental results were previously published by Koval'chuk (1977).

[b]Group 2 for $T < 125$ K, group 3 for $T > 125$ K.

[c]Uncertainties are given in the text.

to group 1. Group 2 is restricted to data which deviate by less than $\pm 0.2\%$ from the group 1 data in general. Most of the data sets had to be placed in group 3 because of their large scatter or because of systematic deviations of up to $\pm 1\%$ from the group 1 data.

The simple vapor-pressure equation established by Gilgen et al. (1994b) represents the group 1 data without any systematic deviation and was thus adapted for this work:

$$\ln\left(\frac{p_s}{p_c}\right) = \frac{T_c}{T}(a_1\vartheta + a_2\vartheta^{1.5} + a_3\vartheta^2 + a_4\vartheta^{4.5}), \quad (2.9)$$

with $\vartheta = (1 - T/T_c)$, $T_c = 150.687$ K, $p_c = 4.863$ MPa, $a_1 = -5.940\,978\,5$, $a_2 = 1.355\,388\,8$, $a_3 = -0.464\,976\,07$ and $a_4 = -1.539\,904\,3$.

In Fig. 4 the group 1 and group 2 data are compared with values calculated from Eq. (2.9). A detailed comparison of the group 1 data and vapor pressures from Eq. (2.9) with values calculated from the new fundamental equation, Eq. (4.1), is given in Sec. 5.1.1.

2.7. Saturated Liquid Density

Twenty-three data sets for the saturated liquid density are available in the literature. These data sets are summarized in
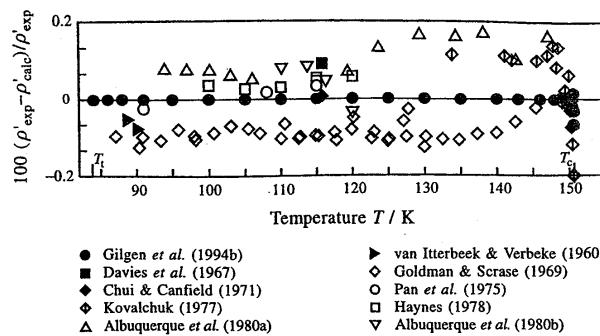
FIG. 5. Percentage deviations of experimental saturated liquid-density data assigned to groups 1 and 2 from values calculated from the saturated liquid-density equation, Eq. (2.10).

Table 8. Again, only the data of Gilgen et al. (1994b) with a typical uncertainty of $\Delta\rho'/\rho' \leq \pm 0.015\%$ were assigned to group 1. All data sets which deviate by not more than $\pm 0.2\%$ from these data (except for the critical region) were placed in group 2. For the group 3 data sets large systematic deviations of up to $\pm 1\%$ from the group 1 data can be observed.

On the basis of the data set of Gilgen et al. (1994b), we established the following equation for the density of the saturated liquid:

$$\ln\left(\frac{\rho'}{\rho_c}\right) = a_1\vartheta^{0.334} + a_2\vartheta^{2/3} + a_3\vartheta^{7/3} + a_4\vartheta^4, \quad (2.10)$$

with $\vartheta = (1 - T/T_c)$, $T_c = 150.687$ K, $\rho_c = 535.6$ kg m^{-3}, $a_1 = 1.500\,426\,2$, $a_2 = -0.313\,812\,90$, $a_3 = 0.086\,461\,622$ and $a_4 = -0.041\,477\,525$. Equation (2.10) is one term shorter than the saturated-liquid-density equation given by Gilgen et al. (1994b), but nevertheless the representation of the group 1 data is almost identical.

Figure 5 shows a comparison between values calculated from Eq. (2.10) and the experimental data which were assigned to groups 1 and 2. The data situation is characterized by systematic differences between the group 2 sets and only the data sets of Haynes (1978) and Pan et al. (1975) are

TABLE 9. Summary of the data sets for the saturated vapor density of argon

Authors	Year	Number of data	Temperature range/K	Group
Crommelin	1911	4	132–148	3
Mathias et al.	1912	8	90–148	3
Michels et al.	1958	11	120–150.7	2
Voronel et al.	1973	49	148–150.7	3
Shavandrin et al.	1976	32	102–150.6	3
Koval'chuk	1977	26	148–150.7	3
Anisimov et al.	1978	26	148–150.7	3
Gilgen et al.	1994b	27	84–150.7	1–2[a,b]
This work (Table 10)		28[c]	83.8–110	1[b]

[a]Group 1 for $T \geq 110$ K, group 2 for $T < 110$ K (see text).

[b]Uncertainties are given in the text.

[c]Calculated values (see text).

TABLE 10. Values for the saturated vapor density of argon determined in this work (see text)

T/K	$\rho''/(\text{kg m}^{-3})$	T/K	$\rho''/(\text{kg m}^{-3})$	T/K	$\rho''/(\text{kg m}^{-3})$
83.8058	4.054 72	93	9.680 16	103	20.924 80
84	4.138 47	94	10.530 22	104	22.431 69
85	4.590 69	95	11.434 89	105	24.019 39
86	5.079 34	96	12.396 43	106	25.691 09
87	5.606 26	97	13.417 18	107	27.450 12
88	6.173 35	98	14.499 54	108	29.299 95
89	6.782 52	99	15.645 97	109	31.244 25
90	7.435 75	100	16.859 03	110	33.286 86
91	8.135 05	101	18.141 36		
92	8.882 49	102	19.495 67		

confirmed by the group 1 data within their claimed uncertainty of about ±0.1%. The volume of the measuring cell used by Albuquerque et al. (1980a), (1980b) was calibrated with saturated liquid densities of nitrogen and methane measured by Haynes et al. (1976) and Nunes da Ponte et al. (1978), respectively. Since these data proved to be incorrect by about +0.1%−+0.2% in comparison with the very accurate data for nitrogen [Nowak et al. (1997a)] and for methane [Kleinrahm and Wagner (1986) and Händel et al. (1992)] it is not astonishing that the data sets of Albuquerque et al. deviate in a similar way.

2.8. Saturated Vapor Density

Only very few data sets are available in the literature for the saturated vapor density. These data sets are summarized in Table 9. The most accurate experimental values were again published by Gilgen et al. (1994b), but nevertheless these data were assigned to group 1 only for temperatures above 110 K. As a result of the analysis of the data sets in the homogeneous low density region it turned out that there are very small but systematic errors in the density measurements of Gilgen et al. (1994a) at low temperatures. When developing the new equation of state and taking into account the new, highly accurate experimental values of the speed of sound in this region (see Table 19), it was not possible to represent Gilgen et al.'s low-temperature density data without systematic deviations. These deviations range up to about −0.02% in density, but they never exceed the claimed experimental uncertainties, which go up to ±0.024% in this region because of special experimental difficulties. Since Gilgen et al. (1994b) determined the densities of the saturated vapor from measurements in the homogeneous region extremely close to the phase boundary, such inconsistencies were also observed for the saturated vapor densities.

Based on this knowledge, we developed a preliminary equation of state for the low density region which is able to represent both the speed of sound measurements *and* the $p\rho T$ data of Gilgen et al. within their uncertainty. Then, new values for the saturated vapor density were determined from the virial equation as $\rho(T_s, p_s)$, where $p_s(T_s)$ was calculated from the vapor-pressure equation, Eq. (2.9). The saturated

vapor densities obtained in this way are listed in Table 10. Taking into account the uncertainty of the vapor-pressure equation and of the preliminary gas-phase equation of state the uncertainty of the new saturated vapor densities is estimated to be less than ±0.03% in density at the triple-point temperature and ±0.025% in density at 110 K.

The new saturated vapor densities together with the experimental data of Gilgen et al. (1994b) for $T \geq 110$ K form the group 1 data set which was used to establish the equation for the saturated vapor density:

$$\ln\left(\frac{\rho''}{\rho_c}\right) = \frac{T_c}{T}(a_1\vartheta^{0.345} + a_2\vartheta^{5/6} + a_3\vartheta^{1} + a_4\vartheta^{13/3}),$$

(2.11)

with $\vartheta = (1 - T/T_c)$, $T_c = 150.687$ K, $\rho_c = 535.6$ kg m^{-3}, $a_1 = -1.706\,956\,56$, $a_2 = -4.027\,394\,48$, $a_3 = 1.551\,775\,58$ and $a_4 = -2.306\,832\,28$.

Figure 6 shows a comparison between experimental data and values calculated from Eq. (2.11). Data sets with deviations exceeding the range of the diagram were omitted. All of the data sets which were published before 1994 lie outside the uncertainties of the group 1 data. The best agreement was found for the data set of Michels et al. (1958), which shows a systematic deviation from the group 1 data of about −0.1.% Only this data set was assigned to group 2.

● Gilgen et al. (1994b)	□ This work (Table 10)
◇ Michels et al. (1958)	▥ Shavandrin et al. (1976)
♣ Kovalchuk (1977)	
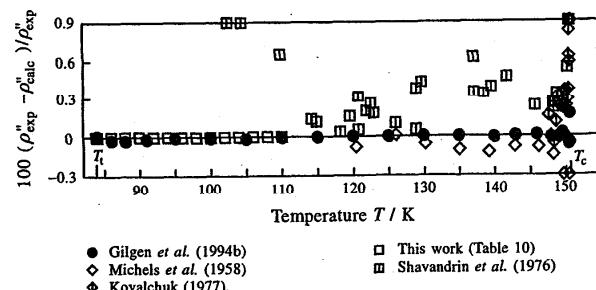
FIG. 6. Percentage deviations of experimental saturated vapor-density data from values calculated from the saturated vapor-density equation, Eq. (2.11).

TABLE 11. Summary of the data sets for the speed of sound on the liquid–vapor phase boundary of argon

Authors	Year	Property	Number of data Total	Number of data Selected	Temperature range/K	Group
Liepmann	1939	w'	36	–	83–87	3
Galt	1948	w'	1	–	85	2
v. Itterbeek & Verhaegen	1949	w'	7	–	84–87	3
van Itterbeek et al.	1959b	w'	10	–	84–90	2
van Dael[a]	1962	w'	2	–	86–90	2
Radovskii	1963	w'	38	–	84–151	2–3
		w''	39	29	84–151	1–2
van Dael et al.	1966	w'	27	23	85–149	1
Aziz et al.	1967	w'	14	14	84–146	1
Blagoi et al.	1967	w'	13	–	89–120	2
Lim & Aziz	1967	w'	19	–	84–88	2
Fleury & Boon	1969	w'	8	–	85–100	2
Thoen et al.	1969	w'	6	6	100–145	1–2
Thoen et al.	1971	w'	19	6	146–151	1–2
		w''	35	21	110–151	1–2
Mikhailenko et al.	1975	w'	14	–	145–149	3

[a]The data were taken from the publication of Thoen et al. (1969).

2.9. Caloric Data on the Liquid–Vapor Phase Boundary

No auxiliary equations have been developed for the caloric properties on the liquid–vapor phase boundary, but the group 1 data have been taken into account directly to develop the new equation of state (see Sec. 4.4).

Speed of Sound. The existing data sets for the speed of sound on the saturated-liquid and saturated-vapor line are summarized in Table 11. A graphical comparison of the group 1 and group 2 data is given in Sec. 5.1.2.

For the saturated liquid, the data sets of van Dael et al. (1966), Aziz et al. (1967), Lim and Aziz (1967), Thoen et al. (1969), and for temperatures above 110 K the data set of Radovskii (1963) confirm each other to within ±0.3%.

TABLE 12. Summary of the data sets for heat capacities of saturated liquid argon

Authors	Year	Property	Number of data	Temperature range/K
Eucken & Hauck	1928	c_σ	6	90–140
Clusius	1936	c_σ	3	86.6–88.9
Walker	1956	c_p'	6[a]	90–140
Flubacher et al.	1961	c_σ	3	84.6–86.3
Gladun	1971	c_v'	12[b]	87.8–149
		c_σ	13[c]	87.8–150.5
		c_p'	13[c]	87.8–150.5

[a]Determined from measurements of the isobaric heat capacity in the homogeneous liquid region.
[b]Determined from measurements of the isochoric heat capacity in the homogeneous liquid region.
[c]The author calculated these values from his c_v' data. The data at $T = 150.5$ K are extrapolated values which are very uncertain.

These data are also consistent with speed of sound measurements in the homogeneous region and with the experimental values of Thoen et al. (1971) in the critical region. These data were used for the development of the new equation of state with the exception of a few outliers, of data in the immediate vicinity of the critical point, and of the data sets of Lim and Aziz (1967) and Radovskii (1963).

For the saturated vapor, only the two data sets of Radovskii (1963) and Thoen et al. (1971) exist for the speed of sound. The uncertainty of these data is about ±1%. Since the homogeneous gas phase is covered by highly accurate speed of sound measurements, these data were used for the development of the new equation of state only with very low weights.

Heat Capacities. Table 12 summarizes the information on the available data sets for heat capacities on the saturated liquid line. Among these properties, only the heat capacity along the saturated liquid line c_σ can be measured directly. The data for the isobaric and isochoric heat capacities c_p' and

TABLE 13. Summary of the data sets for the enthalpy of vaporization of argon

Authors	Year	Number of data	Temperature range/K
Eucken	1916	1	87.3
Frank & Clusius	1939	1	87.3
Flubacher et al.	1961	1	85.7
Kurilenok et al.	1973	15	85.3–87.7
Kim	1974	3[a]	129–145

[a]Kim (1974) determined the enthalpy of vaporization as a function of vapor pressure. For this work the corresponding saturation temperatures were calculated from Eq. (2.9).

TABLE 14. Summary of the $p\rho T$ data sets which were assigned to group 1

| | | Number of data | | Temperature | Pressure | | Uncertainty[a] | |
Authors	Year	Total	Selected	range/K	range/MPa	ΔT/mK	Δp	$\Delta\rho_{total}$
Michels et al.	1949	355	161	273–423	1.9–293			(0.1%–0.15%)
Robertson et al.	1969	287	168	308–673	120–1050	300	0.1%	(0.4%)
Morris & Wylie	1980	43	—	253–308	200–480	5	0.03%	0.05%
Barreiros et al.	1982	73	50[b]	129–147	5.6–142	10	0.01 MPa	(0.05%–0.1%)
Morris	1984	145[c]	145	253–308	100–620			0.03%–(0.06%)
Biswas et al.	1988	19	19	298	100–1000	2	0.1%	(0.1%)
Hoinkis	1989	46	6	298–333	0.2–58			(0.1%)
Guo et al.	1992	28	—	273–293	1.1–4.7	5	0.007%	0.02%
Gilgen et al.	1994a	638	628[d]	90–340	0.2–12.1	1.5–3	0.006%	0.020%
Gilgen et al.	1994b	58	58	148–151	4.4–4.9	3	0.006%	0.010%–0.017%[e]
Estrada-Alexanders & Trusler	1996	565	100[f]	110–450	0.02–27.2			0.025%–(0.04%)
Klimeck et al.	1998	137	137	235–520	2.0–30.1	10–16	0.006%	0.02%–0.03%

[a]The uncertainty values for ΔT and Δp correspond to the uncertainty of the measured values for T and p, whereas $\Delta\rho_{total}$ refers to the total uncertainty which covers all contribution from ΔT, Δp and $\Delta\rho$. Values given in brackets were estimated by ourselves.
[b]Corrected data (see text).
[c]No numerical values, but only an equation of state in the form $\rho(T,p)$ which was fitted to the measured $p\rho T$ data can be found in the article. Therefore, $p\rho T$ values were calculated from this equation.
[d]The experimental values in the gas phase on the isotherms 110 and 120 K were not selected.
[e]Total uncertainty in pressure (critical region).
[f]Data calculated from measured speeds of sound, selected only for $T \leq 125$ K.

c_v' were determined from measurements in the homogeneous liquid region by extrapolation. These data show systematic deviations of up to ±6% (see Sec. 5.1.2). With regard to caloric properties on the saturated liquid line, the behavior of the new equation of state is more accurately determined by the speed of sound measurements discussed above. Thus, the data for heat capacities on the saturated liquid line were not used.

Enthalpy of Vaporization. Only a few values for the enthalpy of vaporization can be found in the literature. The corresponding data sets are summarized in Table 13 and are compared with values calculated from the new equation of state in Sec. 5.1.2. The data sets mainly cover the temperature range between the triple point and the normal boiling point. For higher temperatures only three values were published by Kim (1974).

The enthalpy of vaporization is related to the vapor pressure and to the densities of the saturated liquid and the saturated vapor by the equation of Clausius–Clapeyron. Since there are very accurate data for the thermal properties on the phase boundary, experimental values for the enthalpy of vaporization were not taken into account.

3. Experimental Results for the Single-Phase Region

In this section, experimental data sets for thermodynamic properties in the single-phase region of argon are presented. For each of the considered properties, both general information on all available data sets and more detailed information on the selected data sets is given in corresponding tables.

Where it seemed appropriate, data sets have again been classified into three groups as explained in Sec. 2. Since the situation in the homogeneous region is not always as clear as for the different properties on the phase boundary, numerous data sets are associated with more than one group. Usually these data sets are selected in regions with a poor data situation, but used only for comparison in regions in which more reliable data exist.

Where uncertainties are given, these values usually correspond to estimations given by the authors. Since we noticed, however, that a few authors have published none or overly optimistic estimations of the experimental uncertainties of their data, we had to estimate more realistic values for the experimental uncertainties in some cases; in the tables, these uncertainty values are presented in parentheses.

3.1. Thermal Properties

3.1.1. $p\rho T$ Data

During the last 100 years the thermal behavior of argon has been examined by numerous authors. Seventy data sets are available for the $p\rho T$ relation in the single-phase region, but most of them do not meet present quality standards. Table 14 gives detailed information on the data sets which were assigned to group 1. Table 15 summarizes data sets which were assigned to group 2 or 3.

Up to temperatures of 340 K and pressures of 12 MPa, the description of the $p\rho T$ relation is mainly based on measurements performed with the "two-sinker" buoyancy method, which probably provides the most accurate $p\rho T$ data today. Among these measurements, the most comprehensive data

TABLE 15. Summary of the $p\rho T$ data sets which were assigned to groups 2 and 3

Authors	Year	Number of data	Temperature range/K	Pressure range/MPa	Group
Ramsay & Travers	1901	35	284–546	3.1–9.5	3
Kamerlingh Onnes & Crom.	1910	125	124–293	1.4–6.3	3
Holborn & Schultze	1915	41	273–473	1.8–10	3
Leduc	1918	1	273	0.1	3
Masson & Dolley	1923	25	298	0.5–13	3
Bridgman	1923	15	328	196–1471	3
Holborn & Otto	1924[a]	16	573–673	2.5–10	3
Holborn & Otto	1924[b]	14	173–223	2.0–7.2	3
Baxter & Starkweather	1927	3	273	0.3–10	3
Simon & Kippert	1928	7	84.5–90	35–59	3
Baxter & Starkweather	1929	3	273	0.3–10	3
Bridgman	1935	78[a]	101–328	69–1471	3
Oishi	1949	4	273	1.2	3
Getzen	1956	173	273–573	2.2–43	2–3
Townsend	1956	36	298–323	0.2–14	2
Walker	1956	283	91.9–221	1.7–53	3
Michels et al.	1958	295	118–248	0.6–104	2
Lecocq	1960	126	573–1226	2.1–93	2–3
van Itterbeek & Verbeke	1960	50	86.6–90.6	1.3–15	2
Rogovaya & Kaganer	1961	74	90.1–248	2.5–20	3
Lahr & Eversole	1962	15	137–360	242–1828	3
van Itterbeek et al.	1963	115	90.2–148	1.1–29	3
Crain & Sonntag	1965	78	143–273	0.2–52	2
Streett	1967	26	102–121	0.4–55	3
Crawford & Daniels	1968	11[b]	94.7–201	45–634	2–3
Grigor & Steele	1968	83[c]	144–155	3.0–6.0	3
van Witzenburg & Stryland	1968	114	96.4–154	6.8–203	2
Crawford & Daniels	1969	270	94.7–210	20–646	2–3
		11[b,d]	94.7–201	45–634	2–3
Lippold	1969	68	96.7–149	9.8–98	3
Streett & Staveley	1969	139	101–143	0.35–69	3
Verbeke et al.	1969	315	87.1–202	0.2–15	2
		6	125–172	143–233	3
Blancett et al.	1970	72	223–323	0.3–71	2
Polyakov & Tsiklis	1970	68	373–673	152–1013	3
Rabinovich et al.	1970	61	287–773	10–55	3
Sorokin & Blagoi	1970	48	89.9–129	0.1–49	3
Stishov et al.	1970	3[b]	292–322	1297–1553	2
Theeuwes & Bearman	1970	3	138	5.1–13	2
Dobrovolskii & Golubev	1971	179	92.8–156	1.1–49	2–3
Provine & Canfield	1971	62	143–183	0.3–67	3
Schönmann	1971	71[e]	373–573	0.4–59	2–3
Stishov & Fedosimov	1971	9[b]	198–323	614–1535	2–3
Waxman & Hastings	1971	3	298	1.0–20	2
Cheng	1972	269	200–309	29–1066	2
		4[b]	156–253	357–996	2
Pope	1972	37	101–138	0.1–2.6	2
Cheng et al.	1973	4[b,f]	156–253	357–996	2
Gielen	1973	53	149–153	4.6–5.3	2
Liebenberg et al.	1974	27	295	70–1324	2
Santafe et al.	1976	96	273–323	0.1	3
Lallemand & Vidal	1977	4	298	409–890	2
Kosov & Brovanov	1979	6	290	15–60	3
Vidal et al.	1979	10	298	100–1000	2
Albuquerque et al.	1980	80	93.9–147	0.8–6.1	2
Nunes da Ponte et al.	1981	99	110–120	1.3–138	2–3
Ronchi	1981	313[g]	300–2300	9.9–23884	2
Manov et al.	1984	38	298–363	0.2–15	2–3
Vacek & Hany	1991	72	233–288	4.7–47	2
Vrabec & Fischer	1996	7[h]	200–2000	401–2818	2

[a]The data on the 328 K isotherm had been published before by Bridgman (1924).
[b]Experimental values for the density of the liquid on the solid–liquid phase boundary.
[c]Experimental results were only given in graphical form.
[d]The data had been previously published by Crawford und Daniels (1968).
[e]The experimental results of Schönmann (1971) were reevaluated by Hoinkis (1989) and can be found in the corresponding reference.
[f]The data are identical with the experimental results of Cheng (1972).
[g]No experimental, but calculated values for the Lennard-Jones potential of the form (12-7). The parameters of the potential were fitted to experimental data.
[h]No experimental results, but data from molecular dynamic studies (Lennard-Jones potential of the form (12-6) with $\sigma = 3.3947$ Å and $\varepsilon/k = 117.113$ K).

129 K – 130 K
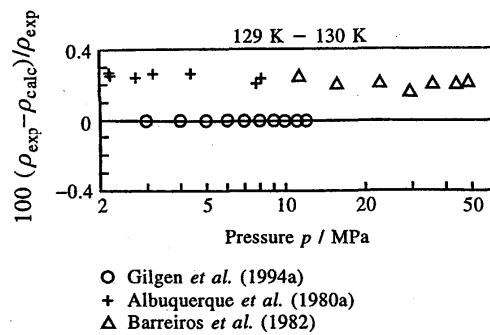
FIG. 7. Percentage density deviations of experimental $p\rho T$ data from values calculated from the new equation of state, Eq. (4.1). This figure illustrates the systematic error in the density measurements of Albuquerque *et al.* (1980a), (1980b) and Barreiros *et al.* (1982).

O   Gilgen *et al.* (1994a)
+   Albuquerque *et al.* (1980a)
△   Barreiros *et al.* (1982)

set was published by Gilgen *et al.* (1994a). These data are supported by the experimental results of Gilgen *et al.* (1994b) for states near the phase boundary at temperatures close to the critical temperature and by the data set of Guo *et al.* (1992) for pressures up to 5 MPa at temperatures between 273 and 293 K.

To enlarge the operational range of buoyancy densimeters without substantial loss of accuracy, Wagner *et al.* (1995) developed a new "single-sinker" densimeter for pressures up to 30 MPa at temperatures from 233 to 523 K. With this apparatus Klimeck *et al.* (1998) measured densities of argon, which supplement the data of Gilgen *et al.* (1994a). The total

uncertainty of data from single- and two-sinker densimeters is generally less than ±0.02% in density, except for data in the critical region and at very low densities.

The $p\rho T$ data of Estrada-Alexanders and Trusler (1996) were not measured directly, but were determined from speed of sound measurements by numerical integration of thermo-dynamic differential equations. The data cover temperatures from 110 to 450 K for densities up to half the critical density and deviate systematically from the experimental values of Gilgen *et al.* (1994a) and Klimeck *et al.* (1998) by up to ±0.04% in density. These data were used only in the gas phase at temperatures below 125 K, where the total uncertainty of the results of Gilgen *et al.* (1994a) increases from ±0.02% to about ±0.035% due to the increasing influence of absolute contribution in σ_ρ and σ_p. In this region, the results of Estrada-Alexanders and Trusler (1996) are more consistent with accurate speed of sound measurements of different authors than any direct $p\rho T$ measurements.

For pressures above 12 MPa, most data sets in the liquid phase $(T<T_c)$ show systematic deviations of up to ±1.4% from each other. In this region, only the data set published by Barreiros *et al.* (1982), which extends to pressures up to 147 MPa for temperatures between 129 and 147 K, could be selected for the description of the $p\rho T$ relation. Barreiros *et al.* (1982) used the same apparatus as Albuquerque *et al.* (1980a), (1980b) which was calibrated with data for the satu-rated liquid density of methane and nitrogen. These data were incorrect by +0.2%−+0.35% (see Sec. 2.7). This faulty calibration is the reason for the systematic deviations

X   Michels *et al.* (1949)
▼   Barreiros *et al.* (1982), corr.
◨   Biswas *et al.* (1988)
O   Gilgen *et al.* (1994a)
★   Estrada-Alexanders & Trusler (1996)

+   Robertson *et al.* (1969)
▷   Morris (1984)
◻   Hoinkis (1989)
◉   Gilgen *et al.* (1994b)
◇   Klimeck *et al.* (1998)
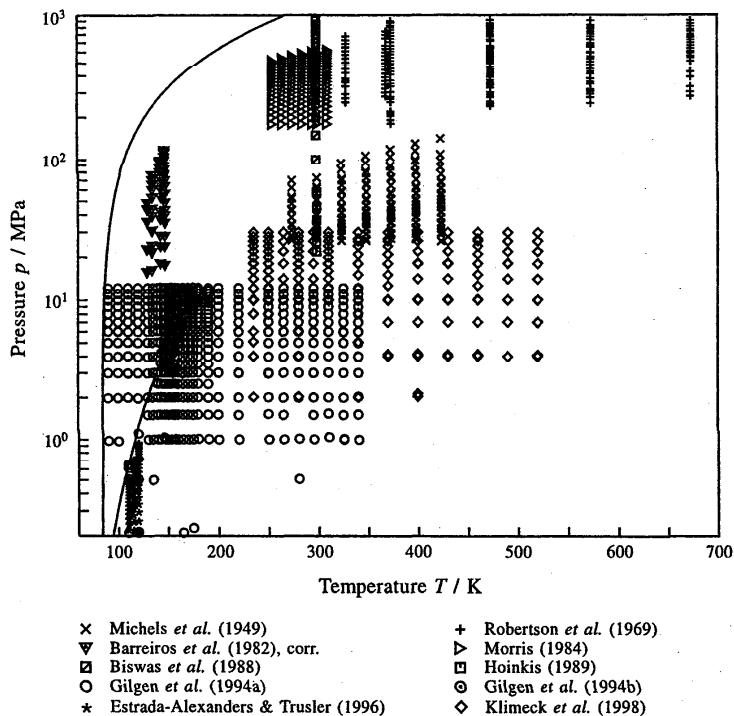
FIG. 8. Distribution of the experimental $p\rho T$ data used for the establishment of the residual part of the new equation of state, Eq. (4.1), in a p-T diagram.

TABLE 16. Second and third virial coefficients of argon determined by reevaluation of the $p\rho T$ data of Gilgen et al. (1994a)

T/K	$B/(cm^3\,mol^{-1})$	$C/(cm^6\,mol^{-2})$	T/K	$B/(cm^3\,mol^{-1})$	$C/(cm^6\,mol^{-2})$
120	-130.28 ± 1.30		170	-67.60 ± 0.25	2012.5 ± 100
130	-112.71 ± 0.60	2231.7 ± 300	175	-63.71 ± 0.25	1913.0 ± 100
135	-105.28 ± 0.30	2389.2 ± 100	180	-60.13 ± 0.25	1864.3 ± 100
140	-98.29 ± 0.25	2344.0 ± 100	190	-53.62 ± 0.25	1718.4 ± 100
143	-94.46 ± 0.25	2326.3 ± 100	200	-48.00 ± 0.25	1635.0 ± 100
146	-90.83 ± 0.25	2314.3 ± 100	220	-38.52 ± 0.25	1455.5 ± 100
148	-88.51 ± 0.25	2289.0 ± 100	250	-27.74 ± 0.25	1292.5 ± 100
150.7	-85.60 ± 0.25	2293.5 ± 100	265	-23.38 ± 0.25	1210.6 ± 100
153	-83.04 ± 0.25	2216.2 ± 100	280	-19.59 ± 0.25	1157.3 ± 100
155	-80.98 ± 0.25	2187.3 ± 100	295	-16.26 ± 0.25	1113.7 ± 100
157	-79.04 ± 0.25	2181.6 ± 100	310	-13.27 ± 0.25	1052.4 ± 100
160	-76.27 ± 0.25	2171.3 ± 100	325	-10.66 ± 0.25	1033.8 ± 100
165	-71.68 ± 0.25	2053.3 ± 100	340	-8.30 ± 0.25	1005.3 ± 100

between the data of Barreiros et al. and the accurate results of Gilgen et al. (1994a), see Fig. 7. Therefore, the data of Barreiros et al. were corrected on each isotherm to form a smooth continuation of the values of Gilgen et al. The numerical values of the corrections on the 129, 134, 143 and 147 K isotherm are -0.22%, -0.34%, -0.33% and -0.16% in density, respectively.

At temperatures between 273 and 423 K the $p\rho T$ data of Michels et al. (1949) were assigned to group 1. Within its uncertainty, this data set is consistent with the new "single-sinker" data for pressures up to 30 MPa, but it extends to significantly higher pressures ($p\leqslant293$ MPa). For temperatures from 253 to 308 K, the most accurate data in the high pressure range ($p>200$ MPa) were published by Morris and Wylie (1980) and Morris (1984). These data have uncertainties of less than $\pm0.06\%$ in density. The region up to 673 K and 1050 MPa is covered by the data of Robertson et al. (1969). Since this data set shows a rather large scatter and systematic deviations of about -0.2% from the more accurate data of Morris (1984), an uncertainty of $\pm0.4\%$ had to be assumed for the data set of Robertson et al.

In a p-T diagram, Fig. 8 shows the $p\rho T$ data which were used to establish the new equation of state. Although the data sets of Morris and Wylie (1980) and Guo et al. (1992) were assigned to group 1, they were not used in the end. These data do not contain significant additional experimental information since they confirm other data sets, which cover a larger region with at least the same accuracy, far within their uncertainties.

3.1.2. Thermal Virial Coefficients

Virial coefficients cannot be measured directly; in most cases they are determined from isothermal fits to $p\rho T$ measurements. Therefore, such data do not contain new information if the original $p\rho T$ data are used to establish an equation of state. However, since a reasonable representation of the virial coefficients is considered as important particularly for

an equation of state for argon, some selected data for the second and third virial coefficient were used here.

In a preliminary data set, we used the second and third virial coefficients given by Gilgen et al. (1994a), who determined these data from a virial equation which was fitted to their low-density $p\rho T$ data. But when the phase-equilibrium condition was taken into account, none of the preliminary equations could represent the data for the third virial coefficient in the region of its maximum near T_c. However, the original $p\rho T$ data were always represented within their uncertainty. Therefore, we reevaluated the $p\rho T$ data of Gilgen et al. by the method which was used for ethylene and nitrogen by Nowak et al. (1996), (1997b). The new results for the second and third virial coefficients are given in Table 16 together with their uncertainties. The values for the second virial coefficient do not differ from the data given by Gilgen et al. significantly, but the third virial coefficients confirm the lower values which were predicted by preliminary equations of state. For the third virial coefficient, Fig. 9 compares the data given by Gilgen et al. with the new results and with values calculated from the new equation of state, Eq. (4.1).

In the data set which was finally used to establish the new equation of state, the new data for the virial coefficients were selected instead of the data of Gilgen et al. As expected, the inconsistency with the very accurate speed of sound data at low temperatures, which was previously discussed for the $p\rho T$ data, was also observed for the derived values of the second virial coefficient. Therefore, only low weights were given to the data for B and C at 120 K.

The data of Aziz and Slaman (1986), (1990) and Sevastyanov and Chernyavskaya (1987) were used at temperatures up to 1100 and 3000 K, respectively. Although these data were calculated from different models for the intermolecular potential, the data sets for the second virial coefficient confirm each other within $\pm0.7\,cm^3\,mol^{-1}$, whereas experimental values show systematic deviations of up to $\pm3\,cm^3\,mol^{-1}$. Table 17 summarizes the selected data sets
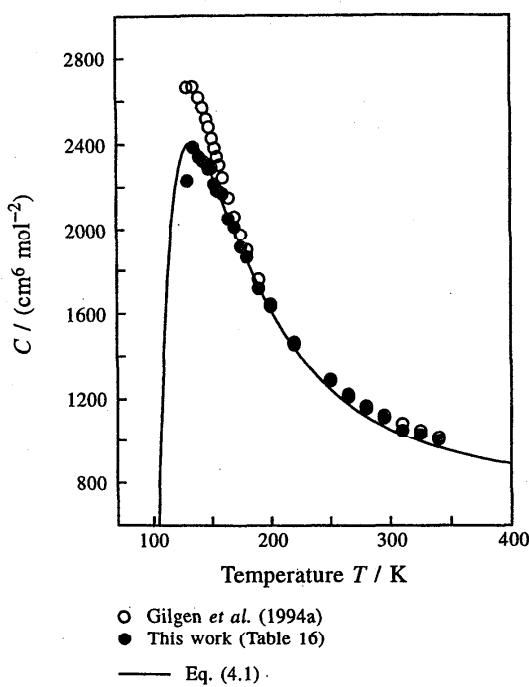
FIG. 9. Plot of the data determined by Gilgen *et al.* (1994a) for the third virial coefficient and of the data determined in this work by reevaluation of the *ppT* data of Gilgen *et al.* (1994a).

and Table 18 gives information on the data sets which were assigned to groups 2 and 3.

3.2. Acoustic Properties

3.2.1. Speed of Sound Data

Forty seven data sets have been published concerning the speed of sound in argon. Table 19 gives detailed information on the selected data sets (group 1). The data sets which were assigned to groups 2 and 3 are summarized in Table 20.

Speed of Sound Data Measured with Spherical Resonators. Today, the most accurate speed of sound measurements in gaseous fluids are performed with spherical resonators. Provided that the radius of the resonator is known in the

TABLE 18. Summary of data sets for the second and third virial coefficient which were assigned to groups 2 and 3

Authors	Year	Number of data B,C	Temperature range/K	Group[a]
Kamerlingh Onnes & Crom.	1910	12,12	152–294	3
Cath & Kamerlingh Onnes	1922	20,—	83–273	3
Holborn & Otto	1925	9, 8	173–673	3
Tanner & Masson	1930	7, 7	298–447	3
Michels *et al.*	1949	14,14	273–423	2
Whalley *et al.*	1953	9, 6	273–873	3
Cottrell *et al.*	1956	3,—	303–363	3
Getzen	1956	13,13	273–573	3
Michels *et al.*	1958	12,12	133–248	2
Knobler *et al.*	1959	1,—	90	3
Hilsenrath	1960	81,62	80–5000	3
Lecocq	1960	6, 6	573–1226	3
Fender & Halsey	1962	10,—	85–124	2
Pool *et al.*	1962	1,—	90	3
Thomaes *et al.*	1962	5,—	109–295	3
Gyorog & Obert	1964	11,10	120–600	2
Crain & Sonntag	1965	4, 4	143–273	2
Davies *et al.*	1967	2,—	104–116	3
Kalfoglou & Miller	1967	6, 6	303–773	2
Weir *et al.*	1967	17,17	80–191	3
Byrne *et al.*	1968	18,—	84–271	3
Lichtenthaler & Schäfer	1969	5,—	288–323	2
Blancett *et al.*	1970	3, 3	223–323	2
Bose & Cole	1970	1,—	323	3
Provine & Canfield	1971	3, 3	143–183	2
Schönmann	1971	3, 3	373–573	2
Levelt Sengers *et al.*	1972	65,31	80–1100	3
Osborne	1972	14,14	300–1024	3
Pope *et al.*	1973	3, 3	101–138	3
Bellm *et al.*	1974	10,—	300–550	3
Hahn *et al.*	1974	5,—	200–573	2
Schramm & Hebgen	1974	3,—	77–90	3
Santafe *et al.*	1976	12,—	273–323	3
Rentschler & Schramm	1977	6,—	325–713	3
Schramm *et al.*	1977	11,—	202–500	3
Ewing & Marsh	1979	2,—	303–340	3
Dymond & Smith	1980	18,—[b]	81–1000	2
Zykov *et al.*	1983	—,12	148–423	—
Kerl & Häusler	1984	5,—	299–345	3
Hoinkis	1989	2, 2	298–333	2
Gilgen *et al.*	1994a	27,25	110–340	2

[a]Assignment based on the evaluation of the data for *B*
[b]Not directly determined by measurement, but averaging of values taken from literature.

TABLE 17. Summary of data sets for the second and third virial coefficient which were assigned to group 1. Uncertainty values in brackets were estimated by ourselves

Authors	Year	Property	Number of data Total	Number of data Selected	Temperature range/K	Uncertainty
Aziz & Slaman	1986	B	39[a,b]	9	80–1100	$(1 \text{ cm}^3 \text{ mol}^{-1})$
Sevastyanov	1987	B	18[c]	11	81–3000	$(1 \text{ cm}^3 \text{ mol}^{-1})$
& Chernyavskaya		C	17	11	110–3000	$(200 \text{ cm}^6 \text{ mol}^{-2})$
Aziz & Slaman	1990	B	39[a,d]	9	80–1100	$(1 \text{ cm}^3 \text{ mol}^{-1})$
This work, Table 16		B	26	26	120–340	$0.25–1.3 \text{ cm}^3 \text{ mol}^{-1}$
		C	25	25	130–340	$100–300 \text{ cm}^6 \text{ mol}^{-2}$

[a]Numerical results for argon communicated by Aziz (1994).
[b]Results for a HFD-B2-potential.
[c]Results for a Lennard–Jones (12-7) potential.
[d]Results for a HFD-B3-potential.

TABLE 19. Summary of speed of sound data sets which were assigned to group 1. Uncertainty values were estimated by ourselves

Authors	Year	Number of data		Temperature range/K	Pressure range/MPa	Uncertainty
		Total	Selected			
Bowman et al.	1968	47	46	86.2–147	0.4–6.6	(0.4%)
Pitaevskaya et al.	1969	136	106	298–473	50–400	(2%–4%)
Thoen et al.	1969	171	145	100–150	0.8–52	(0.6%)[a]
Streett & Costantino	1974	234	215	90.1–160	0.1–345	(0.5%)
Kachanov et al.	1983	15	15	373–423	100–800	(1%)
Kortbeek et al.	1985	85	85	148–298	100–1000	(0.4%)
Ewing et al.	1989	92	92	100–304	0.01–0.5	(0.003%)
Boyes	1992	152	151	252–350	0.05–10	(0.01%–0.015%)
Ewing & Goodwin	1992	50	50	255–300	0.06–7.0	(0.005%)
Ewing & Trusler	1992	90	90	90.1–373	0.01–0.6	(0.003%)
Estrada-Alexanders & Trusler	1995	236	236	110–450	0.01–19	(0.001%–0.03%)

[a]Uncertainty increased for data in the critical region.

TABLE 20. Summary of speed of sound data sets which were assigned to groups 2 and 3

Authors	Year	Number of data	Temperature range/K	Pressure range/Mpa	Group
van Itterbeek & van Paemel	1938	41	78.9–90.2	0.3–20	3
Lacam & Noury	1953a	60	297–298	9.2–93	3
Lacam & Noury	1953b	12	298	1.1–13	3
Lacam	1956	144	298–473	5.1–111	2–3
Martin	1957	90	298–348	8.7–97	2–3
van Itterbeek et al.	1959a	79	174–300	0.2–7.3	3
van Itterbeek et al.	1959b	57[a]	84.8–90.3	0.5–7.4	—
Dobbs & Finegold	1960	42	87.2–90.0	0.1–14	2
van Itterbeek & van Dael	1961	25	87.3–90.3	0.3–20	2
Lestz	1963	14	273–304	0.1–1.2	3
Smith & Harlow	1963	2	273–303	0.1	3
Radovskii	1964	256	90.0–170	0.01–6.0	2–3
El-Hakeem	1965	10	273–294	0.1–7.1	3
Carome et al.	1968	56	90.3–140	0.5–11	3
Nierode et al.	1970	9[a]	273	0.1–7.9	—
Goring	1971	12	302–540	0.1	3
Thoen et al.	1971	187	121–169	0.3–6.9	2–3
Law & Bezanson	1972	1	293	0.1	3
Susekov	1972	11	321	0.3–6.8	3
Liebenberg et al.	1974	27	295	70–1324	2
Hanayama	1975	23	298	12–1275	2
Nishitake & Hanayama	1975	13[b]	298	101–1275	2
Quinn et al.	1976	98	273	0.03–0.2	3
Akdemir	1977	9	303	0.004–0.1	3
Colclough et al.	1979	146[c]	273	0.03–1.3	2
Vidal et al.	1979a	10	298	150–1000	2
Yang	1983	8	298	1.1–92	3
Tam & Leung	1984	1	295	0.1	3
Ewing et al.	1985	71	251–330	0.02–0.1	2
Ewing et al.	1986	116	273	0.02–0.25	2
Goodwin	1988	294	255–300	0.02–7.0	2
Moldover et al.	1988	70	273	0.025–0.5	2
Moldover & Trusler	1988	45	303	0.025–0.04	2
Colgate et al.	1990	7	298–473	0.1	3
Beckermann	1993	78	250–350	0.5–10	2

[a]The results were given only in graphical form.
[b]These results were also published by Hanayama (1975).
[c]Reevaluation of the experimental results of Quinn et al. (1976) and new measurements.

investigated temperature range, the speed of sound in the fluid can be calculated from the measured resonance frequencies. Since measurements on monoatomic gases at low pressures are suitable for the determination of the temperature dependence of the resonator radius, numerous measurements of the speed of sound in argon were carried out in the low pressure region. The most comprehensive data set was published by Estrada-Alexanders and Trusler (1995), which covers temperatures from 110 to 450 K at densities up to half the critical density and pressures up to 19 MPa. The low-temperature limit is extended down to 90 K by the data set of Ewing and Trusler (1992). The other data sets cover only parts of this region.

Unfortunately, most authors did not publish estimates for the overall uncertainty of their speed of sound data. Instead of uncertainties, values for the standard mean deviation, which results from a numerical evaluation of the experimental data or only individual uncertainties of the measured pressure and temperature, are given. An assessment of the overall uncertainty which considers all known sources of errors is given only by Beckermann (1993) and Estrada-Alexanders and Trusler (1995). Beckermann estimated that the overall uncertainty of his data is less than $\pm 0.04\% - \pm 0.06\%$. A comparison with other data sets shows that these values are realistic. Estrada-Alexanders and Trusler claim an uncertainty of less than $\pm 0.007\%$ for their measurements in the worst case, i.e., at the highest density close to the critical temperature. This value neglects the uncertainty of the temperature measurement "because of the manner in which a_0 was determined." Nevertheless, a critical analysis of the data set indicated that the overall uncertainties given in the article are too small in some regions. Therefore, we estimated new values for the overall uncertainties which consider *all* sources of uncertainties which are discussed by Estrada-Alexanders and Trusler. The basis of our assessment will be outlined in the following paragraph in some detail.

The speed of sound cannot be deduced from the measured resonance frequencies of the resonator directly. The experiment yields only the quotient w/a of the speed of sound w and the inner radius of the resonator a. Thus, the temperature dependent value of the radius a has to be known for the determination of the speed sound w. In practice, the radius a is determined by extrapolation of the measured values w/a to zero pressure. In this way, the radius at zero pressure, a_0, can be calculated from the known speed of sound in the ideal gas state ($w_0 = \sqrt{\kappa^\circ RT}$, where κ° is the ratio of ideal gas heat capacities c_p° and c_v°, R is the specific gas constant of argon and T is the temperature). Based on a_0, the radius a at higher pressures is calculated from the known derivative $(\partial a/\partial p)_T$, which depends on the geometry of the resonator and on known properties of the material. Therefore, the uncertainty of the temperature measurement (± 5 mK) has an influence on the value for the radius of the resonator. This effect is considered by Estrada-Alexanders and Trusler with a contribution of ± 10 ppm to the overall uncertainty of the speed of sound. This value corresponds to the contribution of the uncertainty in temperature to the uncertainty of the speed

of sound *at zero pressure*. It is assumed that this contribution remains constant *at higher pressures*. An analysis of the pressure and temperature dependency of the speed of sound shows that this is not true for the whole covered temperature and pressure range. Especially close to the saturated vapor line and at the highest densities close to the critical temperature, the influence of the uncertainty of the measured temperature increases. At a temperature of 150 K, for example, the value of $w^{-1}(\partial w/\partial T)_p$ increases from 3.3×10^{-3} K^{-1} at $\rho = 0$ to 38×10^{-3} K^{-1} at $\rho = 0.5\,\rho_c$.

Close to the saturated vapor line and for temperatures within ± 10 K around the critical temperature this effect results in overall uncertainties which are up to three times larger than the uncertainties given by Estrada-Alexanders and Trusler.

Other Speed of Sound Data. Compared with the spherical resonator data the other data sets for the speed of sound in argon are less accurate by one or two orders of magnitude. No speed of sound measurements are available at temperatures between 160 and 298 K for pressures from 15 to 100 MPa. [The data of Estrada-Alexanders and Trusler (1995) reach up to pressures of 19 MPa only for temperatures above 298 K.]

In the liquid region the experimental results of Bowman *et al.* (1968), Thoen *et al.* (1969) and Streett and Costantino (1974) are consistent with the selected speed of sound data on the saturated liquid line. The high pressure data of Kortbeek *et al.* (1985) and the data set of Streett and Costantino overlap at 148 K and confirm each other far within the claimed uncertainties. In the high pressure region, the data sets of Pitaevskaya *et al.* (1969) and Kachanov *et al.* (1983) had to be used at temperatures above 298 K, but only low weights were given to these data since they scatter by more than $\pm 1\%$.

Figure 10 shows the selected speed of sound data in a p-T diagram.

3.2.2. Acoustic Virial Coefficients

Similar to thermal properties, the speed of sound in the gas phase can be written in a virial expansion in density:

$$\frac{w^2}{\kappa^\circ RT} = 1 + \beta_a(T) \cdot \rho + \gamma_a(T) \cdot \rho^2 + \delta_a(T) \cdot \rho^3 + \ldots .$$

$$(3.1)$$

Like thermal virial coefficients, data for the acoustic virial coefficients ($\beta_a, \gamma_a, \ldots$) do not contain any new information if the original speed of sound data are considered to set up an equation of state. But unlike the speed of sound data, values for the second acoustic virial coefficient β_a can be used *directly* in linear optimization procedures. In this way, more information on the speed of sound becomes accessible for the linear algorithms which were used here to optimize the functional form of preliminary equations of state (cf. Sec. 4.2).

The acoustic virial coefficients are related to the thermal virial coefficients by differential equations. From recent
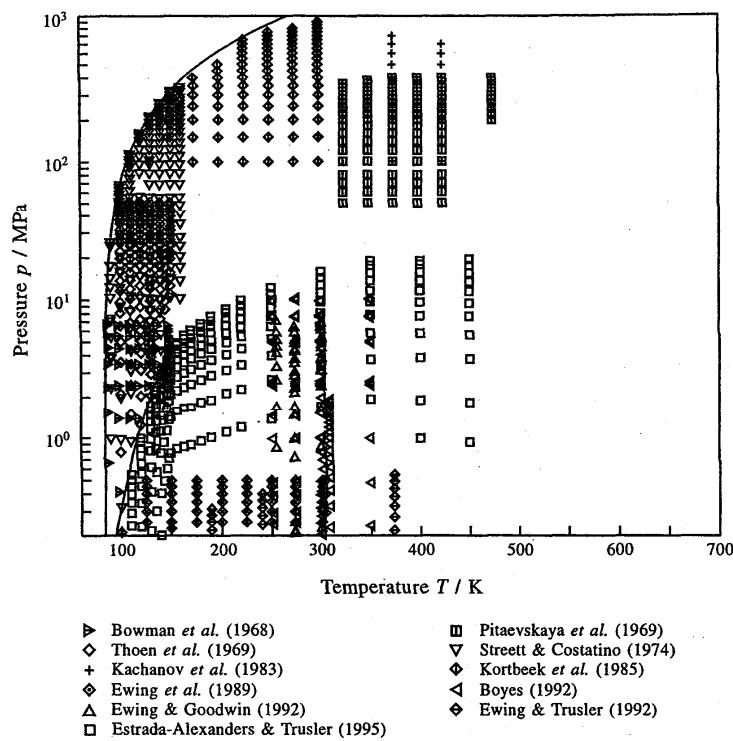
FIG. 10. Distribution of the experimental speed of sound data used to establish the residual part of the new equation of state, Eq. (4.1), in a p-T diagram.
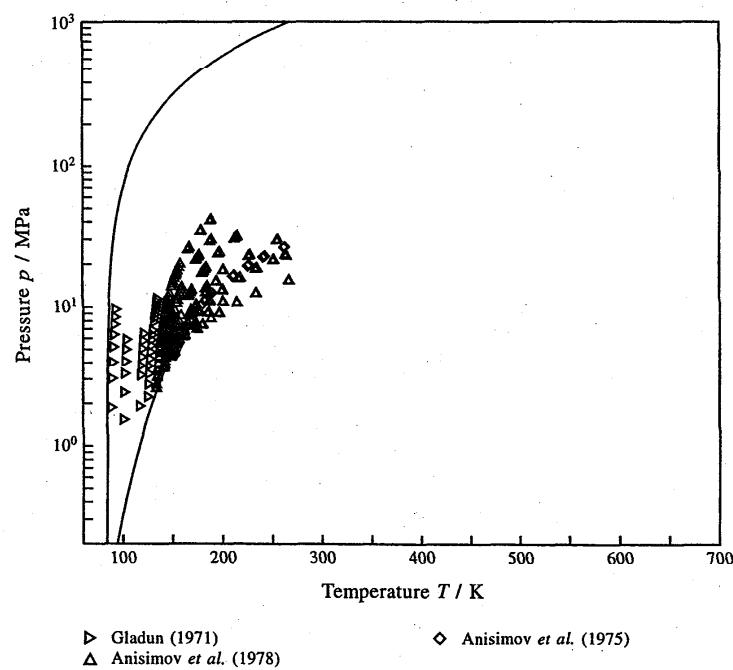
FIG. 11. Distribution of the experimental isochoric heat capacity data used to establish the residual part of the new equation of state, Eq. (4.1), in a p-T diagram.

TABLE 21. Summary of data sets for the second and third acoustic virial coefficients of argon. Uncertainty values were estimated by ourselves

Authors	Year	Number of data Total (β_a, γ_a)	Number of data Selected (β_a)	Temperature range/K	Uncertainty[a]
Colclough et al.	1979	1, —	—	273	$(1 \text{ cm}^3 \text{ mol}^{-1})$
Ewing et al.	1985	8, —	—	251–330	$(4 \text{ cm}^3 \text{ mol}^{-1})$
Ewing et al.	1986	1, —	—	273	$(0.2 \text{ cm}^3 \text{ mol}^{-1})$
Moldover & Trusler	1988	2, —	—	273–303	$(0.2 \text{ cm}^3 \text{ mol}^{-1})$
Moldover et al.	1988	1, —	—	273	$(0.2 \text{ cm}^3 \text{ mol}^{-1})$
Ewing et al.	1989	9, 9	5	100–304	$(0.2–0.5 \text{ cm}^3 \text{ mol}^{-1})$
Boyes	1992	7, —	—	275–350	$(0.2 \text{ cm}^3 \text{ mol}^{-1})$
Ewing & Goodwin	1992	4, —	4	255–300	$(0.2 \text{ cm}^3 \text{ mol}^{-1})$
Ewing & Trusler	1992	8, 8	8	90–373	$(0.2 \text{ cm}^3 \text{ mol}^{-1})$
Beckermann	1993	8, —	—	250–350	$(1 \text{ cm}^3 \text{ mol}^{-1})$
Estrada-Alexanders & Trusler	1995	21, 21	21	110–450	$(0.2 \text{ cm}^3 \text{ mol}^{-1})$

[a]Only for β_a data.

speed of sound measurements with spherical resonators the second acoustic virial coefficient β_a can be determined with high accuracy even at low temperatures, where the uncertainty of thermal virial coefficients determined from $p\rho T$ data increases strongly because of experimental difficulties. Therefore, reliable β_a data provide information on B and its first and second derivatives, which is very useful for the development of equations of state.

Table 21 gives detailed information on the data sets which are available for the acoustic virial coefficients of argon. With the exception of the value of Colclough et al. (1979) all values were determined from measurements with spherical resonators. While the β_a data of most authors confirm each other within $\pm 0.3 \text{ cm}^3 \text{mol}^{-1}$, systematic deviations of up to $500 \text{ cm}^6 \text{mol}^{-2}$ occur between the values for the third acoustic virial coefficient γ_a given by Estrada-Alexanders and Trusler (1995), Ewing et al. (1989) and Ewing and Trusler (1992). Therefore, only data for the second acoustic virial coefficient were selected.

3.3. Isochoric Heat Capacity

Table 22 summarizes the data sets which are available for the isochoric heat capacity of argon. The majority of these data describe the critical region. The most reliable measurements were made by Anisimov et al. (1975), (1978). The authors claim an uncertainty of $\pm 0.3\%$ for these data but because of the scatter of the data it is obvious that the uncertainty is at least $\pm 2\%$. Only the values for the homogeneous region were selected from these data sets; the data in the two-phase region were used only for comparison.

For temperatures from 110 to 450 K and densities up to half the critical density the gas phase is covered by the data of Estrada-Alexanders and Trusler (1996), which were determined from the speed of sound data of Estrada-Alexanders and Trusler (1995) by numerical integration. A critical analysis of all data sets shows that these values, in combination

with the original speed of sound data, are not consistent to the $p\rho T$ data of Gilgen et al. (1994a) on a very high level of accuracy. Due to the observed inconsistencies and to the fact that they are not primary data, the c_v data of Estrada-Alexanders and Trusler were only used for comparisons. Figure 11 shows the selected c_v data in a p-T diagram.

For temperatures up to 2000 K and pressures up to 2700 MPa, where no experimental results are available, Vrabec and Fischer (1996) calculated c_v data for a density of 1600 kg m^{-3} by molecular simulation. These data were used as an indicator for the course of the isochoric heat capacity at high temperatures and pressures. However, since it is not clear how accurately they describe the isochoric heat capacity of argon, only four of these values were used with low weights.

3.4. Isobaric Heat Capacity

Information on the data sets published for the isobaric heat capacity of argon is given in Table 23. Again, we did not use the c_p values calculated by Estrada-Alexanders and Trusler (1996) from the speed of sound data previously published by Estrada-Alexanders and Trusler (1995) due to the reasons which were discussed in Sec. 3.3. All other data sets show a large scatter ranging from $\pm 2\%$ to $\pm 10\%$. Although these data were not selected, they are represented by the new equation of state within their uncertainty.

3.5. Enthalpy Differences

Only two data sets are available for the enthalpy of argon, see Table 24. To avoid problems with different reference states, enthalpy data are considered as enthalpy differences $\Delta h = h_1(T_1, p_1) - h_2(T_2, p_2)$ in this work. Roebuck and Osterberg (1934) measured temperature and pressure on lines of

TABLE 22. Summary of data sets for the isochoric heat capacity of argon. Uncertainty values were estimated by ourselves

Authors	Year	Number of data		Temperature range/K	Density range/(kg m^{-3})	Uncertainty
		Total	Selected			
Eucken	1916	5	—	87.9–92.2	1403	(10%)
Eucken & Hauck	1928	11	—	90.0–190	976–1389	(10%)
Walker	1956	113[a]	—	99.4–197	671–1327	(5%–15%)
Voronel et al.	1965	89	—	133–153	530–538	(10%)
Voronel & Chashkin	1967	153	—	139–154	504–666	(6%)
Gladun	1971	82	82	87.8–151	738–1393	(4%)
Voronel et al.	1973	191	—	136–152	531	(3%)
Anisimov et al.	1974	108	—	151–263	496–532	(3%)
Anisimov et al.	1975	152	57	84.1–263	295–693	(1.5%–3%)
Koval'chuk	1977	92[b]	—	148–151	458–632	(1%–2%)
Anisimov et al.	1978	507[b]	306	130–267	310–1022	(1%–3%)
Estrada-Alexanders & Trusler	1996	565[c]	—	110–450	1–272	(0.1%–0.3%)
Vrabec & Fischer	1996	7[d]	4	200–2000	1600	(3%)

[a]Densities recalculated by evaluating the liquid density equation, Eq. (2.10), for the saturation temperatures given by Walker (1956).
[b]For every experimental c_v value, Koval'chuk (1977) gives two measured temperatures $\{c_{v,\exp}=[\Delta u_{\exp}/(T_2-T_1)]_v\}$. The article of Anisimov et al. (1978) contains the same data but here the measured c_v values are related to mean temperatures.
[c]Data calculated from measured speeds of sound.
[d]Not determined by experiment, but by molecular simulation [Lennard–Jones potential of the form (12-6) with $\sigma=3.3947$ Å and $\varepsilon/k=117.113$ K].

constant enthalpy. With the pressure correction given by Roebuck and Osterberg (1940), the data were interpreted as states with $\Delta h=0$.

The data sets of Roebuck and Osterberg (1934) and Kim (1974) were always represented within their scatter of about $\pm1\%$ by preliminary equations of state, since the region described by the data is also covered by accurate $p\rho T$ and speed of sound data. Hence we did not use the enthalpy data for the development of the new equation of state.

TABLE 23. Summary of data sets for the isobaric heat capacity of argon

Authors	Year	Number of data	Temperature range/K	Pressure range/MPa
Heuse	1919	2	93.2–288	0.1
Walker	1956	204	92.6–176	1.0–9.1
Lestz	1963	14[a]	273–304	0.1–1.2
Kim	1974	209	116–378	2.0–14
Shul'ga et al.	1985	48	87.3–144	0.3–39
Roder et al.	1989	232	113–324	0.6–68
Perkins et al.	1991	84	103–324	0.3–11
Baba et al.	1992	33	323–423	5.0–21
Estrada-Alexanders & Trusler	1996	565[a]	110–450	0.02–27

[a]Data calculated from measured speeds of sound.

3.6. Throttling Coefficients

Table 25 summarizes the data sets for the Joule–Thomson coefficient $\mu=(\partial T/\partial p)_h$ and the isothermal throttling coefficient $\delta_T=(\partial h/\partial p)_T$ of argon. Roebuck and Osterberg (1934) and Kim (1974) derived values for the throttling coefficients from the enthalpy data published in the same paper (cf. Sec. 3.5), but these data are much less accurate than the original experimental results (scatter and systematic deviations of about $\pm5\%-\pm10\%$). The uncertainty of the data published by Strakey (1970) is estimated to be $\pm3\%$ in most cases. The data for the isothermal throttling coefficient by Ishkin and Rogovaya (1957) deviate systematically from the data of Kim (1974) by about -5%, which are more consistent with data for other properties. For the same reason as for the enthalpy data (see Sec. 3.5), no data for the throttling coefficients were used to develop the new equation of state.

TABLE 24. Summary of data sets for the enthalpy of argon

Authors	Year	Number of data	Temperature range/K	Pressure range/MPa
Roebuck & Osterberg	1934	252	122–573	0.1–21
Kim	1974	276	123–378	0–14

TABLE 25. Summary of data sets for the Joule–Thomson coefficient μ and the isothermal throttling coefficient δ_T of argon

Authors	Year	Property	Number of data	Temperature range/K	Pressure range/MPa
Roebuck & Osterberg	1934	μ	134	103–573	0.1–20
Ishkin & Rogovaya	1957	δ_T	54	133–299	0.3–4.7
Strakey	1970	μ	88	153–383	0.6–19
Kim	1974	μ	12	122	1.7–14
		δ_T	76	139–348	0.01–14

4. The New Fundamental Equation of State

The new equation of state for argon is an empirical description of the Helmholtz free energy. For the development of such empirical formulations, the application of linear optimization procedures and nonlinear multiproperty fitting algorithms is state-of-the-art. The details of this strategy were extensively discussed, e.g., by Setzmann and Wagner (1989), (1991). Due to the high demands regarding the representation of highly accurate speed of sound data, a new nonlinear optimization procedure had to be used for the first time during the development of our new equation of state for argon. This nonlinear regression analysis will be presented and explained in detail in a separate paper [Tegeler et al. (1999)]. Therefore, only some fundamentals and a brief description of the procedure which was used to develop the new formulation will be given in Secs. 4.1, 4.2, 4.3, and 4.4.

4.1. Thermodynamic Properties Derived from the Helmholtz Energy

The equation of state described in this paper is explicit in the Helmholtz energy A with the two independent variables density ρ and temperature T. The dimensionless Helmholtz energy $\alpha = A/(RT)$ is commonly split into a part α^o which represents the properties of the ideal gas at given T and ρ and a part α^r which takes into account the residual fluid behavior. This convention can be written as

$$\alpha(\delta,\tau) = \alpha^o(\delta,\tau) + \alpha^r(\delta,\tau), \qquad (4.1)$$

where $\delta = \rho/\rho_c$ is the reduced density and $\tau = T_c/T$ is the inverse reduced temperature. Both the density ρ and the temperature T are reduced with their critical values, ρ_c and T_c, respectively.

Since the Helmholtz energy as a function of density and temperature is one of the four fundamental forms of an equation of state, all thermodynamic properties of a pure substance can be obtained by combining derivatives of Eq. (4.1). Table 26 gives the relations between Eq. (4.1) and its derivatives and the thermodynamic properties considered in this paper. At a given temperature, the vapor pressure and the densities of the coexisting phases can be determined by simultaneous solution of the equations:

$$\frac{p_s}{RT\rho'} = 1 + \delta'\,\alpha_\delta^r(\delta',\tau), \qquad (4.2a)$$

$$\frac{p_s}{RT\rho''} = 1 + \delta''\alpha_\delta^r(\delta'',\tau), \qquad (4.2b)$$

$$\frac{p_s}{RT}\left(\frac{1}{\rho''} - \frac{1}{\rho'}\right) - \ln\left(\frac{\rho'}{\rho''}\right) = \alpha^r(\delta',\tau) - \alpha^r(\delta'',\tau). \qquad (4.2c)$$

These equations represent the phase equilibrium conditions, i.e., the equality of pressure, temperature and specific Gibbs energy (Maxwell criterion) in the coexisting phases.

4.2. The Equation for the Helmholtz Energy of the Ideal Gas

The Helmholtz energy of the ideal gas is given by

$$A^o(\rho,T) = h^o(T) - RT - Ts^o(\rho,T). \qquad (4.3)$$

The enthalpy h^o of the ideal gas is a function of temperature only, and the entropy s^o of the ideal gas depends on temperature and density. Both properties can be calculated if an equation for $c_p^o(T)$ is known. When c_p^o is inserted into the expression for $h^o(T)$ and $s^o(\rho,T)$ in Eq. (4.3) one obtains

$$A^o(\rho,T) = \left(\int_{T_0}^T c_p^o\,dT + h_0^o\right) - RT - T$$
$$\times\left[\int_{T_0}^T \frac{c_p^o - R}{T}\,dT - R\ln\left(\frac{\rho}{\rho_0^o}\right) + s_0^o\right], \qquad (4.4)$$

where all variables with the index "0" refer to an arbitrary reference state. Usually the enthalpy h_0^o and the entropy s_0^o are taken to be zero for $T_0 = 298.15$ K, $p_0 = 0.101\,325$ MPa and the corresponding density $\rho_0 = p_0/(RT_0)$.

For the temperatures considered in this work, only the translational contribution to the ideal-gas heat capacity of argon, $c_{p,tr}^o = 2.5R$, has to be taken into account:

$$c_p^o = 0.520\,333\,3\ \text{kJ kg}^{-1}\,\text{K}^{-1}. \qquad (4.5)$$

Since the characteristic temperature of the first excited electronic state is about 135 000 K [Kelly (1987)] for argon, the contribution of electronic excitation to c_p^o is only 0.01% even at a temperature of 10 000 K. Hence, for the present work this effect is negligible.

From Eqs. (4.4) and (4.5) the expression for the ideal-gas part of the Helmholtz energy α^o can be derived easily:

$$\alpha^o = \ln(\delta) + a_1^o + a_2^o\tau + 1.5\cdot\ln(\tau), \qquad (4.6)$$

with $a_1^o = 8.316\,662\,43$ and $a_2^o = -4.946\,511\,64$. The coefficients a_1^o and a_2^o were adjusted to give zero for the ideal-gas enthalpy at $T_0 = 298.15$ K and the ideal-gas entropy at $T_0 = 298.15$ K and $p_0 = 0.101\,325$ MPa. In Table 27, all derivatives of the ideal-gas part α^o required for the calculation of thermodynamic properties are explicitly given.

TABLE 26. Relations of thermodynamic properties to the dimensionless Helmholtz function α consisting of α^o and α^r, see Eq. (4.1)

Property and common thermodynamic definiton	Relation to the reduced Helmholtz energy α and its derivatives[a]
Pressure $p(T,\rho) = -(\partial A/\partial v)_T$	$\dfrac{p(\delta,\tau)}{\rho RT} = 1 + \delta\alpha_\delta^r$
Entropy $s(T,\rho) = -(\partial A/\partial T)_v$	$\dfrac{s(\delta,\tau)}{R} = \tau(\alpha_\tau^o + \alpha_\tau^r) - \alpha^o - \alpha^r$
Internal energy $u(T,\rho) = A - T(\partial A/\partial T)_v$	$\dfrac{u(\delta,\tau)}{RT} = \tau(\alpha_\tau^o + \alpha_\tau^r)$
isochoric heat capacity $c_v(T,\rho) = (\partial u/\partial T)_v$	$\dfrac{c_v(\delta,\tau)}{R} = -\tau^2(\alpha_{\tau\tau}^o + \alpha_{\tau\tau}^r)$
Enthalpy $h(T,p) = A - T(\partial A/\partial T)_v$ $\qquad - v(\partial A/\partial v)_T$	$\dfrac{h(\delta,\tau)}{RT} = 1 + \tau(\alpha_\tau^o + \alpha_\tau^r) + \delta\alpha_\delta^r$
Isobaric heat capacity $c_p(T,p) = (\partial h/\partial T)_p$	$\dfrac{c_p(\delta,\tau)}{R} = -\tau^2(\alpha_{\tau\tau}^o + \alpha_{\tau\tau}^r) + \dfrac{(1 + \delta\alpha_\delta^r - \delta\tau\alpha_{\delta\tau}^r)^2}{1 + 2\delta\alpha_\delta^r + \delta^2\alpha_{\delta\delta}^r}$
Saturated liquid heat capacity $c_\sigma(T) = (\partial h/\partial T)_p + T(\partial p/\partial T)_v$ $\qquad \cdot(\mathrm{d}p_s/\mathrm{d}T)/(\partial p/\partial v)_T\|_{v=v'}$	$\dfrac{c_\sigma(\tau)}{R} = -\tau^2(\alpha_{\tau\tau}^o + \alpha_{\tau\tau}^r) + \dfrac{1 + \delta\alpha_\delta^r - \delta\tau\alpha_{\delta\tau}^r}{1 + 2\delta\alpha_\delta^r + \delta^2\alpha_{\delta\delta}^r}$ $\qquad \cdot\left[(1 + \delta\alpha_\delta^r - \delta\tau\alpha_{\delta\tau}^r) - \dfrac{\rho_c}{R\delta}\dfrac{\mathrm{d}p_s}{\mathrm{d}T}\right]$
Speed of sound $w(T,p) = \sqrt{(\partial p/\partial\rho)_s}$	$\dfrac{w^2(\delta,\tau)}{RT} = 1 + 2\delta\alpha_\delta^r + \delta^2\alpha_{\delta\delta}^r - \dfrac{(1 + \delta\alpha_\delta^r - \delta\tau\alpha_{\delta\tau}^r)^2}{\tau^2(\alpha_{\tau\tau}^o + \alpha_{\tau\tau}^r)}$
Joule–Thomson coefficient $\mu(T,p) = (\partial T/\partial p)_h$	$\mu R\rho = \dfrac{-(\delta\alpha_\delta^r + \delta^2\alpha_{\delta\delta}^r + \delta\tau\alpha_{\delta\tau}^r)}{(1 + \delta\alpha_\delta^r - \delta\tau\alpha_{\delta\tau}^r)^2 - \tau^2(\alpha_{\tau\tau}^o + \alpha_{\tau\tau}^r)(1 + 2\delta\alpha_\delta^r + \delta^2\alpha_{\delta\delta}^r)}$
Isothermal throttling coefficient $\delta_T(T,p) = (\partial h/\partial p)_T$	$\delta_T\rho = 1 - \dfrac{1 + \delta\alpha_\delta^r - \delta\tau\alpha_{\delta\tau}^r}{1 + 2\delta\alpha_\delta^r + \delta^2\alpha_{\delta\delta}^r}$
Second acoustic virial coefficient[b] $\beta_a(T) = \lim_{\rho\to 0}\{\partial[w^2/(\kappa^o RT)]/\partial\rho\}_T$	$\beta_a(\tau)\rho_c = \lim_{\delta\to 0}\left[2\alpha_\delta^r - 2\dfrac{\kappa^o - 1}{\kappa^o}\tau\alpha_{\delta\tau}^r + \dfrac{(\kappa^o - 1)^2}{\kappa^o}\tau^2\alpha_{\delta\tau\tau}^r\right]$
Second thermal virial coefficient $B(T) = \lim_{\rho\to 0}\{\partial[p/(\rho RT)]/\partial\rho\}_T$	$B(\tau)\rho_c = \lim_{\delta\to 0}\alpha_\delta^r(\delta,\tau)$
Third thermal virial coefficient $C(T) = \tfrac{1}{2}\lim_{\rho\to 0}\{\partial^2[p/(\rho RT)]/\partial\rho^2\}_T$	$C(\tau)\rho_c^2 = \lim_{\delta\to 0}\alpha_{\delta\delta}^r(\delta,\tau)$

[a]$\alpha_\delta = [\partial\alpha/\partial\delta]_\tau$, $\alpha_{\delta\delta} = [\partial^2\alpha/\partial\delta^2]_\tau$, $\alpha_\tau = [\partial\alpha/\partial\tau]_\delta$, $\alpha_{\tau\tau} = [\partial^2\alpha/\partial\tau^2]_\delta$, $\alpha_{\delta\tau} = [\partial^2\alpha/\partial\delta\partial\tau]$, and $\alpha_{\delta\tau\tau} = [\partial^3\alpha/\partial\delta\partial\tau^2]$.
[b]$\kappa^o = c_p^o/c_v^o = 5/3$ (isentropic coefficient of argon in the ideal gas state).

4.3. The Equation for the Residual Part of the Helmholtz Energy

While statistical thermodynamics can predict the behavior of fluids in the ideal-gas state with high accuracy, no physically founded equation is known which describes accurately the real thermodynamic behavior of fluids in the whole fluid region. Thus, for this purpose an equation for the residual fluid behavior, in this case for the residual part of the Helmholtz energy α^r, has to be determined in an empirical way. Since the Helmholtz energy itself is not accessible to direct

TABLE 27. The ideal-gas part of the dimensionless Helmholtz function α^o and its derivatives[a]

$\alpha^o = \ln\delta + a_1^o + a_2^o\tau + 1.5\ln\tau$
$\alpha_\delta^o = 1/\delta + 0 + 0 + 0$
$\alpha_{\delta\delta}^o = -1/\delta^2 + 0 + 0 + 0$
$\alpha_{\delta\tau}^o = 0 + 0 + 0 + 0$
$\alpha_\tau^o = 0 + 0 + a_2^o + 1.5/\tau$
$\alpha_{\tau\tau}^o = 0 + 0 + 0 - 1.5/\tau^2$

[a]$\alpha_\delta^o = [\partial\alpha^o/\partial\delta]_\tau$, $\alpha_{\delta\delta}^o = [\partial^2\alpha^o/\partial\delta^2]_\tau$, $\alpha_\tau^o = [\partial\alpha^o/\partial\tau]_\delta$, $\alpha_{\tau\tau}^o = [\partial^2\alpha^o/\partial\tau^2]_\delta$, and $\alpha_{\delta\tau}^o = [\partial^2\alpha^o/\partial\delta\partial\tau]$.

measurements, it is necessary to determine a suitable mathematical structure and the fitted coefficients from properties for which experimental data are available.

4.3.1. Fitting an Equation for α^r to Data

If a certain functional form has been selected for $\alpha^r(\delta,\tau,\bar{n})$, data for J different properties z_j (e.g., pressure p, speed of sound $w,\ldots$) can be used to determine the unknown coefficients n_i (expressed as vector $\bar{n}$) by minimizing the following sum of squares:

$$\chi^2 = \sum_{j=1}^{J} \chi_j^2 = \sum_{j=1}^{J} \sum_{m=1}^{M_j} \left[\frac{[z_{\exp} - z_{\text{calc}}(x_{\exp},y_{\exp},\bar{n})]^2}{\sigma_{\exp}^2} \right]_{j,m},$$

(4.7)

where M_j is the number of data points used for the jth property, $z_{\exp}$ is the experimental value for any property z and z_{calc} is the value for the property calculated from the equation for α with the parameter vector $\bar{n}$ at $x_{\exp}$ and $y_{\exp}$. The measured independent variables x and y may vary for the different properties of z, but usually one of them corresponds to temperature T, while the other corresponds to density ρ or pressure p [e.g., $p(T,\rho)$ or $w(T,p)$]. The variance $\sigma_{\exp}^2$ represents the total uncertainty of a single data point, which can be calculated according to the Gaussian error propagation formula:

$$\sigma_{\exp}^2 = \left(\frac{\partial \Delta z}{\partial x}\right)_{y,z}^2 \sigma_x^2 + \left(\frac{\partial \Delta z}{\partial y}\right)_{x,z}^2 \sigma_y^2 + \left(\frac{\partial \Delta z}{\partial z}\right)_{x,y}^2 \sigma_z^2,$$

(4.8)

where Δz is the residual $(z_{\exp} - z_{\text{calc}})$ in Eq. (4.7) and σ_x, σ_y, and σ_z are the isolated uncertainties of the single variables x, y and z, respectively. The partial derivatives of Δz have to be calculated from a preliminary equation of state.

The determination of $\bar{n}$ by minimizing χ^2 for data of more than one property is called "multiproperty fitting." This problem leads to a linear system of normal equations if each of the properties z depends on the same independent variables as the function used (e.g., T and ρ for the Helmholtz energy) and if the relations between z and the function or its derivatives is linear for all properties considered. Data for such properties are called "linear data." For functions in terms of the Helmholtz energy, such properties are, e.g., $p(T,\rho)$ and $c_v(T,\rho)$, see Table 26. If one or both of the conditions are not fulfilled [e.g., for $h(T,p)$, $w(T,p)$, $c_p(T,p),\ldots$], more complicated and time consuming nonlinear algorithms have to be used to minimize the sum of squares, Eq. (4.7).

4.3.2. The Procedure for Optimizing the Mathematical Form of α^r

Since the functional form of an equation for the residual part of the Helmholtz energy is not known from the start, a suitable mathematical structure has to be established before any coefficients n_i can be fitted to the data. In the past, the structure of most correlation equations had been determined subjectively, based on the experience of the correlator or by

trial and error. To improve this situation, Wagner and coworkers developed different optimization strategies [Wagner (1974), Ewers and Wagner (1982), and Setzmann and Wagner (1989)] which introduce objective criteria for the selection of the mathematical structure.

For the development of the new equation of state for argon, highly accurate speed of sound data (see Sec. 3.2.1) were available in large parts of the fluid region for the first time. Since all existing optimization procedures use linear algorithms and are hence restricted to linear data, nonlinear data such as speeds of sound can only be used if they are linearized by suitable methods. For the new, very precise speed of sound data the previously described cyclic process [see, e.g., Setzmann and Wagner (1991)] did not converge. This well known process consists of the steps linearizing nonlinear data with a preliminary equation of state, optimizing the functional form of a new preliminary equation of state, nonlinear fitting of its coefficients to the original data, and then repeated linearization of the data with the new preliminary equation of state. Detailed investigations showed that there are two reasons for the convergence problem: the loss of a part of the original experimental information caused by the linearization and the error introduced by the (imperfect) preliminary equation of state which is used for the linearization. Both effects became significant here for the first time because of the exceptionally high accuracy of the speed of sound data. As a consequence these data could not be represented within their uncertainties.

Therefore, Tegeler et al. (1999) developed a new nonlinear optimization procedure, which uses nonlinear data directly, i.e., without linearization. The new procedure is essentially a nonlinear regression analysis, similar to the one which is incorporated in the linear optimization procedure of Setzmann and Wagner (1989), OPTIM. Based on the experience that a simple regression analysis does not provide sufficient flexibility for complex optimization problems, the nonlinear regression analysis was reembedded in OPTIM to obtain a more powerful tool for the nonlinear optimization of equations of state. Due to the unavoidable use of nonlinear algorithms for the determination of sums of squares the nonlinear realization of OPTIM is too time consuming for the development of wide-range fundamental equations despite growing computing speeds. Thus, the following procedure was used:

(i) First of all we focused on the region which is covered by the highly accurate speed of sound data ($T \leq 450$ K, $\rho \leq 0.5\rho_c$). With the nonlinear optimization procedure, a simple equation of state has been developed which represents (almost) all data in this low-density region within their uncertainties. Since this optimization problem is much less complex than the development of a wide-range equation of state the nonlinear version of OPTIM could be applied with reasonable computing times.

(ii) In the next step the whole fluid region was investigated and preliminary wide-range equations of state were estab-

TABLE 28. Summary of the selected data used in the linear optimization procedure and in the nonlinear regression analysis

Property	For details see	Linear optimization procedure	Nonlinear regr. analysis
$p(\rho,T)$	Table 14	1472	1472
$p(\rho,T)$	Sec. 5.4.1	33[a]	33
$p_s(\rho',T)$		179[b]	—
$p_s(\rho'',T)$		179[b]	—
Maxwell criterion		179[b]	—
$p_s(T)$	Table 7	—	47
$\rho'(T)$	Table 8	—	27
$\rho''(T)$	Table 9	—	48
$B(T)$	Table 17	67	67
$C(T)$	Table 17	48	48
$\beta_a(T)$	Table 21	38	38
$c_v(\rho,T)$	Table 22	449	449
$c_v(\rho,T)$	Sec. 4.3.2	317[a]	—
$(\partial c_v/\partial T)_\rho$	Sec. 5.2.3	58[a]	58[a]
$w(\rho^p,T,\gamma_1^p,\gamma_2^p,\gamma_3^p)$	Table 19	619[c]	—
$w(\rho^p,T,\gamma^p)$	Table 19	612[d]	—
$w(\rho,T)$	Table 19	—	1231
$w'(\rho^p,T,\gamma^p)$	Table 11	49[d]	—
$w'(T)$	Table 11	—	49
$w''(\rho^p,T,\gamma^p)$	Table 11	50[d]	—
$w''(T)$	Table 11	—	50
$\Delta u(\rho,T)$	Sec. 5.4.1	33	33

[a]Auxiliary data calculated from preliminary equations of state.
[b]Linearized solution of the Maxwell criterion with data calculated from the auxiliary Eqs. (2.9)–(2.11); see e.g., Wagner (1972).
[c]Linearized data in the low density region; see Sec. 4.3.2.
[d]Linearized data; see Setzmann and Wagner (1991).

TABLE 29. Parameters of the modified Gaussian terms in the bank of terms, Eq. (4.10) ($\eta_i=20$ and $\varepsilon_i=1$ for $1 \le i \le 48$)

i	d_i	t_i	β_i	γ_i	i	d_i	t_i	β_i	γ_i
1	1	0	250	1.11	25	1	0	300	1.17
2	1	1	250	1.11	26	1	1	300	1.17
3	1	2	250	1.11	27	1	2	300	1.17
4	1	3	250	1.11	28	1	3	300	1.17
5	2	0	250	1.11	29	2	0	300	1.17
6	2	1	250	1.11	30	2	1	300	1.17
7	2	2	250	1.11	31	2	2	300	1.17
8	2	3	250	1.11	32	2	3	300	1.17
9	3	0	250	1.11	33	3	0	300	1.17
10	3	1	250	1.11	34	3	1	300	1.17
11	3	2	250	1.11	35	3	2	300	1.17
12	3	3	250	1.11	36	3	3	300	1.17
13	1	0	275	1.14	37	1	0	325	1.20
14	1	1	275	1.14	38	1	1	325	1.20
15	1	2	275	1.14	39	1	2	325	1.20
16	1	3	275	1.14	40	1	3	325	1.20
17	2	0	275	1.14	41	2	0	325	1.20
18	2	1	275	1.14	42	2	1	325	1.20
19	2	2	275	1.14	43	2	2	325	1.20
20	2	3	275	1.14	44	2	3	325	1.20
21	3	0	275	1.14	45	3	0	225	1.11
22	3	1	275	1.14	46	3	1	225	1.11
23	3	2	275	1.14	47	3	2	225	1.11
24	3	3	275	1.14	48	3	3	225	1.11

lished using the linear version of OPTIM. Thus, the nonlinear data had to be considered in a linearized form. While the common cyclic process has been applied to most of the nonlinear data with the linearizations explained, e.g., by Setzmann and Wagner (1991), we used a different procedure for the highly accurate speed of sound data in the low-density region. To make use of the high accuracy of the "low-density equation" we linearized the highly accurate speed of sound data with the low-density equation. In this way, the error introduced by the linearization could be minimized. Moreover, we used a new linearization method, where speeds of sound are linearized as

$$\frac{w^2}{RT} = 1 + 2\delta\alpha_\delta^r + \delta^2\alpha_{\delta\delta}^r + \gamma_1^p + \gamma_2^p\delta\alpha_\delta^r - \gamma_3^p\delta\tau\alpha_{\delta\tau}^r,$$

(4.9)

with the precorrelation factors

$$\gamma_1^p = \frac{1}{-\tau^2(\alpha_{\tau\tau}^o + \alpha_{\tau\tau}^r)}, \quad \gamma_2^p = \frac{2+\delta\alpha_\delta^r}{-\tau^2(\alpha_{\tau\tau}^o + \phi_{\tau\tau}^r)},$$

$$\gamma_3^p = \frac{2+2\delta\alpha_\delta^r - \delta\tau\alpha_{\delta\tau}^r}{-\tau^2(\alpha_{\tau\tau}^o + \alpha_{\tau\tau}^r)}.$$

Thus, each of the very accurate data points $w(T,p)$ was linearized by calculating values for the corresponding density ρ

and for γ_1^p, γ_2^p and γ_3^p from the equation for the low-density region. In contrast to the common linearization method [see Setzmann and Wagner (1991)], which has still been applied to less accurate speed of sound data, the use of Eq. (4.9) preserves some of the information on $\alpha_{\delta\tau}^r$ which is included in the original speed of sound data. The representation of the speed of sound data was further improved by consideration of 317 data points for the isochoric heat capacity c_v, which were calculated from the equation of state for the low-density region.

(iii) Finally, the new equation of state was obtained in a run of the new nonlinear regression analysis. The best equation from the linear optimization procedure was used as a starting solution for this regression run. As a result, the quality of the representation of all nonlinear data was improved further.

4.4. The Data Sets Used and the Bank of Terms

The experimental data which were selected to establish the new equation of state have been presented in Secs. 2 and 3. Table 28 gives a brief summary of the data which were used in the linear optimization procedure and in the nonlinear regression analysis.

The bank of terms used for the optimization of the functional form of the final equation of state consisted of 650 terms and can be written as

TABLE 30. Coefficients and exponents of Eq. (4.11)

i	n_i	d_i	t_i	c_i	η_i	β_i	γ_i	ε_i
1	0.887 223 049 900 11×10⁻¹	1	0.00					
2	0.705 148 051 672 98	1	0.25					
3	−0.168 201 156 540 90×10¹	1	1.00					
4	−0.149 090 144 314 86	1	2.75					
5	−0.120 248 046 009 40	1	4.00					
6	−0.121 649 787 985 99	2	0.00					
7	0.400 359 336 267 52	2	0.25					
8	−0.271 360 626 991 29	2	0.75					
9	0.242 119 245 796 45	2	2.75					
10	0.578 895 831 855 70×10⁻²	3	0.00					
11	−0.410 973 356 153 41×10⁻¹	3	2.00					
12	0.247 107 615 416 14×10⁻¹	4	0.75					
13	−0.321 813 917 507 02	1	3.00	1				
14	0.332 300 176 957 94	1	3.50	1				
15	0.310 199 862 873 45×10⁻¹	3	1.00	1				
16	−0.307 770 860 024 37×10⁻¹	4	2.00	1				
17	0.938 911 374 195 81×10⁻¹	4	4.00	1				
18	−0.906 432 106 820 31×10⁻¹	5	3.00	1				
19	−0.457 783 492 766 54×10⁻³	7	0.00	1				
20	−0.826 597 290 251 97×10⁻⁴	10	0.50	1				
21	0.130 134 156 031 47×10⁻³	10	1.00	1				
22	−0.113 978 400 019 96×10⁻¹	2	1.00	2				
23	−0.244 551 699 605 35×10⁻¹	2	7.00	2				
24	−0.643 240 671 759 55×10⁻¹	4	5.00	2				
25	0.588 894 710 936 74×10⁻¹	4	6.00	2				
26	−0.649 335 521 129 65×10⁻³	8	6.00	2				
27	−0.138 898 621 584 35×10⁻¹	3	10.00	3				
28	0.404 898 392 969 10	5	13.00	3				
29	−0.386 125 195 947 49	5	14.00	3				
30	−0.188 171 423 322 33	6	11.00	3				
31	0.159 776 475 964 82	6	14.00	3				
32	0.539 855 185 138 56×10⁻¹	7	8.00	3				
33	−0.289 534 179 580 14×10⁻¹	7	14.00	3				
34	−0.130 254 133 813 84×10⁻¹	8	6.00	3				
35	0.289 486 967 757 78×10⁻²	9	7.00	3				
36	−0.226 471 343 047 96×10⁻²	5	24.00	4				
37	0.176 164 561 963 68×10⁻²	6	22.00	4				
38	0.585 524 544 827 74×10⁻²	2	3.00		20		1.11	1
39	−0.692 519 082 700 28	1	1.00		20	375		
40	0.153 154 900 305 16×10¹	2	0.00		20	300	1.17	1
41	−0.273 804 474 497 83×10⁻²	3	0.00		20	225	1.11	1

$R = 0.208\,133\,3$ kJ kg⁻¹ K⁻¹ $T_c = 150.687$ K $\rho_c = 535.6$ kg m⁻³

$$\alpha^r = \sum_{i=1}^{4} \sum_{j=0}^{20} n_{i,j} \delta^i \tau^{j/4} + e^{-\delta} \sum_{i=1}^{10} \sum_{j=0}^{10} n_{i,j} \delta^i \tau^{j/2}$$

$$+ e^{-\delta^2} \sum_{i=1}^{12} \sum_{j=1}^{12} n_{i,j} \delta^i \tau^j + e^{-\delta^3} \sum_{i=1}^{10} \sum_{j=4}^{14} n_{i,j} \delta^i \tau^j$$

$$+ e^{-\delta^4} \sum_{i=2}^{8} \sum_{j=2}^{15} n_{i,j} \delta^i \tau^{2j} + e^{-\delta^6} \sum_{i=3}^{10} \sum_{j=2}^{8} n_{i,j} \delta^i \tau^{2j}$$

$$+ \sum_{i=1}^{48} n_i \delta^{d_i} \tau^{t_i} e^{-\eta_i(\delta - \varepsilon_i)^2 - \beta_i(\delta - \gamma_i)^2}. \tag{4.10}$$

In view of the extrapolation behavior of the new equation of state, no terms with negative exponents for the inverse re-

duced temperature τ were introduced into the bank of terms. Such functions may cause unreasonable plots of the virial coefficients calculated from the equation of state at very high temperatures. In the region of very high densities the extrapolation behavior of the equation of state is dominated by the pure polynomial terms. Based on the experience that equations of state, which include polynomial terms with density exponents d_i greater than 4, tend to behave unreasonably when being extrapolated to high densities, we restricted the exponents of these terms to $d_i \leq 4$ [see also Span and Wagner (1997)]. The modified Gaussian terms [last sum in Eq. (4.10)] were originally introduced by Setzmann and Wagner (1991). The slightly changed parameters of these terms are given in Table 29.

TABLE 31. The residual part of the Helmholtz energy α^r and its derivatives[a]

$$\alpha^r = \sum_{i=1}^{12} n_i \delta^{d_i} \tau^{t_i} + \sum_{i=13}^{37} n_i \delta^{d_i} \tau^{t_i} e^{-\delta^{c_i}} + \sum_{i=38}^{41} n_i \delta^{d_i} \tau^{t_i} e^{-\eta_i(\delta-\varepsilon_i)^2 - \beta_i(\tau-\gamma_i)^2}$$

$$\alpha^r_\delta = \sum_{i=1}^{12} n_i d_i \delta^{d_i-1} \tau^{t_i} + \sum_{i=13}^{37} n_i e^{-\delta^{c_i}} [\delta^{d_i-1} \tau^{t_i}(d_i - c_i \delta^{c_i})] + \sum_{i=38}^{41} n_i \delta^{d_i} \tau^{t_i} e^{-\eta_i(\delta-\varepsilon_i)^2 - \beta_i(\tau-\gamma_i)^2} \left[\frac{d_i}{\delta} - 2\eta_i(\delta-\varepsilon_i) \right]$$

$$\alpha^r_{\delta\delta} = \sum_{i=1}^{12} n_i d_i (d_i-1) \delta^{d_i-2} \tau^{t_i} + \sum_{i=13}^{37} n_i e^{-\delta^{c_i}} \{ \delta^{d_i-2} \tau^{t_i}[(d_i - c_i \delta^{c_i})(d_i - 1 - c_i \delta^{c_i}) - c_i^2 \delta^{c_i}] \} + \sum_{i=38}^{41} n_i \tau^{t_i} e^{-\eta_i(\delta-\varepsilon_i)^2 - \beta_i(\tau-\gamma_i)^2}$$

$$\cdot [-2\eta_i \delta^{d_i} + 4\eta_i^2 \delta^{d_i}(\delta-\varepsilon_i)^2 - 4d_i \eta_i \delta^{d_i-1}(\delta-\varepsilon_i) + d_i(d_i-1)\delta^{d_i-2}]$$

$$\alpha^r_\tau = \sum_{i=1}^{12} n_i t_i \delta^{d_i} \tau^{t_i-1} + \sum_{i=13}^{37} n_i t_i \delta^{d_i} \tau^{t_i-1} e^{-\delta^{c_i}} + \sum_{i=38}^{41} n_i \delta^{d_i} \tau^{t_i} e^{-\eta_i(\delta-\varepsilon_i)^2 - \beta_i(\tau-\gamma_i)^2} \left[\frac{t_i}{\tau} - 2\beta_i(\tau-\gamma_i) \right]$$

$$\alpha^r_{\tau\tau} = \sum_{i=1}^{12} n_i t_i (t_i-1) \delta^{d_i} \tau^{t_i-2} + \sum_{i=13}^{37} n_i t_i (t_i-1) \delta^{d_i} \tau^{t_i-2} e^{-\delta^{c_i}} + \sum_{i=38}^{41} n_i \delta^{d_i} \tau^{t_i} e^{-\eta_i(\delta-\varepsilon_i)^2 - \beta_i(\tau-\gamma_i)^2} \left[\left(\frac{t_i}{\tau} - 2\beta_i(\tau-\gamma_i) \right)^2 - \frac{t_i}{\tau^2} - 2\beta_i \right]$$

$$\alpha^r_{\delta\tau} = \sum_{i=1}^{12} n_i d_i t_i \delta^{d_i-1} \tau^{t_i-1} + \sum_{i=13}^{37} n_i e^{-\delta^{c_i}} \delta^{d_i-1} t_i \tau^{t_i-1}(d_i - c_i \delta^{c_i}) + \sum_{i=38}^{41} n_i \delta^{d_i} \tau^{t_i} e^{-\eta_i(\delta-\varepsilon_i)^2 - \beta_i(\tau-\gamma_i)^2} \left[\frac{d_i}{\delta} - 2\eta_i(\delta-\varepsilon_i) \right] \left[\frac{t_i}{\tau} - 2\beta_i(\tau-\gamma_i) \right]$$

$$\alpha^r_{\delta\tau\tau} = \sum_{i=1}^{12} n_i d_i t_i (t_i-1) \delta^{d_i-1} \tau^{t_i-2} + \sum_{i=13}^{37} n_i e^{-\delta^{c_i}} t_i (t_i-1) \tau^{t_i-2} \delta^{d_i-1}(d_i - c_i \delta^{c_i})$$

$$+ \sum_{i=38}^{41} n_i \delta^{d_i} \tau^{t_i} e^{-\eta_i(\delta-\varepsilon_i)^2 - \beta_i(\tau-\gamma_i)^2} \left[\left(\frac{t_i}{\tau} - 2\beta_i(\tau-\gamma_i) \right)^2 - \frac{t_i}{\tau^2} - 2\beta_i \right] \left[\frac{d_i}{\delta} - 2\eta_i(\delta-\varepsilon_i) \right]$$

[a] $\alpha^r_\delta = [\partial\alpha^r/\partial\delta]_\tau$, $\alpha^r_{\delta\delta} = [\partial^2\alpha^r/\partial\delta^2]_\tau$, $\alpha^r_\tau = [\partial\alpha^r/\partial\tau]_\delta$, $\alpha^r_{\tau\tau} = [\partial^2\alpha^r/\partial\tau^2]_\delta$, $\alpha^r_{\delta\tau} = [\partial^2\alpha^r/\partial\delta\partial\tau]$, and $\alpha^r_{\delta\tau\tau} = [\partial^3\alpha^r/\partial\delta\partial\tau^2]$.

4.5. The New Equation of State

Proceeding from the bank of terms defined by Eq. (4.10) the following combination of terms was obtained for the residual part of the Helmholtz energy by the procedure described in Sec. 4.3.2:

$$\alpha^r = \sum_{i=1}^{12} n_i \delta^{d_i} \tau^{t_i} + \sum_{i=13}^{37} n_i \delta^{d_i} \tau^{t_i} e^{-\delta^{c_i}}$$

$$+ \sum_{i=38}^{41} n_i \delta^{d_i} \tau^{t_i} e^{-\eta_i(\delta-\varepsilon_i)^2 - \beta_i(\tau-\gamma_i)^2}. \qquad (4.11)$$

The final values of the parameters were determined by the nonlinear regression analysis and are given in Table 30. The coefficients n_i resulted from a nonlinear fit which is included in this procedure.

The new equation of state for argon, Eq. (4.1), in combination with the formulation for α^o given in Eq. (4.6) and the formulation for α^r given in Eq. (4.11), was constrained to the critical parameters given in Sec. 2.2 and to the first and second partial derivatives of pressure with respect to density being zero at the critical point. It is valid for the entire fluid region covered by reliable experimental data, namely for

$$83.8058 \text{ K} \le T \le 700 \text{ K}$$

and

$$0 \text{ MPa} \le p \le 1000 \text{ MPa}.$$

Estimations for the uncertainty of Eq. (4.1) are given in Sec. 6 and the quality of the new equation of state is discussed in Sec. 5. The necessary derivatives of α^r are given in Table 31.

5. Comparison of the New Equation of State with Experimental Data and Other Equations of State

In this section, the quality of the new equation of state is discussed based on comparisons with selected experimental data. Most figures also show results of the equation of state published by Stewart and Jacobsen (1989), which is the most recent equation of state to compare with. The representation of thermodynamic properties in the critical region is discussed in Sec. 5.3. Additionally, the crossover equation of Tiesinga et al. (1994) is included in these comparisons. Since both equations are valid on the IPTS-68 temperature scale, temperatures were reconverted to the IPTS-68 scale before values were calculated from these equations.

5.1. Liquid–Vapor Phase Boundary

5.1.1. Thermal Properties

Figure 12 shows deviations between selected data for the vapor pressure, the saturated liquid and saturated vapor density and values calculated from Eq. (4.1). The additional lines correspond to values calculated from the auxiliary

O   Gilgen et al. (1994b)
□   This work (Table 10)

— — —   Aux. eqs. (see Sec. 2.6 to 2.8)
—·—·—   Stewart & Jacobsen (1989)
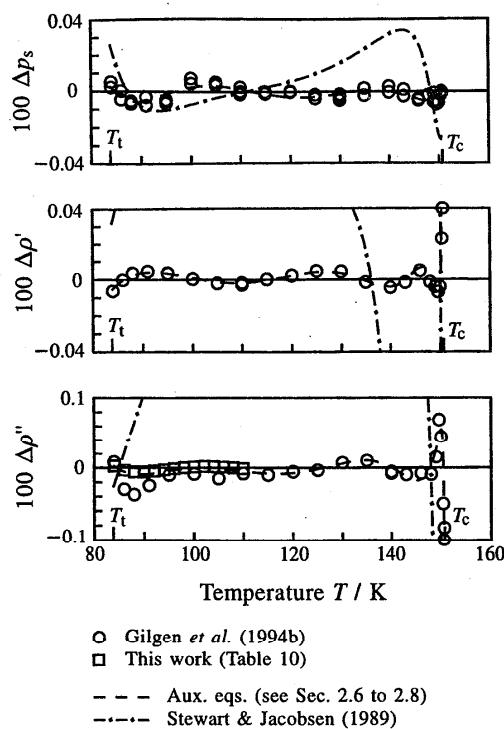
FIG. 12. Percentage deviations $\Delta y = (y_{exp} - y_{calc})/y_{exp}$ $(y = p_s, \rho', \rho'')$ of the selected thermal data at saturation from values calculated from Eq. (4.1). For temperatures below 110 K the saturated vapor-density data of Gilgen et al. (1994b) were not used and are plotted in this figure only for comparison. Values calculated from the auxiliary equations presented in Sec. 2 and from the equation of state of Stewart and Jacobsen (1989) are plotted for comparison.

◆ Galt (1948)   ⋏ Lim & Aziz (1967)
▷ van Itterbeek et al. (1959)   ◈ Fleury & Boon (1996)
■ van Dael (1962)   ◇ Thoen et al. (1969)
▽ van Dael et al. (1966)   ◉ Thoen et al. (1971)
O Aziz et al. (1967)   △ Radovskii (1963)
□ Blagoi et. al. (1967)

—·—·—   Stewart & Jacobsen (1989)
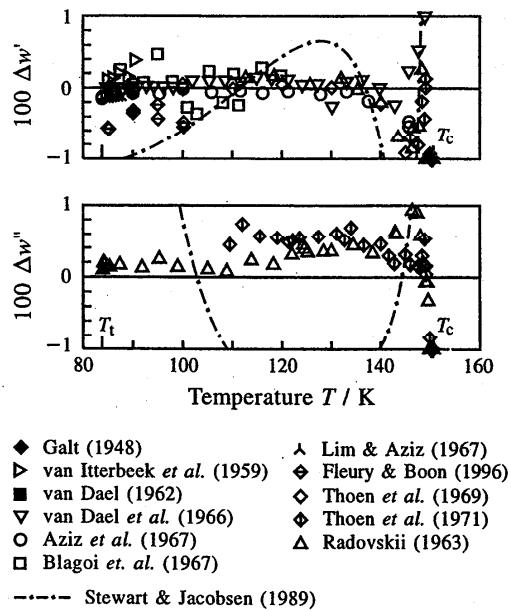
FIG. 13. Percentage deviations $\Delta y = (y_{exp} - y_{calc})/y_{exp}$ $(y = w', w'')$ of speed of sound data on the saturated-liquid and saturated-vapor line from values calculated from Eq. (4.1). Values calculated from the equation of state of Stewart and Jacobsen (1989) are plotted for comparison.

□   Eucken & Hauck (1928)
◇   Clusius (1936)
O   Walker (1956)
◆   Flubacher et al. (1961)
▷   Gladun (1971)

—·—·—   Stewart & Jacobsen (1989)
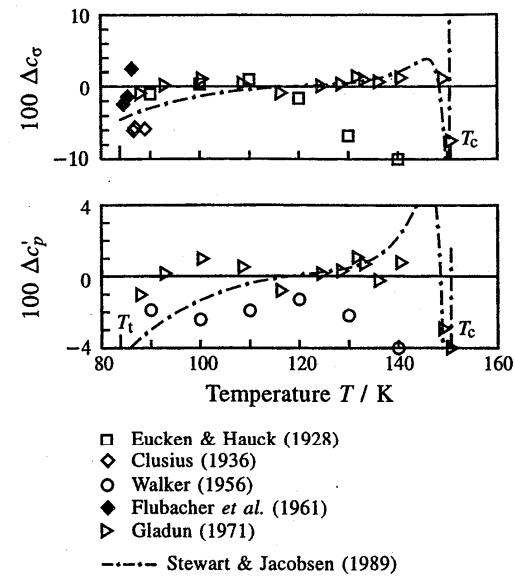
FIG. 14. Percentage deviations $\Delta y = (y_{exp} - y_{calc})/y_{exp}$ $(y = c_\sigma, c_p')$ of heat capacities on the saturated-liquid line from values calculated from Eq. (4.1). Values calculated from the equation of state of Stewart and Jacobsen (1989) are plotted for comparison.

equations given in Sec. 2 and to values calculated from the equation of state of Stewart and Jacobsen (1989).

Equation (4.1) represents the selected data far within their uncertainties. The deviations to the vapor-pressure data of Gilgen et al. (1994b) do not exceed ±0.01%. For temperatures below 150 K the same is true for the saturated liquid densities. The saturated vapor density data of Gilgen et al. were selected only for temperatures above 110 K, while at lower temperatures the saturated vapor density data determined in this work (see Sec. 2.8) were used. For $T \leqslant 149$ K the data are represented to within ±0.02%. For the saturated vapor density data of Gilgen et al. which were not used to establish Eq. (4.1) the greatest deviation occurs for the ρ'' data point at 88 K with $\Delta \rho'' = -0.038\%$. In this region, this

▼   Eucken (1916)
▲   Frank & Clusius (1939)
◆   Flubacher et al. (1961)
+   Kurilenok et al. (1973)
□   Kim (1974)

—·—·—   Stewart & Jacobsen (1989)
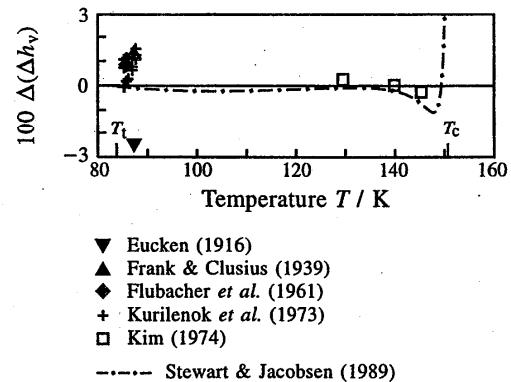
FIG. 15. Percentage deviations $\Delta(\Delta h_v) = (\Delta h_{v,exp} - \Delta h_{v,calc})/\Delta h_{v,exp}$ of experimental data for the enthalpy of vaporization from values calculated from Eq. (4.1). Values calculated from the equation of state of Stewart and Jacobsen (1989) are plotted for comparison.

FIG. 16. Percentage density deviations of highly accurate $p\rho T$ data from values calculated from Eq. (4.1). Values calculated from the equation of state of Stewart and Jacobsen (1989) are plotted for comparison.
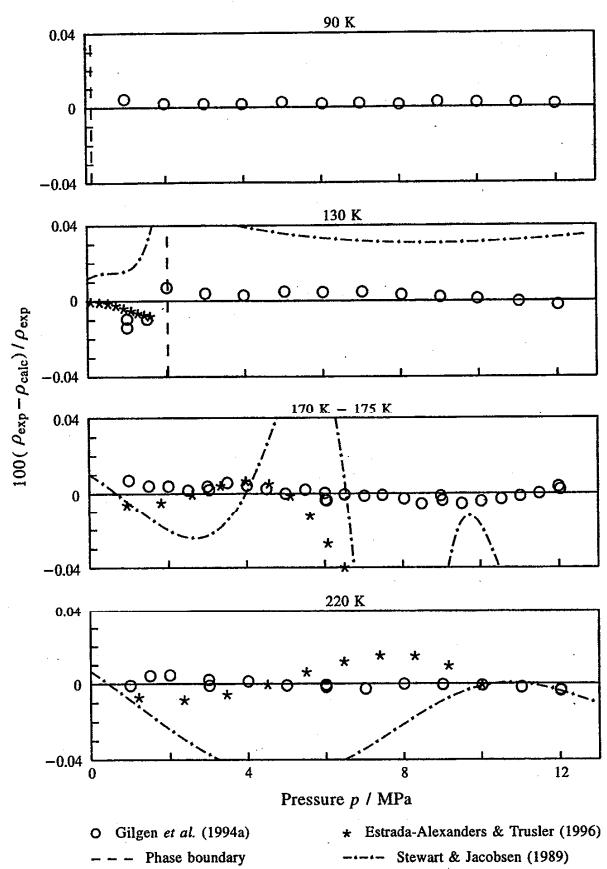
FIG. 17. Percentage density deviations of highly accurate $p\rho T$ data from values calculated from Eq. (4.1). Values calculated from the equation of state of Stewart and Jacobsen (1989) are plotted for comparison.

is still within the uncertainty of the data. With the exception of the vapor-pressure data for temperatures below 130 K the equation of Stewart and Jacobsen (1989) is not able to predict the selected data within their uncertainties.

5.1.2. Caloric Properties

Figure 13 gives a comparison between experimental speed of sound data on the liquid–vapor coexistence curve which were assigned to groups 1 and 2 and values calculated from Eq. (4.1). With the exception of the critical region, the data are represented by Eq. (4.1) without significant systematic deviations. Due to the high uncertainty of the speed of sound data on the saturated vapor line these data were only used with low weights in the development of the new equation of state. Since the speed of sound calculated from Eq. (4.1) is fixed by highly accurate speed of sound data in the gas phase (see Sec. 3.2.1), the positive systematic deviations shown in the lower diagram of Fig.13 are obviously caused by an offset in the data on the saturated vapor line.

The values calculated for w' from the equation of state of Stewart and Jacobsen (1989) differ by more than 1% from the reliable experimental data. For the description of speeds
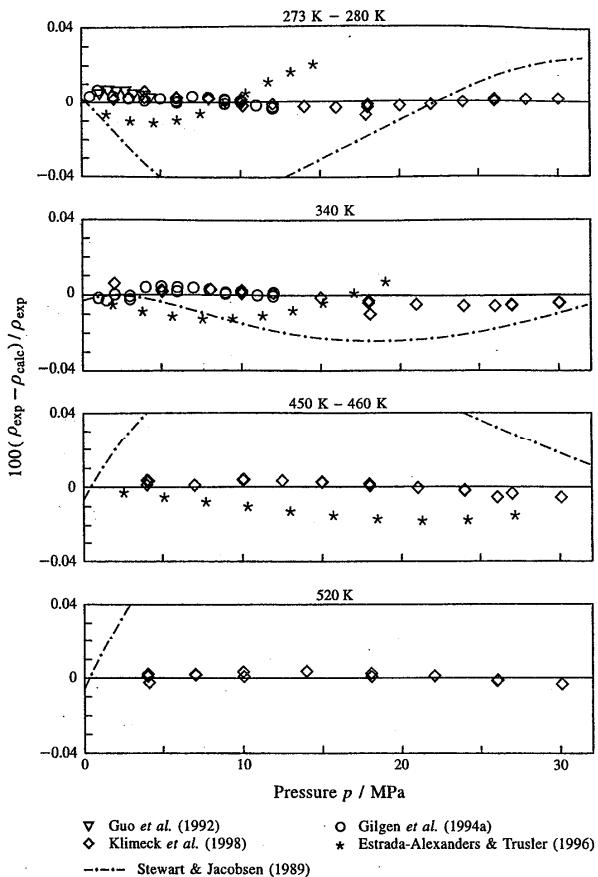
of sound in the saturated vapor this equation yields even less satisfactory results; close to the triple-point temperature deviations of more than 10% occur. Probably this behavior is connected to the unreasonable plot of the third virial coefficient calculated from the equation of Stewart and Jacobsen at low temperatures (see Sec. 5.2.1).

Figure 14 shows comparisons between experimental data for the heat capacities c_σ and c_p' on the saturated liquid line and values calculated from Eq. (4.1). Figure 15 shows the corresponding deviations for the enthalpy of evaporation Δh_v. These data were not used to establish the new equation of state and are represented within their large uncertainties both by Eq. (4.1) and by the equation of Stewart and Jacobsen (1989).

5.2. Single Phase Region

5.2.1. Thermal Properties

Figures 16 and 17 give comparisons between $p\rho T$ data sets which were assigned to group 1 and values calculated from Eq. (4.1). The plotted pressure and temperature range correspond to the region which is covered by the state-of-the-art measurements of Gilgen *et al.* (1994a) and Klimeck
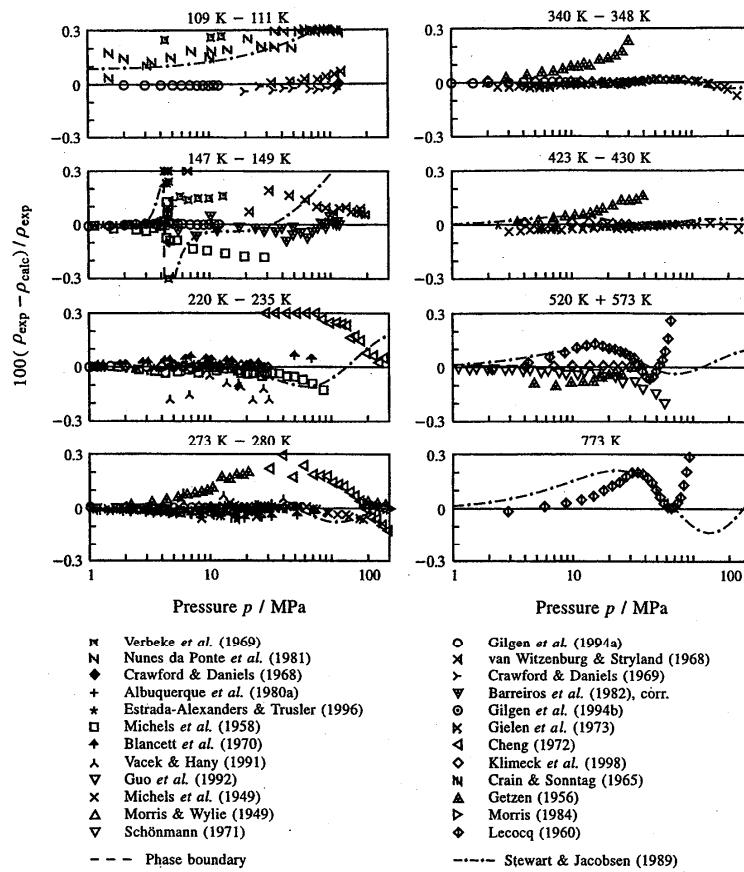
FIG. 18. Percentage density deviations of $p\rho T$ data assigned to groups 1 and 2 from values calculated from Eq. (4.1). Values calculated from the equation of state of Stewart and Jacobsen (1989) are plotted for comparison.
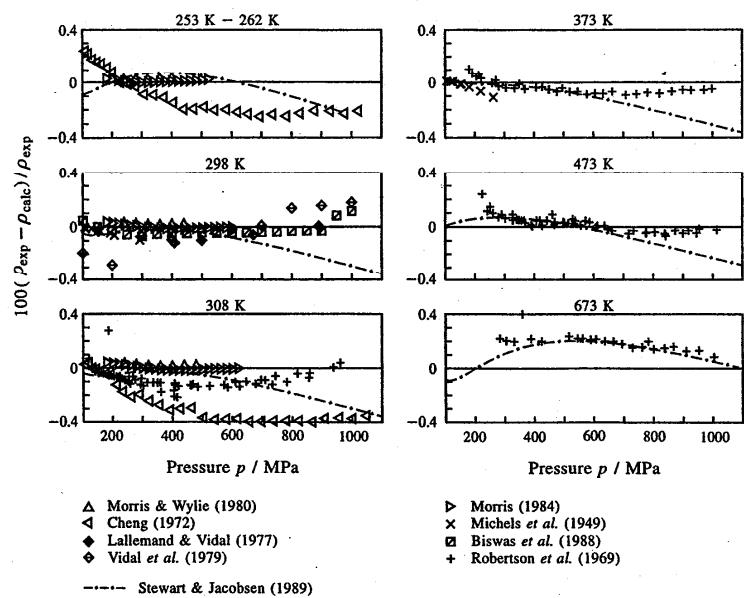
FIG. 19. Percentage density deviations of $p\rho T$ data in the high pressure range from values calculated from Eq. (4.1). Values calculated from the equation of state of Stewart and Jacobsen (1989) are plotted for comparison.

Temperature T / K

● This work (Table 16)   ⊕ Sevastyanov & Chernyavskaya (1987)
◆ Aziz & Slaman (1986)   ⊟ Aziz & Slaman (1990)

—·—·— Stewart & Jacobsen (1989)
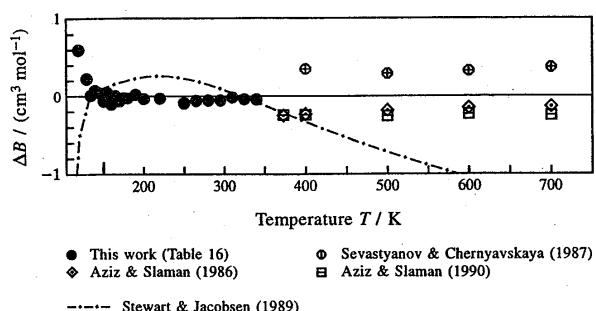
FIG. 20. Percentage deviations of the selected data for the second virial coefficient from values calculated from Eq. (4.1). Values calculated from the equation of state of Stewart and Jacobsen (1989) are plotted for comparison.

et al. (1998). The data of Gilgen *et al.* for temperatures up to 340 K and pressures up to 12 MPa are supplemented by the data of Klimeck *et al.*, which extend to 30 MPa for temperatures between 235 and 520 K. In this region the description of the $p\rho T$ surface is mainly based on these data sets. However, as discussed in Sec. 3.1.1, the data of Estrada Alexanders and Trusler (1996) were used in the gas phase for temperatures below 125 K. Equation (4.1) represents the data of Gilgen *et al.* and Klimeck *et al.* far within their uncertainties except in the low temperature gas region. Since the equation of Stewart and Jacobsen (1989) had no access to recent $p\rho T$ data, it is not surprising that the equation is not able to reproduce these data. The oscillating deviations between the values calculated from the equation of Stewart and Jacobsen and the experimental data increase to +0.1% in density at low temperatures in the liquid state and at temperatures above 400 K.

Figure 18 gives a representative view on the group 1 and 2 data sets for pressures up to 300 MPa. As mentioned in Sec. 3.1.1, at temperatures below 235 K and pressures above 12 MPa only the corrected data of Barreiros *et al.* (1982) were used to establish the new equation of state, Eq. (4.1). These

data are reproduced within their uncertainty which, despite the correction (see Sec. 3.1.1), ranges from ±0.1% to ±0.2% in density. When other $p\rho T$ data sets were taken into account on a trial basis the representation of the speed of sound data in this region became considerably worse. At temperatures between 273 and 473 K, Eq. (4.1) follows the $p\rho T$ data of Michels *et al.* (1949), which are confirmed by the data of Klimeck *et al.* (1998) within ±0.05% in the range of overlap. To enable the representation of the accurate data of Morris and Wylie (1980) and Morris (1984) at high pressures, a deviation of up to −0.1% in density had to be accepted for the data of Michels *et al.* (1949) at pressures above 100 MPa.

In the plotted pressure range the deviations between Eq. (4.1) and the equation of state of Stewart and Jacobsen (1989) do not exceed ±0.1% for temperatures between 250 and 450 K. These deviations increase at higher temperatures, where Stewart and Jacobsen tried to reproduce the data of Lecocq (1960). The plots for the isotherms at 520 and 573 K illustrate that this prevents the equation from reproducing the recent data of Klimeck *et al.* (1998). Therefore, the data set of Lecocq (1960) was not used in this work. The largest difference between these data and the values calculated from Eq. (4.1) occurs at 1226 K, the highest temperature measured by Lecocq, with a deviation of +0.6% in density.

Comparisons for $p\rho T$ data at pressures up to 1000 MPa are given in Fig. 19. In this region, the very accurate data of Morris and Wylie (1980) and Morris (1984) are represented by Eq. (4.1) to within ±0.04% in density. Unfortunately, these data are restricted to temperatures between 253 and 308 K at pressures up to 620 MPa. At higher pressures Eq. (4.1) follows the data of Biswas *et al.* (1988) on the 298 K isotherm, which can be reproduced within ±0.05% with the exception of the two last points. For the data of Robertson *et al.* (1969) systematic deviations of about +0.2% had to be accepted at the highest temperature (673 K). A better repre-

Temperature T / K

● This work (Table 16)

——— Eq. (4.1)

Temperature T / K

⊕ Sevastyanov & Chernyavskaya (1987)

—·—·— Stewart & Jacobsen (1989)
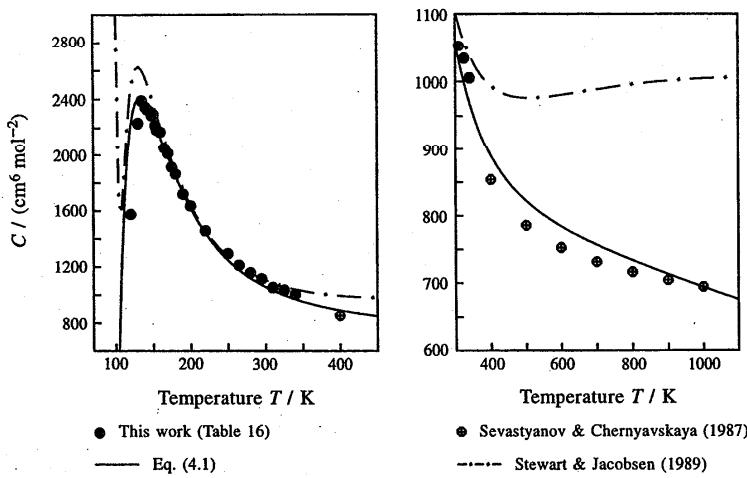
FIG. 21. Representation of the selected data for the third virial coefficient for temperatures up to 450 K and in the high temperature range. The plotted curves correspond to values calculated from Eq. (4.1) and from the equation of state of Stewart and Jacobsen (1989).
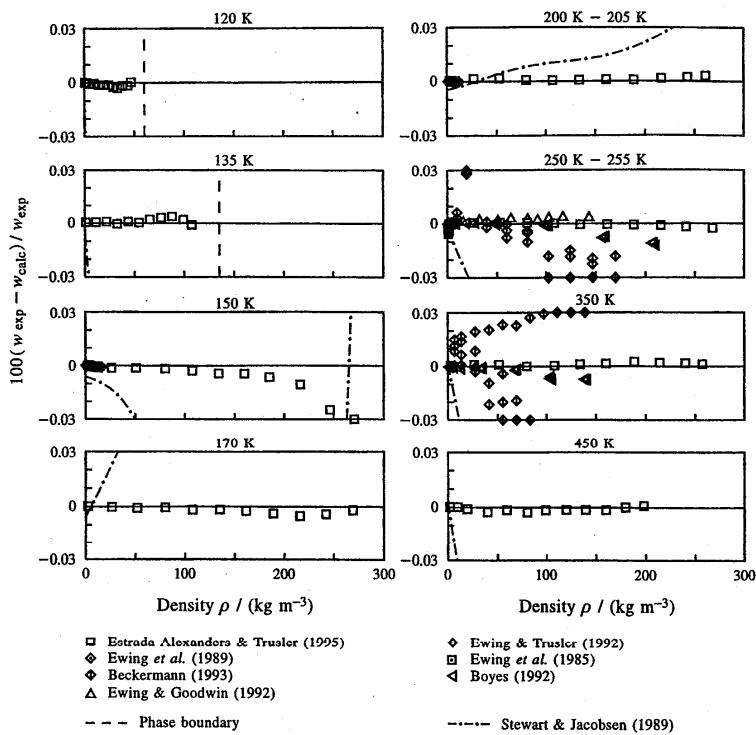
FIG. 22. Percentage deviations of highly accurate speed of sound data for densities up to about half the critical density from values calculated from Eq. (4.1). Values calculated from the equation of state of Stewart and Jacobsen (1989) are plotted for comparison.

sentation of these data could not be achieved in combination with a good extrapolation behavior.

The representation of $p\rho T$ data in the critical region is discussed in Sec. 5.3.1.

Thermal Virial Coefficients. Deviations between the selected data for the second thermal virial coefficient B and values calculated from Eq. (4.1) are shown in Fig. 20. The calculated second virial coefficients are in good agreement with the data derived from the $p\rho T$ measurements of Gilgen *et al.* (1994a) in this work for temperatures below 340 K. For higher temperatures, the data calculated from different intermolecular potentials are confirmed within $\pm 0.5\,\text{cm}^3\,\text{mol}^{-1}$.

FIG. 23. Percentage deviations of data for the second acoustic virial coefficient from values calculated from Eq. (4.1). Values calculated from the equation of state of Stewart and Jacobsen (1989) are plotted for comparison.

In Fig. 21 the course of the third thermal virial coefficient C calculated from Eq. (4.1) and from the equation of state of Stewart and Jacobsen (1989) is plotted together with the selected data. Both equations yield the expected maximum near T_c, but only the new equation of state shows reasonable behavior over the whole temperature range. When approaching low temperatures, the values calculated from the equation of state of Stewart and Jacobsen suddenly increase again and at temperatures above 500 K a minimum in the course of C is predicted. This behavior is neither physically justified nor confirmed by any data.

5.2.2. Acoustic Properties

Figure 22 shows the representation of speeds of sound in the gas phase for densities up to half the critical density. This region is covered by very accurate speed of sound data measured with spherical resonators. Since a very high resolution had to be chosen to discuss these data, other data sets could not be drawn in the same figure because of their much higher uncertainties. The most comprehensive data set was measured by Estrada-Alexanders and Trusler (1995). With the exception of three data points, Eq. (4.1) is able to reproduce these data to within their uncertainty. During the development of the new equation of state problems occurred at near-critical temperatures and at the highest densities measured by Estrada-Alexanders and Trusler, where none of the preliminary equations of state could represent all data with the desired accuracy. The final equation of state does not meet the

FIG. 24. Representation of data for the third acoustic virial coefficient. The plotted curves correspond to values calculated from Eq. (4.1) and from the equation of state of Stewart and Jacobsen (1989).

The equation of Stewart and Jacobsen (1989) is not able to reproduce the new speed of sound data at least roughly within their uncertainty. Even at very low densities the deviations to the speed of sound data increase to a few percent, which indicates that the acoustic virial coefficients calculated from this equation are systematically incorrect. This conclusion is confirmed by Figs. 23 and 24. While Eq. (4.1) represents the reliable data for the second acoustic virial coefficient β_a within $\pm 0.2\,cm^3\,mol^{-1}$, the equation of Stewart and Jacobsen shows large systematic deviations over the whole temperature range. At low temperatures, it yields values which are too low by more than $-20\,cm^3\,mol^{-1}$ and at 450 K its deviation is about $-3\,cm^3\,mol^{-1}$. For the third acoustic virial coefficient γ_a, the same abnormal behavior as for the third thermal virial coefficient C is observed (see Fig. 24). At temperatures above 250 K, discrepancies of about $500\,cm^6\,mol^{-2}$ occur between the γ_a data of Estrada-Alexanders and Trusler (1995) and the two data sets of Ewing et al. (1989) and Ewing and Trusler (1992). Since the γ_a data of Estrada-Alexanders and Trusler were determined from speed of sound measurements which are represented by Eq. (4.1) to within their uncertainties, our new equation of state represents the γ_a data of these authors also.

Figure 25 shows deviation plots for the speed of sound in the liquid region at pressures up to 300 MPa. The selected data of Streett and Costantino (1974), Thoen et al. (1969) and Bowman et al. (1968) are represented by Eq. (4.1) to within their estimated uncertainties ($\pm 0.4\% - \pm 0.6\%$). On some isotherms the data of Streett and Costantino and Thoen et al. show discrepancies of up to $\pm 0.8\%$ for pressures below 10 MPa. In these regions, the data of Bowman et al., which proved to be consistent with the selected speed of sound data on the saturated liquid line, were preferred. The equation of state published by Stewart and Jacobsen (1989) shows systematic offsets and oscillating deviations from re-

last two data points on the 150 K isotherm and the last data point on the 163.15 K isotherm within their uncertainties. The deviations of the experimental data from values calculated from Eq. (4.1) are -0.025%, -0.054% and $+0.017\%$, respectively. Other high quality data sets at appreciable pressures are only available for temperatures between 250 and 350 K, where the data of Ewing and Goodwin (1992) for pressures up to 7 MPa are represented to within $\pm 0.003\%$ and the data of Boyes (1992) for pressures up to 10 MPa show deviations which increase to -0.012%.

FIG. 25. Percentage deviations of speed of sound data in the liquid and supercritical (for $T = 160$ K) region from values calculated from Eq. (4.1). Values calculated from the equation of state of Stewart and Jacobsen (1989) are plotted for comparison.

**X** Lacam (1953a)   **Z** Hanayama (1975)
⋈ Lacam (1956)   **▥** Pitaevskaya *et al.* (1969)
✦ Martin (1957)   **◁** Vidal *et al.* (1979)
◆ Yang (1983)   **◈** Kortbeek *et al.* (1985)

—·—·— Stewart & Jacobsen (1989)
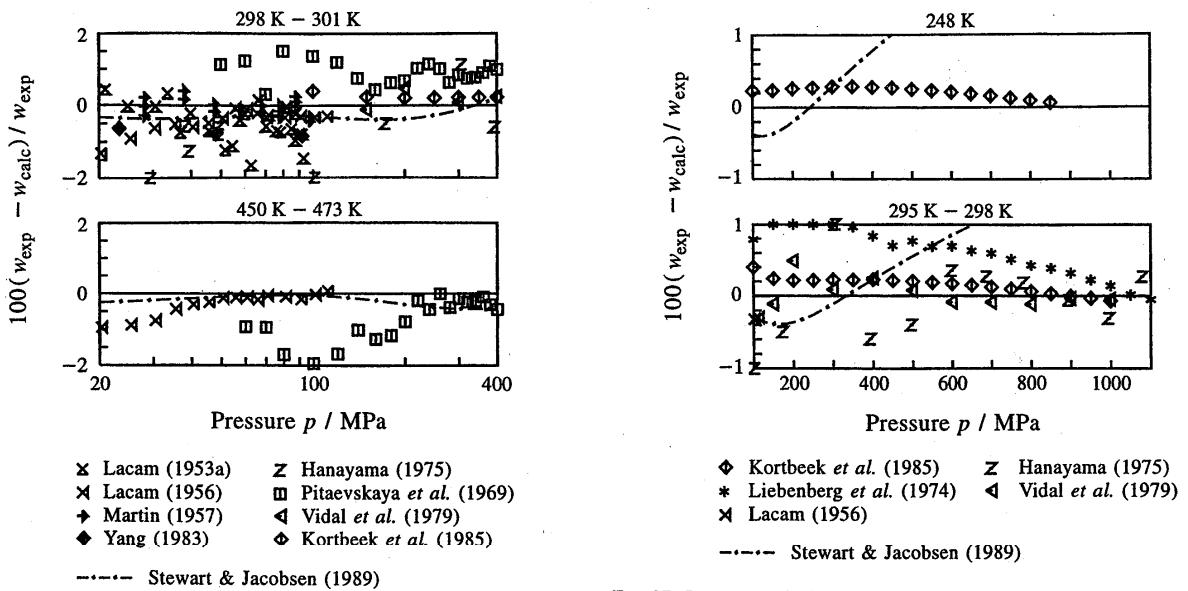
FIG. 26. Percentage deviations of speed of sound data in the supercritical region from values calculated from Eq. (4.1). Values calculated from the equation of state of Stewart and Jacobsen (1989) are plotted for comparison.


◆ Kortbeek *et al.* (1985)   **Z** Hanayama (1975)
✳ Liebenberg *et al.* (1974)   **◁** Vidal *et al.* (1979)
⋈ Lacam (1956)

—·—·— Stewart & Jacobsen (1989)

FIG. 27. Percentage deviations of speed of sound data in the high pressure region from values calculated from Eq. (4.1). Values calculated from the equation of state of Stewart and Jacobsen (1989) are plotted for comparison.

liable data, which in some cases exceed ±1%.

At pressures between 15 and 100 MPa, speed of sound data are only available for temperatures up to 160 and above 298 K. The data above 298 K are shown in Fig. 26 together with the results of Pitaevskaya *et al.* (1969), which extend to pressures of 400 MPa. In this region, Eq. (4.1) and the equation of Stewart and Jacobsen (1989) agree within ±0.5%, which is excellent compared with the uncertainty of the different data sets.

For temperatures between 148 and 298 K, the high pressure range is covered by the speed of sound data of Kortbeek *et al.* (1985). Only Eq. (4.1) is able to represent these data within their estimated uncertainty of ±0.5%, (see Fig. 27). However, small systematic deviations of up to 0.3% occur.

Other data sets are available only at 298 K in this pressure range. The representation of speed of sound data in the critical region is discussed in Sec. 5.3.2.

5.2.3. Isochoric Heat Capacity

Deviation plots for the specific isochoric heat capacity are presented in Fig. 28. For the development of the new equation of state only the data sets of Gladun (1971) and Anisimov *et al.* (1975), (1978) were used in the homogeneous region—in the deviation plots at temperatures above the "phase boundary." With the exception of the critical region, which is discussed in Sec. 5.3, the deviations of these data from values calculated from Eq. (4.1) and from the equation of Stewart and Jacobsen (1989) remain within the uncer-

◇ Anisimov *et al.* (1975)   **△** Anisimov *et al.* (1978)
◁ Kovalchuk (1977)   **+** Walker (1956)
▷ Gladun (1971)

— — — Phase boundary   —·—·— Stewart & Jacobsen (1989)
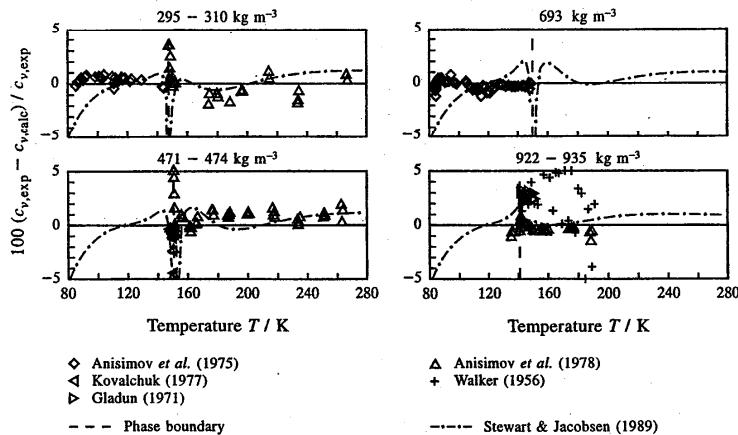
FIG. 28. Percentage deviations of isochoric heat capacity data from values calculated from Eq. (4.1). Data at temperatures below the saturation temperature are within the two-phase region. Values calculated from the equation of state of Stewart and Jacobsen (1989) are plotted for comparison.
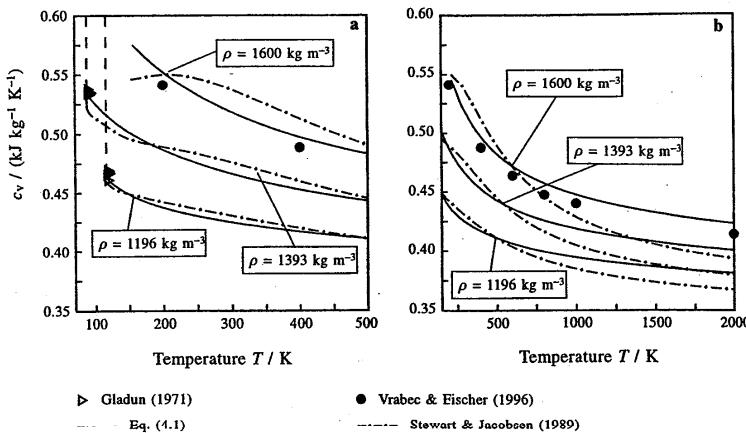
FIG. 29. Representation of the isochoric heat capacity at high densities up to 550 K (a) and up to 2000 K (b). The plotted curves correspond to values calculated from Eq. (4.1) and from the equation of state of Stewart and Jacobsen (1989).

tainty of the experimental data. In the two-phase region, Eq. (4.1) confirms the data of Anisimov *et al.* (1975), while the equation of Stewart and Jacobsen differs from these data by up to -5%.

Figure 29 shows plots of the isochoric heat capacity on three high density isochores. The isochores with $\rho = 1196\,\mathrm{kg\,m^{-3}}$ and $\rho = 1393\,\mathrm{kg\,m^{-3}}$ correspond to densities below the density of the liquid at the triple point and are hence limited by the saturated liquid line at low temperatures. The isochore $\rho = 1600\,\mathrm{kg\,m^{-3}}$ is limited by the solidification line. The values calculated from Eq. (4.1) result in smooth curves without any turning points and maxima. In contrast to the plot of the equation of state published by Stewart and Jacobsen (1989) the behavior of Eq. (4.1) seems to be physically reasonable. Since only very few c_v data are available in this region, preliminary equations often resulted in plots similar to that of the equation of Stewart and Jacobsen. In order to avoid maxima and turning points in the plot of c_v without fixing the equations to arbitrary c_v values, we calculated $58(\partial c_v/\partial T)_\rho$ values for densities between 1300

and $1400\,\mathrm{kg\,m^{-3}}$ at temperatures up to 300 K from preliminary equations which behaved reasonably in this region. These data were introduced into the final data set with low weights.

As can be seen in Fig. 29(b), Eq. (4.1) is able to reproduce the course of the isochoric heat capacity predicted by the data of Vrabec and Fischer (1996) up to very high temperatures. However, systematic deviations between -1% and -2.3% occur. Since these data were calculated from molecular dynamics based on a (12,6) Lennard-Jones potential, it is not known to what extent the data describe the real behavior of fluid argon. Therefore, we did not try to achieve a better representation of these data.

5.2.4. Isobaric Heat Capacity

Figure 30 shows deviations between selected c_p data and values calculated from Eq. (4.1). The data sets of Roder *et al.* (1989) and Perkins *et al.* (1991) are not included in the graphs because of their large scatter and their systematic de-
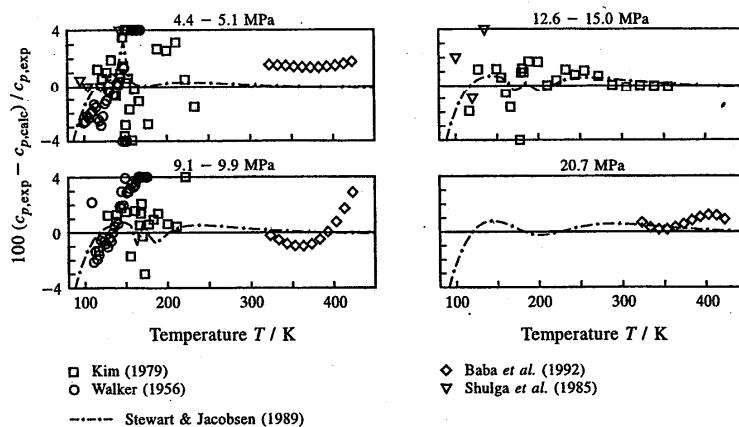
FIG. 30. Percentage deviations of isobaric heat capacity data from values calculated from Eq. (4.1). Values calculated from the equation of state of Stewart and Jacobsen (1989) are plotted for comparison.
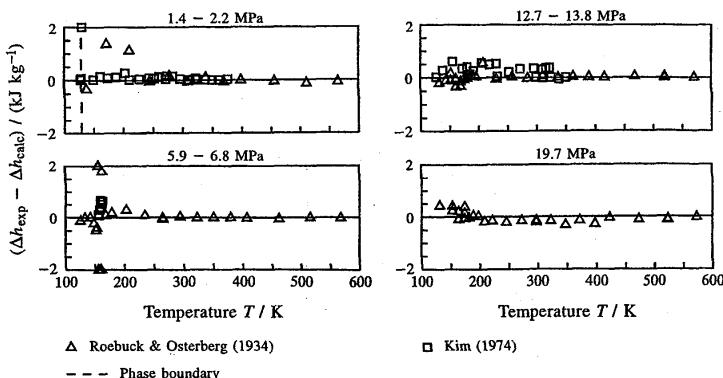
FIG. 31. Absolute deviations of data for differences of enthalpy from values calculated from Eq. (4.1).

/iations which reach up to ±10%. As mentioned in Sec. 3.4, no c_p data were used to establish the new equation of state. Both Eq. (4.1) and the equation of state of Stewart and Jacobsen (1989) represent the available data within their experimental uncertainty. At high temperatures, where the data of Baba et al. (1992) show systematic deviations of up to 3%, the equations agree with each other within less than 1%. The deviations between the equations increase to more than 4% at low temperatures, where the equation of Stewart and Jacobsen represents the data of Walker (1956) better than Eq. (4.1). Since Eq. (4.1) describes the thermal properties and the speed of sound with uncertainties of $\Delta\rho/\rho \leqslant \pm0.03\%$ and $\Delta w/w \leqslant \pm0.8\%$ in this region, an error of a few percent in c_p can hardly result from the equation of state. Obviously, the c_p data are incorrect in this region.

5.2.5. Enthalpy Differences

Absolute deviations between enthalpy differences Δh which were measured by Roebuck and Osterberg (1934) and Kim (1974) and Δh values calculated from Eq. (4.1) are presented in Fig. 31. In Fig. 31, all data are plotted for the final temperature of the corresponding experiment. Although Δh data were not used in the development of Eq. (4.1), the

experimental results are reproduced by Eq. (4.1) to $\pm 1\ \mathrm{kJ\,kg^{-1}}$ with the exception of a few outliers.

5.2.6. Throttling Coefficients

The deviation plots in Fig. 32 illustrate that the data for the Joule–Thomson coefficient μ are generally represented to within $\pm0.2\ \mathrm{K\,MPa^{-1}}$ by both Eq. (4.1) and the equation of state of Stewart and Jacobsen (1989). Larger deviations between the equations occur in the gas phase at low temperatures. This fact can be explained by a misbehavior of the equation of Stewart and Jacobsen, which became obvious for thermal properties and for speeds of sound in this region (see Secs. 5.2.1. and 5.2.2.).

For some selected isotherms, data for the isothermal throttling coefficient δ_T are plotted in an absolute δ_T-p diagram, Fig. 33, together with values calculated from Eq. (4.1) and from the equation of Stewart and Jacobsen (1989). Both equations support the data of Kim (1974), while the values published by Ishkin and Rogovaya (1957) seem to be slightly too low, especially at low temperatures.
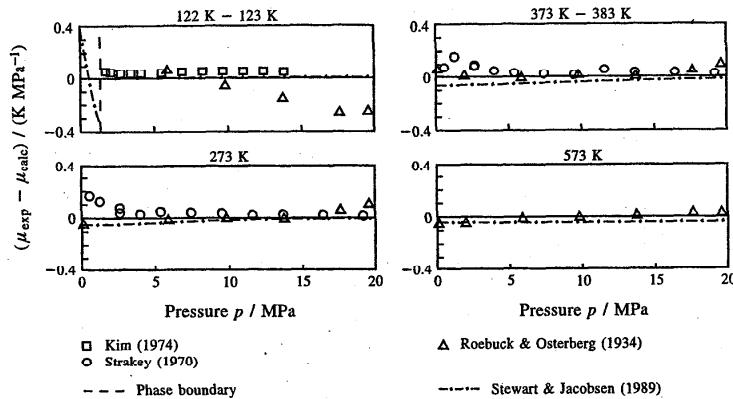
FIG. 32. Absolute deviations of data for the Joule–Thomson coefficient from values calculated from Eq. (4.1). Values calculated from the equation of state of Stewart and Jacobsen (1989) are plotted for comparison.

A   Ishkin & Rogovaya (1957)
□   Kim (1974)

———   Eq. (4.1)
—·—·—   Stewart & Jacobsen (1989)
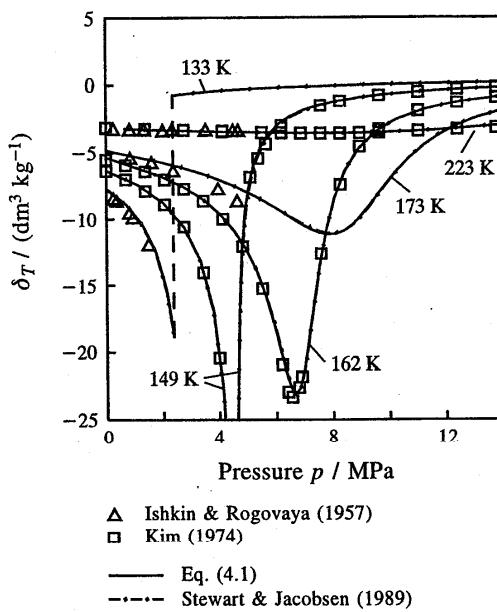
FIG. 33. Representation of the isothermal throttling coefficient. The plotted curves correspond to values calculated from Eq. (4.1) and from the equation of state of Stewart and Jacobsen (1989).


O   Gilgen et al. (1994b)

— — —   Aux. eqs. (see Sec. 2.6 to 2.8)
—·—·—   Stewart & Jacobsen (1989)
—··—··—   Tiesinga et al. (1994)

FIG. 34. Percentage deviations $\Delta y = (y_{exp} - y_{calc})/y_{exp}$ $(y = p_s, \rho', \rho'')$ of the near-critical saturation data of Gilgen et al. (1994b) from values calculated from Eq. (4.1). Values calculated from the auxiliary equations presented in Sec. 2 and from the equation of state of Stewart and Jacobsen (1989) are plotted for comparison.

5.3. Results in the Critical Region

For an assessment of Eq. (4.1) with regard to the representation of properties close to the critical point a comparison with results from the crossover equation of Tiesinga et al. (1994) is of special interest. This numerically very complex equation was developed especially for the description of thermodynamic properties in the critical region. Assuming that the behavior of fluids can be described by the three-dimensional Ising model close to the critical point, Tiesinga et al. used critical exponents, which are consistent with the results of the renormalization group theory [Wilson (1974)]. Analytical equations of state result in different values for the critical exponents, which are either integer values or reciprocals of integer values (see Table 32). From this fact it is usually concluded that analytical equations of state are not able to describe thermodynamic properties in the critical region correctly. It will be shown that this is only true for the limiting behavior of Eq. (4.1) with regard to the isochoric heat capacity c_v and the speed of sound w.

5.3.1. Thermal Properties

Figure 34 illustrates the representation of the group 1 data for the thermal properties on the phase boundary close to the critical temperature. Equation (4.1) represents all data within their experimental uncertainties. Compared with the data of Gilgen et al. (1994b), the accuracy of the equations of state of Stewart and Jacobsen (1989) and of the crossover equation of Tiesinga et al. (1994) is acceptable only for the vapor pressure. The deviations for orthobaric densities calculated from these equations far exceed the uncertainties of the experimental data.

Figure 35 shows selected $p \rho T$ data in the extended critical region. Equation (4.1) represents the reference data of Gilgen

TABLE 32. Examples of power laws for the description of thermodynamic properties along certain paths throughout the critical region

Described path	Power law	Critical exponent	Values determined by evaluating	
			RG theory[a]	Classical eqs.[b]
Phase boundary	$(\rho' - \rho'') \sim (T_c - T)^\beta$	β	0.326±0.002	0.5
Crit. isotherm	$\lvert p - p_c \rvert \sim \lvert \rho - \rho_c \rvert^\delta$	δ	4.80±0.02	3
Crit. isochore	$c_v \sim (T - T_c)^{-\alpha}$	α	0.110±0.003	0

[a]According to Sengers and Levelt Sengers (1986).
[b]For equations of state constrained at the critical point by the conditions $(\partial p/\partial \rho)_T = 0$, $(\partial^2 p/\partial \rho^2)_T = 0$ and $(\partial^3 p/\partial \rho^3)_T > 0$.
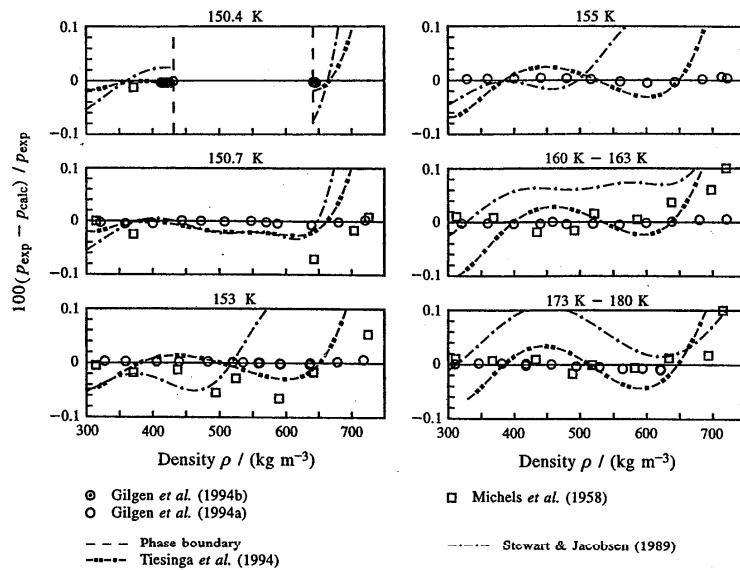
FIG. 35. Percentage pressure deviations of $p\rho T$ data in the extended critical region from values calculated from Eq. (4.1). Values calculated from the equation of state of Stewart and Jacobsen (1989) and from the crossover equation of Tiesinga *et al.* (1994) are plotted for comparison.

et al. (1994a), (1994b) to within their experimental uncertainty, which ranges from ±0.01% to ±0.02% in pressure in this region. The equation of state of Stewart and Jacobsen (1989) represents neither these data nor the data of Michels *et al.* (1958) with comparable uncertainty. The deviations between values calculated from the crossover equation and the accurate data of Gilgen *et al.* remain within ±0.04% only for densities between 400 and 650 kg m^{-3}. Outside of this density range, but still inside the range of validity of the crossover equation, the deviations increase even to much higher values.

5.3.2. Caloric Properties

The behavior of the isochoric heat capacity c_v and the speed of sound w at the critical point can be expressed in terms of the power law

$$c_v \sim (T - T_c)^{-\alpha}. \tag{5.1}$$

The value for the critical exponent α determined by evaluation of the renormalization group theory ($\alpha = 0.110 \pm 0.003$, see Table 32) predicts a weak divergence for the isochoric heat capacity c_v at the critical point. As a consequence, the predicted speed of sound w becomes zero at the critical point. In contrast to this, analytical equations of state yield $\alpha = 0$ and result in finite values for c_v and values greater than zero for w.

Figure 36 shows comparisons for speed of sound data in the critical region. On the 150.67 K isotherm, which is the one closest to the critical temperature, only the crossover equation is able to follow the course indicated by the experimental data. The large deviations between the results of the crossover equation and the data (up to about 10%) are still within the experimental uncertainties. In this region an ex-
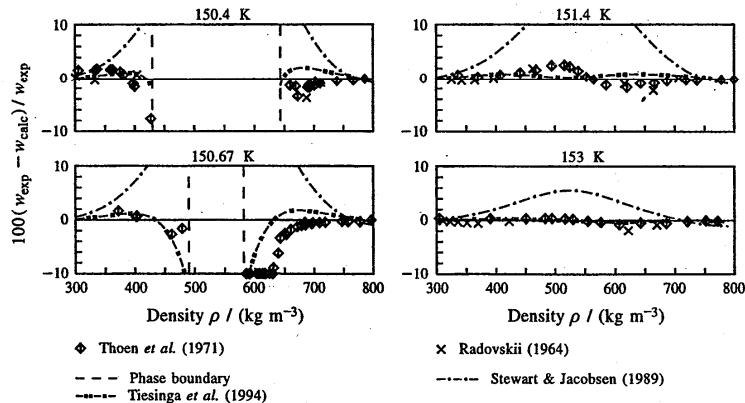

FIG. 36. Percentage deviations of speed of sound data in the extended critical region from values calculated from Eq. (4.1). Values calculated from the equation of state of Stewart and Jacobsen (1989) and from the crossover equation of Tiesinga *et al.* (1994) are plotted for comparison.
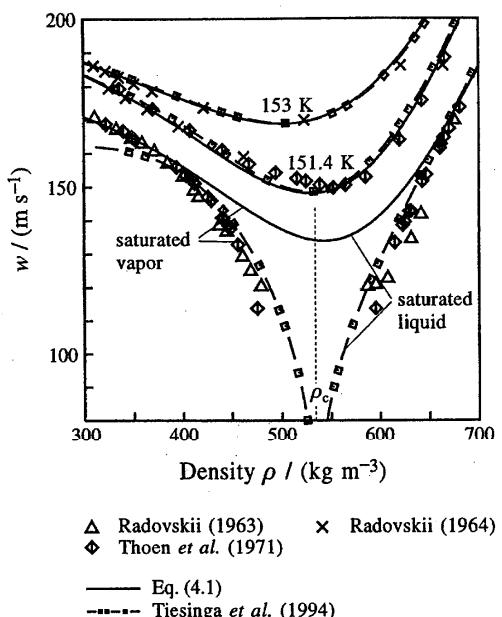
FIG. 37. Representation of the speed of sound on isotherms and on the saturated liquid and saturated vapor line in the critical region. The plotted curves correspond to values calculated from Eq. (4.1), from the equation of state of Stewart and Jacobsen (1989) and from the crossover equation of Tiesinga et al. (1994).

perimental error of, e.g., ±1 mK in the measured temperature results in an error of ±1% in the speed of sound. At 150.67 K, the deviations between values calculated from Eq. (4.1) and the data exceed the experimental uncertainties. But

FIG. 38. Representation of the isochoric heat capacity on an isochore in the critical region. For this isochore, the saturation temperature T_s is only 0.04 mK below the critical temperature. The plotted curves correspond to values calculated from Eq. (4.1), from the equation of state of Stewart and Jacobsen (1989) and from the crossover equation of Tiesinga et al. (1994).

FIG. 39. Representation of experimental data which describe the Hugoniot curve of argon for two different initial states (see text). The Hugoniot curves calculated from the equation of state of Stewart and Jacobsen (1989) are plotted for comparison.

on the 151.4 K isotherm, which is just 0.7 K above the critical temperature, Eq. (4.1) is able to represent the data with sufficient accuracy again. The equation of state of Stewart and Jacobsen (1989) is incorrect by up to 6% even at 153 K.

Figure 37 shows graphs for the speed of sound in the critical region plotted against the density. In contrast to the crossover equation, Eq. (4.1) is not able to follow the experimental data along the saturated liquid and vapor line for densities between 400 and 650 kg m⁻³. However, it is important to note that this density range corresponds to temperatures only 0.5 K below the critical temperature. For densities below 400 kg m⁻³ on the saturated vapor line, the speed of sound values calculated from the crossover equation are clearly too low. Tiesinga et al. (1994) see this behavior as an "indication that care should be taken with any use of the crossover equation in the vapor phase below the critical temperature."

The representation of isochoric heat capacity data in the critical region is shown in Fig. 38 for the 531 kg m⁻³ isochore ($0.99\rho_c$). On this isochore, the saturation temperature T_s, which is marked by the dashed line, is only 0.04 mK below the critical temperature. Again, it is illustrated that Eq. (4.1) is able to represent the available data down to temperatures of about 0.7 K above the critical temperature. Closer to
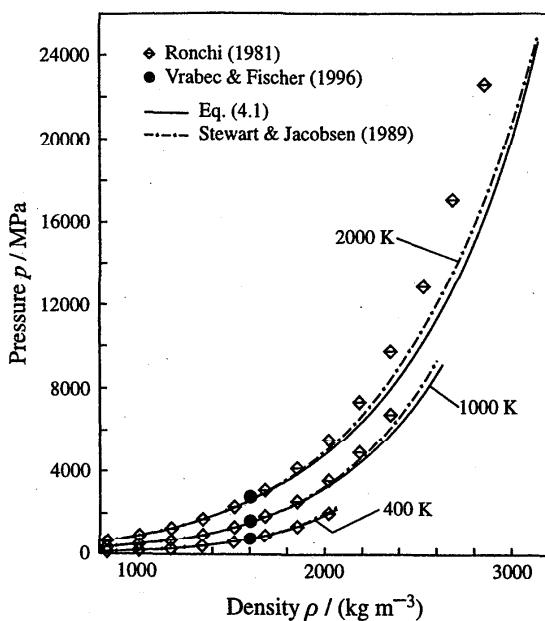
FIG. 40. Representation of $p\rho T$ data at very high densities and temperatures, which are based on calculations for different forms of the Lennard-Jones potential (see text). The plotted curves correspond to values calculated from Eq. (4.1) and from the equation of state of Stewart and Jacobsen (1989).

FIG. 41. The so-called "ideal curves" calculated from Eq. (4.1) and from the equation of state of Stewart and Jacobsen (1989). The curves are plotted in a double logarithmic p/p_c vs T/T_c diagram.

the critical point, only the crossover equation of Tiesinga *et al.* (1994) is able to follow the data.

Summarizing the discussion of the critical region, we assess that Eq. (4.1) is able to represent even caloric data in the critical region accurately with the exception of a small region around the critical point. Systematic errors larger than the uncertainty of the available data occur for the speed of sound and the isochoric heat capacity in the homogeneous region for $T \leqslant (T_c + 0.7 \text{ K})$ at densities between 400 and 650 kg m^{-3} and on the liquid–vapor phase boundary for $T > (T_c - 0.5 \text{ K})$. Within this region the crossover equation of Tiesinga *et al.* (1994) yields better results for these properties, but this equation fails for the description of the vapor phase at subcritical temperatures and generally for data further away from the critical point. The equation of state of Stewart and Jacobsen (1989) fails to represent caloric data for $|T - T_c| < \sim 4 \text{ K}$.

5.4. Extrapolation Behavior of the New Equation of State

Equation (4.1) is valid in the range where reliable experimental data were used to establish the equation of state. The behavior of Eq. (4.1) outside this range will be discussed in the following subsections.

5.4.1. Extrapolation to High Pressures and Temperatures

For very high temperatures and pressures, shock wave measurements are the only available source of experimental information on the thermodynamic behavior of argon. These measurements result in data for the Hugoniot relation

$$u - u_0 = 0.5(p + p_0)(1/\rho_0 - 1/\rho), \qquad (5.2)$$

where u is the internal energy, p the pressure, and ρ the density after releasing the shock wave, and u_0, p_0 and ρ_0 are the initial values. Most experiments were started from the saturated liquid near the boiling-point temperature $(T_0 \approx 87 \text{ K}, p_0 \approx 0.1 \text{ MPa}, \text{"high density curve"})$; however, van Thiel and Alder (1966) made additional measurements for another initial state $(T_0 = 148.2 \text{ K}, p_0 = 7 \text{ MPa}, \text{"low density curve"})$. For both of the initial states, Fig. 39 shows the Hugoniot curves calculated from Eq. (4.1) and from the equation of state of Stewart and Jacobsen (1989) together with the corresponding experimental data.

On the low- and high-density curve, the temperature increases with pressure to 37 000 and 17 000 K at 50 000 MPa, respectively. Above 50 000 MPa, the data of Grigor'ev *et al.* (1985) indicate a flattening of the high density curve, which is probably caused by electronic excitation. Up to this pressure, Eq. (4.1) shows a reasonable behavior for both Hugoniot curves, while the course of the equation of state of Stewart and Jacobsen (1989) is clearly too steep.

The Hugoniot data were not used directly in the development of Eq. (4.1). In order to preserve the reasonable representation of the Hugoniot curves which was achieved for a preliminary equation, 33 $u(T,\rho)$ and $p\rho T$ data were calculated from this equation along these curves. The calculated values were included in the selected data set with low weights. When a new equation showed an improved extrapolation behavior, the data were recalculated from the new equation.
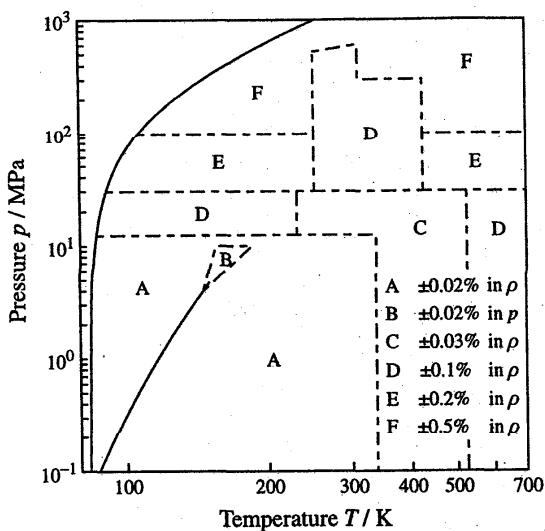
FIG. 42. Tolerance diagram for densities calculated from Eq. (4.1). In region B the uncertainty in pressure is given.

FIG. 44. Tolerance diagram for isobaric and isochoric heat capacity data calculated from Eq. (4.1).

At high densities $p\rho T$ data of Ronchi (1981) and Vrabec and Fischer (1996) are available for temperatures up to 2300 K. The data sets are based on molecular dynamics simulations for Lennard-Jones potentials of the form (12,7) and (12,6), respectively. For three selected isotherms, Fig. 40 compares these data with values calculated from Eq. (4.1) and from the equation of Stewart and Jacobsen (1989). Particularly at high densities, both equations yield pressures that are significantly lower than the simulated ones. No better representation of these data could be achieved, even if they were included in preliminary data sets. This is probably

FIG. 43. Tolerance diagram for speed of sound data calculated from Eq. (4.1).

due to an imperfection of the potential model selected by the authors. As van Thiel and Alder (1966) pointed out, the repulsive forces derived from the Lennard-Jones potential with the exponent 12 are stronger than for the real intermolecular potential of argon and result in higher pressures, especially at high densities.

5.4.2. The "Ideal Curves"

Ideal curves are curves along which one property of a real fluid is equal to the corresponding property of the hypothetical ideal gas in the same state. The most important ideal curves are derived from the compression factor z and its first derivatives, i.e., the classical ideal curve $(z=1)$, the Boyle curve $[(\partial z/\partial p)_T=0]$, the Joule–Thomson inversion curve $[(\partial z/\partial T)_p=0]$, and the Joule inversion curve $[(\partial z/\partial p)_\rho=0]$. Based on theoretical considerations performed in the 1960s, the courses of these curves were expected to be universal for all pure fluids in reduced variables.

Recent investigations [Span and Wagner (1997)] have shown that the representation of the ideal curves is a useful tool for the assessment of the extrapolation behavior of equations of state even though their plot is not as universal as expected in the 1960s. For argon, the range covered by experimental data is very large in terms of reduced variables. Thus, all ideal curves lie within this range. The only relevant exception is the high-temperature part of the Joule inversion curve.

Figure 41 shows the plot of the ideal curves calculated from Eq. (4.1) and from the equation of state of Stewart and Jacobsen (1989). Inside the region where reliable experimental data exist, both equations show the expected courses of the ideal curves. Visible differences occur only for the rep-

resentation of the Joule inversion curve. The equation of
Stewart and Jacobsen shows slightly oscillating behavior at
the high pressure end of the Joule curve, which is still within
its fitted range. This problem might indicate inconsistencies
among the high pressure data sets which were selected by
Stewart and Jacobsen.

6. The Uncertainty of the New Equation of State

Mainly guided by comparisons with experimental data, es-
timates for the uncertainty of calculated densities ρ, speeds
of sound w, and isochoric and isobaric heat capacities c_v and
c_p calculated from Eq. (4.1) have been made. These uncer-
tainties are illustrated in the tolerance diagrams, Figs. 42–44.

Based on the investigation of the extrapolation behavior
(see Sec. 5.4.), Eq. (4.1) should yield reasonable results out-
side of its range of validity for pressures up to 50 000 MPa
and temperatures up to 17 000 K at least for the basic ther-
modynamic properties like pressure and enthalpy. The calcu-
lation of derived properties like the speed of sound or spe-
cific heat capacities is not recommended beyond the limits of
validity.

7. Conclusions

A new equation of state for argon has been developed,
which is written in the form of a fundamental equation ex-
plicit in the reduced Helmholtz free energy. It is valid for
single-phase and saturation states from the melting line to
700 K at pressures up to 1000 MPa. The formulation is based
on selected experimental data for the thermodynamic prop-
erties of argon, which have been compiled in a comprehen-
sive review of the available literature.

Based on new reference data for the thermal properties
and for the speed of sound, the new equation of state yields
outstanding accuracies in the most important parts of the
fluid region. This accuracy could only be achieved by opti-
mizing the mathematical structure of the formulation using
both linear state-of-the-art procedures and a new nonlinear
optimization procedure. The equation of state shows reason-
able thermodynamic behavior even in scarcely measured re-
gions. Furthermore, the extrapolation behavior of the equa-
tion has been tested carefully. For basic properties such as
pressure and enthalpy, the equation should yield reasonable
results up to pressures of 50 000 MPa and temperatures to
17 000 K.

8. Acknowledgments

9. References

Akdemir, B., Istanbul Üniversitesi Fen Fakültesi Mecmuasi, Seri C, Istanbul 39–41, 63 (1977).

Albuquerque, G. M. N., J. C. G. Calado, M. Nunes da Ponte, and L. A. K. Staveley, Cryogenics 20, 416 (1980a).
Albuquerque, G. M. N., J. C. G. Calado, M. Nunes da Ponte, and A. M. F. Palavra, Cryogenics 20, 601 (1980b).
Ancsin, J., Metrologia 9, 147 (1973).
Ancsin, J., and M. J. Phillips, Metrologia 5, 77 (1969).
Angus, S., B. Armstrong, A. L. Gosman, R. D. McCarty, J. G. Hust, A. A. Vassermann, and V. A. Rabinovich, International Thermodynamic Tables of the Fluid State, Argon (Butterworths, London, 1972).
Anisimov, M. A., A. T. Berestov, L. S. Veksler, B. A. Koval'chuk, and V. A. Smirnov, Sov. Phys. JETP 39, 359 (1974).
Anisimov, M. A., B. A. Koval'chuk, V. A. Rabinovich, and V. A. Smirnov, Teplofiz. Svoistva Veshchestv Material. 8, 237 (1975).
Anisimov, M. A., B. A. Koval'chuk, V. A. Rabinovich, and V. A. Smirnov, Teplofiz. Svoistva Veshchestv Material. 12, 86 (1978).
Aziz, R. A., Dep. of Physics, Univ. of Waterloo, Waterloo, Canada (private communication, 1994).
Aziz, R. A., D. H. Bowman, and C. C. Lim, Can. J. Chem. 45, 2079 (1967).
Aziz, R. A. and M. J. Slaman, Mol. Phys. 58, 679 (1986).
Aziz, R. A. and M. J. Slaman, J. Chem. Phys. 92, 1030 (1990).
Baba, M., L. Dordain, J.-Y. Coxam, and J.-P. E. Grolier, Indian J. Technol. 30, 553 (1992).
Bale, H. D., B. C. Dobbs, J. S. Lin, and P. W. Schmidt, Phys. Rev. Lett. 25, 1556 (1970).
Baly, E. C. C., and F. G. Donnan, J. Chem. Soc. (London) 81, 907 (1902).
Bandyopadhyay, A. K., W. Blanke, and J. Jäger, PTB-Mitteilungen 101, 269 (1991).
Barreiros, S. F., J. C. G. Calado, P. Clancy, M. Nunes da Ponte, and W. B. Streit, J. Phys. Chem. 86, 1722 (1982).
Baxter, G. P., and H. W. Starkweather, Proc. Natl. Acad. Sci. USA 14, 57 (1927).
Baxter, G. P., and H. W. Starkweather, Proc. Natl. Acad. Sci. USA 15, 441 (1929).
Beckermann, W., Fortschrittberichte VDI (VDI, Düsseldorf, 1993), Reihe 19, Nr. 67.
Bedford, R. E. and C. G. M. Kirby, Metrologia 5, 83 (1969).
Bellm, J., W. Reineke, K. Schäfer, and B. Schramm, Ber. Bunsenges. Phys. Chem. 78, 282 (1974).
Bender, E., Equations of State Exactly Representing the Phase Behavior of Pure Substances, Proceedings of the 5th Symposium on Thermophysical Properties (American Society of Mechanical Engineers, New York, 1970), p. 227.
Benedict, M., G. B. Webb, and L. C. Rubin, J. Chem. Phys. 8, 334 (1940).
Biswas, S. N., N. J. Trappeniers, P. J. Kortbeek, and C. A. ten Seldam, Rev. Sci. Instrum. 59, 470 (1988).
Blagoi, Yu. P., A. E. Butko, S. A. Mikhailenko, and V. V. Yakuba, Sov. Phys. Acoust. 12, 355 (1967).
Blancett, A. L., K. R. Hall, and F. B. Canfield, Physica 47, 75 (1970).
Bonhoure, J., and R. Pello, Metrologia 19, 21 (1983).
Born, F., Ann. Phys. (Leipzig) 69, 473 (1922).
Bose, T. K., and R. H. Cole, J. Chem. Phys. 52, 140 (1970).
Bourbo, P., and I. Ischkin, Physica 3, 1067 (1936).
Bowman, D. H., R. A. Aziz, and C. C. Lim, Can. J. Phys. 47, 267 (1969).
Bowman, D. H., C. C. Lim, and R. A. Aziz, Can. J. Chem. 46, 1175 (1968).
Boyes, S. J., The speed of sound in gases with application to equations of state and sonic nozzles, PhD thesis, University College, London, 1992.
Bridgman, P. W., Proc. Am. Acad. Arts Sci. 59, 173 (1923).
Bridgman, P. W., Phys. Rev. 46, 930 (1934).
Bridgman, P. W., Proc. Am. Acad. Arts Sci. 70, 1 (1935).
Byrne, M. A., M. R. Jones, and L. A. K. Staveley, Trans. Faraday Soc. 64, 1747 (1968).
Carome, E. F., C. B. Cykowski, J. F. Havlice, and D. A. Swyt, Physica 38, 307 (1968).
Cath, P. G., and H. Kamerlingh Onnes, Natuurkundig Laboratorium, Leiden: Communications from the Physical Laboratory of the University of Leiden 156A, 1 (1922).
Chen, H. H., R. A. Aziz, and C. C. Lim, Can. J. Phys. 49, 1569 (1971).
Chen, H. H., C. C. Lim, and R. A. Aziz, J. Chem. Thermodyn. 7, 191 (1975).
Chen, H. H., C. C. Lim, and R. A. Aziz, J. Chem. Thermodyn. 10, 649 (1978).
Chen, C. T., and R. D. Present, J. Chem. Phys. 57, 757 (1972).

Cheng, V. M., Measurements on the dense-fluid equation of state and the melting parameters of argon, methane and nitrogen at high pressures, PhD thesis, Princeton University, 1972.

Cheng, V. M., W. B. Daniels, and R. K. Crawford, Phys. Lett. **43A**, 109 (1973).

Chui, C.-H., and F. B. Canfield, Faraday Soc. Trans. **67**, 2933 (1971).

Clark, A. M., F. Din, J. Robb, A. Michels, T. Wassenaar, and T. Zwietering, Physica **17**, 876 (1951).

Clusius, K., Z. Phys. Chem. **31B**, 459 (1936).

Clusius, K., and A. Frank, Z. Elektrochem. **49**, 308 (1943).

Clusius, K., K. Schleich, and M. Vogelmann, Helv. Chim. Acta **46**, 1705 (1963).

Clusius, K., and L. Staveley, Z. Phys. Chem. (Leipzig) **49B**, 1 (1941).

Clusius, K., and K. Weigand, Z. Phys. Chem. (Leipzig) **46B**, 1 (1940).

Cohen, E. R., and B. N. Taylor, *The Adjustment of the Fundamental Physical Constants*, CODATA Bulletin No. 63, Commision On Data for Science and Technology, International Council of Scientific Unions (Pergamon, Oxford, 1986).

Colclough, A. R., T. J. Quinn, and T. R. D. Chandler, Proc. R. Soc. London **368A**, 125 (1979).

Colgate, S. O., A. Sivaraman, and K. Reed, J. Chem. Thermodyn. **22**, 245 (1990).

Coplen, T. B., J. Phys. Chem. Ref. Data **26**, 1239 (1997).

Cottrell, T. L., R. A. Hamilton, and R. P. Taubinger, Faraday Soc. Trans. **52**, 1310 (1956).

Crain, Jr., R. W., and R. E. Sonntag, Adv. Cryogen. Eng. **11**, 379 (1965).

Crawford, R. K., and W. B. Daniels, Phys. Rev. Lett. **21**, 367 (1968).

Crawford, R. K., and W. B. Daniels, J. Chem. Phys. **50**, 3171 (1969).

Crommelin, C. A., Natuurkundig Laboratorium, Leiden: Communications from the Physical Laboratory of the University of Leiden **115**, 1 (1910).

Crommelin, C. A., Koninklijk Nederlandse Akademie van Wetenschappen, Afdeeling Natuur, Proceedings **13**, 607 (1911).

Crommelin, C. A., Natuurkundig Laboratorium, Leiden: Communications from the Physical Laboratory of the University of Leiden **138C**, 23 (1913).

Crommelin, C. A., Natuurkundig Laboratorium, Leiden: Communications from the Physical Laboratory of the University of Leiden **140A**, 1 (1914).

Davies, R. H., A. G. Duncan, G. Saville, and L. A. K. Staveley, Trans. Faraday Soc. **63**, 855 (1967).

Dobbs, E. R., and L. Finegold, J. Acoust. Soc. Am. **32**, 1215 (1960).

Dobrovol'skii, O. A., and I. F. Golubev, Chimija i technologija produktov organicheskogo sinteza. Fiziko-chimicheskie issledovanija. Hrsg.: M.S. Furman. Moskva, 1971. (Trudy/Gosudarstvennyi Nauchno-Issledovatel'skij i Proektnyj Institut Azotnoj **8**, Promyshlennosti i Produktov Organicheskogo Sinteza), 14.

Duncan, A. G., and L. A. K. Staveley, Trans. Faraday Soc. **62**, 548 (1966).

Dymond, J. H., and E. B. Smith, *The Virial Coefficients of Pure Gases and Mixtures* (Clarendon, Oxford, 1980).

El-Hakeem, A. S., J. Chem. Phys. **42**, 3132 (1965).

Estrada-Alexanders, A. F., and J. P. M. Trusler, J. Chem. Thermodyn. **27**, 1075 (1995).

Estrada-Alexanders, A. F., and J. P. M. Trusler, Int. J. Thermophys. **17**, 1325 (1996).

Eucken, A., Deutsche Physikalische Gesellschaft: Verhandlungen Deutschen Physikalischen Gesellschaft **18**, 4 (1916).

Eucken, A., and F. Hauck, Z. Phys. Chem. **134**, 161 (1928).

Ewers, J., and W. Wagner, *A Method for Optimizing the Structure of Equations of State and its Application to an Equation of State for Oxygen*, Proceedings of the 8th Symposium on Thermophysical Properties (American Society of Mechanical Engineers, New York, 1982) Vol. 1, p. 78.

Ewing, M. B., and A. R. H. Goodwin, J. Chem. Thermodyn. **24**, 531 (1992).

Ewing, M. B., and K. N. Marsh, J. Chem. Thermodyn. **11**, 793 (1979).

Ewing, M. B., M. L. McGlashan, and J. P. M. Trusler, J. Chem. Thermodyn. **17**, 549 (1985).

Ewing, M. B., M. L. McGlashan, and J. P. M. Trusler, Metrologia **22**, 93 (1986).

Ewing, M. B., A. A. Owusu, and J. P. M. Trusler, Physica **156A**, 899 (1989).

Ewing, M. B., and J. P. M. Trusler, Physica A **184**, 415 (1992).

Fender, B. E. F., and G. D. Halsey, Jr., J. Chem. Phys. **36**, 1881 (1962).

Fender, B. E. F., and G. D. Halsey, Jr., J. Chem. Phys. **42**, 127 (1965).

Finger, L. W., R. M. Hazen, G. Zou, H. K. Mao, and P. M. Bell, Appl. Phys. Lett. **39**, 892 (1981).

Fleury, P. A., and J. P. Boon, Phys. Rev. **186**, 244 (1969).

Flubacher, P., A. J. Leadbetter, and J. A. Morrison, Proc. Phys. Soc. **78**, 1449 (1961).

Frank, A., and K. Clusius, Z. Phys. Chem. (Leipzig) **42B**, 395 (1939).

Freeman, M. P., and G. D. Halsey, Jr., J. Phys. Chem. **60**, 1119 (1956).

Furukawa, G. T., Bureau International des Poids et Mesures (Lèvres)/Comit, Consultatif de Thermometrie, Sessions 12, T100 (1978).

Furukawa, G. T., W. R. Bigge, and J. L. Riddle, Temperature: Its Measurement Control Sci. Industry **4**, 231 (1972).

Galt, J. K., J. Chem. Phys. **16**, 505 (1948).

Getzen, F. W., The compressibility of gaseous argon, PhD thesis, Massachusetts Institute of Technology, 1956.

Gielen, H., V. Jansoone, and O. Verbeke, J. Chem. Phys. **59**, 5763 (1973).

Gilgen, R., Fortschritt-Berichte VDI, Reihe 3 Nr. 317, (VDI, Düsseldorf, 1993).

Gilgen, R., R. Kleinrahm, and W. Wagner, J. Chem. Thermodyn. **26**, 383 (1994a).

Gilgen, R., R. Kleinrahm, and W. Wagner, J. Chem. Thermodyn. **26**, 399 (1994b).

Gladun, C., Cryogenics **11**, 205 (1971).

Goldman, K., and N. G. Scrase, Physica **45**, 1 (1969).

Goodwin, A. R. H., Thermophysical properties from the speed of sound, Ph.D. thesis, University College, London, 1988.

Goring, G. E., J. Chem. Phys. **54**, 4514 (1971).

Gosman, A. L., R. D. McCarty, and J. G. Hust, Natl. Stand. Ref. Data Ser. (U.S., Natl. Bur. Stand.) **27** (1969).

Grigor, A. F., and W. A. Steele, Phys. Chem. Liquids **1**, 129 (1968).

Grigor'ev, F. V., S. B. Kormer, O. L. Mikhailova, M. A. Mochalov, and V. D. Urlin, Sov. Phys. JETP **61**, 751 (1985).

Guo, X.-Y., R. Kleinrahm, and W. Wagner, report for a research project of the Ruhrgas AG, Ruhr-Universität, Bochum (1992).

Gyorog, D. A., and E. F. Obert, AIChE J. **10**, 621 (1964).

Hahn, R., K. Schäfer, and B. Schramm, Ber. Bunsenges. Phys. Chem. **78**, 287 (1974).

Hanayama, Y., Ehime-daigaku-kiyo/Dai-san-bu, Kogaku **8**, 9 (1975).

Händel, G., R. Kleinrahm, and W. Wagner, J. Chem. Thermodyn. **24**, 685 (1992).

Hardy, W. H., R. K. Crawford, and W. B. Daniels, J. Chem. Phys. **54**, 1005 (1971).

Haynes, W. M., Cryogenics **18**, 621 (1978).

Haynes, W. M., M. J. Hiza, and N. V. Frederick, Rev. Sci. Instrum. **47**, 1237 (1976).

Heastie, R., Proc. Phys. Soc. (London) **73**, 490 (1957).

Heuse, W., Ann. Phys. (Leipzig) **53**, 86 (1919).

Hilsenrath, J., Tables of Thermodynamic and Transport Properties **75** (1960).

Hoinkis, J., Dissertation, Universität Karlsruhe, Germany, 1989.

Holborn, L., and J. Otto, Z. Phys. **23**, 77 (1924a).

Holborn, L., and J. Otto, Z. Phys. **30**, 320 (1924b).

Holborn, L., and J. Otto, Z. Phys. **33**, 1 (1925).

Holborn, L., and H. Schultze, Ann. Phys. (Leipzig) **47**, 1089 (1915).

Holst, G., and L. Hamburger, Z. Phys. Chem. (Leipzig) **91**, 513 (1916).

Ishkin, I. P., and I. A. Rogovaya, Zh. Fiz. Khim. **31**, 410 (1957).

Jacobsen, R. T, The thermodynamic properties of nitrogen from 65 to 2000 K with pressures to 10,000 atm, PhD thesis, Washington State University, 1972.

Jacobsen, R. T, R. B. Stewart, M. Jahangiri, and S. G. Penoncello, Adv. Cryog. Eng. **31**, 1161 (1986).

Kachanov, Yu. L., B. E. Kanishchev, and L. L. Pitaevskaya, J. Eng. Phys. **44**, 1 (1983).

Kalfoglou, N. K., and J. G. Miller, J. Phys. Chem. **71**, 1256 (1967).

Kamerlingh Onnes, H., and C. A. Crommelin, Natuurkundig Laboratorium, Leiden: Communications from the Physical Laboratory of the University of Leiden **118B**, 13 (1910).

Kang, K. H., K. S. Gam, and C. Rhee, J. Korean Soc. **21**, 417 (1988).

Kelly, R. L., J. Phys. Chem. Ref. Data **16**, Suppl. 1, 1 (1987).

Kemp, R. C., W. R. G. Kemp, and J. A. Cowan, Metrologia **12**, 93 (1976).

Kemp, R. C., and W. R. G. Kemp, Metrologia **14**, 83 (1978).

Kerl, K., and H. Häusler, Ber. Bunsenges. Phys. Chem. **88**, 992 (1984).

Khnykov, V. M., M. P. Orlova, L. B. Belyanskii, and L. N. Rabukh, Russ. J. Phys. Chem. **52**, 849 (1978).

Kidnay, A. J., K. L. Lewis, J. C. G. Calado, and L. A. K. Staveley, J. Chem. Thermodyn. **7**, 847 (1975).

Kim, K. Y., Calorimetric studies on argon and hexafluoroethane and a gen alized correlation of maxima in isobaric heat capacity, PhD thesis, University of Michigan, 1974.

Kleinrahm, R. and W. Wagner, J. Chem. Thermodyn. **18**, 739 (1986).

Klimeck, J., R. Kleinrahm, and W. Wagner, J. Chem. Thermodyn. **30**, 1571 (1998).

Knobler, C. M., J. J. M. Beenakker, and H. F. P. Knaap, Physica **25**, 909 (1959).

Kortbeek, P. J., M. J. P. Muringer, N. J. Trappeniers, and S. N. Biswas, Rev. Sci. Instrum. **56**, 1269 (1985).

Kosov, N. D., and I. S. Brovanov, J. Eng. Phys. **36**, 413 (1979).

Koval'chuk, B. A., Vsesojuznyi Institut Nauchnoj i Technicheskoj Informacii, Moskva (VINITI) 3402-77, Referativnyi Zhurnal/Chimija 1 (1977).

Krishan, R., J. K. Gupta, and K. D. Baveja, Indian J. Pure Appl. Phys. **27**, 772 (1989).

Kurilenok, K. V., V. A. Medvedev, and M. P. Orlova, Teplofiz. Svoistva Veshchestv Material. **7**, 13 (1974).

Lacam, A., J. Recherches CNRS **34**, 25 (1956).

Lacam, A., and J. Noury, Acad. Sci. Comptes Rendus **236**, 362 (1953a).

Lacam, A., and J. Noury, Acad. Sci. Comptes Rendus **236**, 2039 (1953b).

Lahr, P. H., and W. G. Eversole, J. Chem. Eng. Data **7**, 42 (1962).

Lallemand, M., and D. Vidal, J. Chem. Phys. **66**, 4776 (1977).

Law, A. K., and D. S. Bezanson, Can. J. Phys. **50**, 1764 (1972).

Lecocq, A., J. Recherches Centre National Recherche Scientific **55**, 55 (1960).

Leduc, M. A., Comptes Rendus Hebdomadaire Académie Sciences **167**, 70 (1918).

Lee, M. W., S. Fuks, and J. Bigeleisen, J. Chem. Phys. **53**, 4066 (1970).

Leming, C. W., Sublimation pressures of solid argon, krypton and xenon, PhD thesis, Michigan State University, 1970.

Lestz, S. S., J. Chem. Phys. **38**, 2830 (1963).

Levelt Sengers, J. M. H. NIST, Thermophys. Prop. Div., Gaithersburg MD, (private communication, 1970a).

Levelt Sengers, J. M. H., Ind. Eng. Chem. Fundam. **9**, 470 (1970b).

Levelt Sengers, J. M. H., M. Klein, and J. S. Gallagher, *American Institute of Physics Handbook* (McGraw-Hill, New York, 1972), pp. 4–204.

Lewis, W. F., D. Benson, R. K. Crawford, and W. B. Daniels, J. Phys. Chem. Solids **35**, 383 (1974).

Lichtenthaler, R. N., and K. Schäfer, Ber. Bunsenges. Phys. Chem. **73**, 42 (1969).

Liebenberg, D. H., R. L. Mills, and J. C. Bronson, J. Appl. Phys. **45**, 741 (1974).

Liepmann, H. W., Helv. Phys. Acta **12**, 421 (1939).

Lim, C. C., and R. A. Aziz, Can. J. Phys. **45**, 1275 (1967).

Lippold, H., Cryogenics **9**, 112 (1969).

Lovejoy, D. R., Nature (London) **197**, 353 (1963).

Luettmer-Strathmann, J., S. Tang, and J. V. Sengers, J. Chem. Phys. **97**, 2705 (1992).

Manov, S. V., N. I. Timoshenko, A. L. Yamnov, and A. I. Yartsev, *Trudy Moskovskogo Energeticheskogo Instituta* (MEI, Moskva, 1984) Vol. 622, p. 74.

Martin, A. V. J., J. Recherches C.N.R.S. **41**, 251 (1957).

Masson, I., and L. G. F. Dolley, R. Soc. (London), Phil. Trans. **103A**, 524 (1923).

Mathias, E., H. Kamerlingh Onnes, and C. A. Crommelin, Koninklijk Nederlandse Akademie van Wetenschappen, Afdeeling Natuur, Proc. **15**, 667 (1912).

McCain, Jr., W. D., and W. T. Ziegler, J. Chem. Eng. Data **12**, 199 (1967).

Michels, A., J. M. Levelt, and W. de Graaff, Physica **24**, 659 (1958).

Michels, A., and C. Prins, Physica **28**, 101 (1962).

Michels, A., T. Wassenaar, Th. Sluyters, and W. de Graaff, Physica **23**, 89 (1957).

Michels, A., Hub. Wijker, and H. K. Wijker, Physica **15**, 627 (1949).

Mikhailenko, S. A., B. G. Dudar', and Yu. P. Blagoi, Sov. J. Low Temp. Phys. **1**, 116 (1975).

Moldover, M. R., and J. P. M. Trusler, Metrologia **25**, 165 (1988).

Moldover, M. R., J. P. M. Trusler, T. J. Edwards, J. B. Mehl, and R. S. Davis, J. Res. Natl. Bur. Stands. **93**, 85 (1988).

Morris, E. C., J. Chem. Phys. **81**, 581 (1984).

Morris, E. C., and R. G. Wylie, J. Chem. Phys. **73**, 1359 (1980).

Narinskii, G. B., Kislorod **11**, 9 (1957).

Nellis, W. J., and A. C. Mitchell, J. Chem. Phys. **73**, 6137 (1980).

Nierode, D. E., J. L. Lewis, R. A. Gaggioli, and E. F. Obert, AIChE J. **16**, 472 (1970).

Nishitake, T., and Y. Hanayama, J. Phys. Soc. Jpn. **39**, 1065 (1975).

Nowak, P., R. Kleinrahm, and W. Wagner, J. Chem. Thermodyn. **28**, 1423 (1996).

Nowak, P., R. Kleinrahm, and W. Wagner, J. Chem. Thermodyn. **29**, 1157 (1997a).

Nowak, P., R. Kleinrahm, and W. Wagner, J. Chem. Thermodyn. **29**, 1137 (1997b).

Nunes da Ponte, M., W. B. Streett, R. C. Miller, and L. A. K. Staveley, J. Chem. Thermodyn. **13**, 767 (1981).

Nunes da Ponte, M., W. B. Streett, and L. A. K. Staveley, J. Chem. Thermodyn. **10**, 151 (1978).

Oishi, J., J. Sci. Research Institute **43**, 22 (1949).

Olszweski, K., R. Soc. (London), Phil. Trans. **186A**, 253 (1895).

Osborne, J., Ph.D. thesis, University of London, 1972; J. H. Dymond and E. B. Smith, *The Second Virial Coefficients of Pure Gases* (Oxford University Press, Oxford, 1979).

Pan, W. P., M. H. Mady, and R. C. Miller, AIChE J. **21**, 283 (1975).

Pavese, F., Metrologia **14**, 93 (1978).

Pavese, F., Metrologia **17**, 35 (1981).

Pavese, F., J. Ancsin, D. N. Astrov, J. Bonhoure, G. Bonnier, G. T. Furukawa, R. C. Kemp, H. Maas, R. L. Rusby, H. Sakurai, and L. Shan-Kang, Metrologia **20**, 127 (1984).

Perkins, R. A., D. G. Friend, H. M. Roder, and C. A. Nieto de Castro, Int. J. Thermophys. **12**, 965 (1991).

Pitaevskaya, L. L., A. V. Bilevich, and N. B. Isakova, Russ. J. Phys. Chem. **43**, 1197 (1969).

Polyakov, E. V., and D. S. Tsiklis, Thermophys. Properties Matter Substances **2**, 130 (1970).

Pool, R. A. H., G. Saville, T. M. Herrington, B. D. C. Shields, and L. A. K. Staveley, Faraday Soc. Trans. **58**, 1692 (1962).

Pool, R. A. H., B. D. C. Shields, and L. A. K. Staveley, Nature (London) **181**, 831 (1958).

Pope, G. A., Calculation of argon, methane, and ethane virial coefficients at low reduced temperatures based on data obtained by isochorically coupled Burnett experiments, PhD thesis, Rice University, 1972.

Pope, G. A., P. S. Chappelear, and R. Kobayashi, J. Chem. Phys. **59**, 423 (1973).

Preston-Thomas, H., Metrologia **27**, 3 (1990).

Provine, J. A., and F. B. Canfield, Physica **52**, 79 (1971).

Quinn, T. J., A. R. Colclough, and T. R. D. Chandler, Philos. Trans. R. Soc. London **283**, 367 (1976).

Rabinovich, V. A., L. A. Tokina, and V. M. Berezin, High Temp. **8**, 745 (1970).

Radovskii, I. S., Zh. Prikl. Mech. Techn. Fiz. **3**, 159 (1963).

Radovskii, I. S., Z. Prikl. Mech. Techn. Fiz. **3**, 172 (1964).

Ramsay, W., and M. W. Travers, R. Soc. London, Trans. Ser. A **197**, 47 (1901).

Rentschler, H. P., and B. Schramm, Ber. Bunsenges. Phys. Chem. **81**, 319 (1977).

Robertson, S. L., Jr., S. E. Babb, and G. J. Scott, J. Chem. Phys. **50**, 2160 (1969).

Robinson, D. W., Proc. R. Soc. (London) **A225**, 393 (1954).

Roder, H. M., R. A. Perkins, and C. A. Nieto de Castro, Int. J. Thermophys. **10**, 1141 (1989).

Roebuck, J. R., and H. Osterberg, Phys. Rev. **46**, 785 (1934).

Roebuck, J. R., and H. Osterberg, J. Chem. Phys. **8**, 627 (1940).

Rogovaya, I. A., and M. G. Kaganer, Russ. J. Phys. Chem. **35**, 1049 (1961).

Ronchi, C., J. Nucl. Mater. **96**, 314 (1981).

Rusby, R. L., J. Chem. Thermodyn. **23**, 1153 (1991).

Rusby, R. L., R. P. Hudson, and M. Durieux, Metrologia **31**, 149 (1994).

Saji, Y., and S. Kobayashi, Cryogenics **4**, 136 (1964).

Santafe, J., J. S. Urieta, and C. Gutierrez Losa, Revista Academia Ciencas Exactas, Fisico-Quimicas Naturales Zaragoza **31**, 63 (1976).

Schmidt, R., and W. Wagner, Fluid Phase Equilibria **19**, 175 (1985).

Schönmann, W., Messung der thermischen Eigenschaften und Aufstellung einer empirischen Zustandsgleichung gasförmiger Argon-Kohlendioxid-Gemische, Dissertation, TH Karlsruhe, Germany, 1971.

Schramm, B., and U. Hebgen, Chem. Phys. Lett. **29**, 137 (1974).

Schramm, B., H. Schmiedel, R. Gehrmann, and R. Bartl, Ber. Bunsenges. Phys. Chem. **81**, 316 (1977).

Sengers, J. V., and J. M. H. Levelt Sengers, Annu. Rev. Phys. Chem. **37**, 189 (1986).

Setzmann, U., and W. Wagner, Int. J. Thermophys. **10**, 1103 (1989).

Setzmann, U., and W. Wagner, J. Phys. Chem. Ref. Data **20**, 1061 (1991).

Sevastyanov, R. M., and R. A. Chernyavskaya, J. Eng. Phys. **52**, 703 (1987).

Shavandrin, A. M., N. M. Potapova, and Yu. R. Chashkin, Teplofiz. Svoistva Veshchestv Material. **9**, 141 (1976).

Shiratori, T., Keiryo-Kenkyusho-Hokoku **28**, 248 (1979).

Shul'ga, V. M., F. G. El'darov, and S. B. Kiselev, Teplofiz. Svojstva Veschestv Material. **20**, 133 (1985).

Simon, F., and F. Kippert, Z. Phys. Chem. **135**, 113 (1928).

Simon, F., M. Ruhemann, and W. A. M. Edwards, Z. Phys. Chem. (Leipzig) **6B**, 331 (1930).

Smith, D. H., and R. G. Harlow, Br. J. Appl. Phys. **14**, 102 (1963).

Sorokin, V. A., and Yu. P. Blagoi, Termodinamicheskije Termokhimicheskije Konstanty **97**, Moskva (1970).

Span, R., and W. Wagner, Int. J. Thermophys. **18**, 1415 (1997).

Stewart, R. B., and R. T Jacobsen, J. Phys. Chem. Ref. Data **18**, 639 (1989).

Stewart, R. B., R. T Jacobsen, and J. H. Becker, Center for Applied Thermodynamic Studies, Report No. 81-3, University of Idaho, Moscow, 1981.

Stewart, R. B., R. T Jacobsen, J. H. Becker, J. C. J. Teng, and P. K. K. Mui, *Thermodynamic properties of argon from the triple point to 1200 K with pressures to 1000 MPa*, Proceedings of the 8th Symposium on Thermophysical Properties (American Society of Mechanical Engineers, New York, J. V. Sengers, 1982), Vol. 1, p. 97.

Stishov, S. M., and V. I. Fedosimov, Sov. Phys. JETP Lett. **14**, 217 (1971).

Stishov, S. M., I. N. Makarenko, V. A. Ivanov, and V. I. Fedosimov, Sov. Phys. JETP Lett. **11**, 13 (1970).

Strakey, J. P., The Joule-Thomson coefficients of argon-carbon dioxide mixtures, PhD thesis, Yale University, 1970.

Streett, W. B., Journal of Chemical Physics **46**, 3282 (1967).

Streett, W. B., and M. S. Costantino, Physica **75**, 283 (1974).

Streett, W. B., and L. A. K. Staveley, J. Chem. Phys. **50**, 2302 (1969).

Strobridge, T. R., 1962, Natl. Bur. Stand. Tech. Note No. 129 (1962).

Susekov, O. F., Russ. J. Phys. Chem. **46**, 1115 (1972).

Tam, A. C., and W. P. Leung, Phys. Rev. Lett. **53**, 560 (1984).

Tanner, C. C., and I. Masson, Proc. R. Soc. London, **126A**, 268 (1930).

Teague, R. K., and C. J. Pings, J. Chem. Phys. **48**, 4973 (1968).

Tegeler, Ch., R. Span, and W. Wagner, Int. J. Thermophys. (submitted).

Terry, M. J., J. T. Lynch, M. Bunclark, K. R. Mansell, and L. A. K. Staveley, J. Chem. Thermodyn. **1**, 413 (1969).

Theeuwes, F., and R. J. Bearman, Trans. Kansas Academy Sci. **72**, 342 (1970).

Thoen, J., E. Vangeel, and W. Van Dael, Physica **45**, 339 (1969).

Thoen, J., E. Vangeel, and W. Van Dael, Physica **52**, 205 (1971).

Thomaes, G., R. van Steenwinkel, and W. Stone, Mol. Phys. **5**, 301 (1962).

Tiesinga, B. W., E. Sakonidou, H. R. van den Berg, J. Luettmer-Strathmann, and J. V. Sengers, J. Chem. Phys. **101**, 6944 (1994).

Townsend, P. W., Pressure-volume-temperature relationships of binary gaseous mixtures, PhD thesis, Columbia University, 1956.

Vacek, V., and A. M. Hany, High Temp.-High Pressures **23**, 689 (1991).

van Dael, W., A. van Itterbeek, A. Cops, and J. Thoen, Physica **32**, 611 (1966).

van Itterbeek, A., J. de Boelpaep, O. Verbeke, F. Theeuwes, and K. Staes, Physica **30**, 2119 (1964).

van Itterbeek, A., W. Grevendonk, W. van Dael, and G. Forrez, Physica **25**, 1255 (1959b).

van Itterbeek, A., W. van Dael, and W. Grevendonk, Physica **25**, 640 (1959a).

van Itterbeek, A., and W. van Dael, Cryogenics **1**, 226 (1961).

van Itterbeek, A., and O. van Paemel, Physica **5**, 845 (1938).

van Itterbeek, A., and O. Verbeke, Physica **26**, 931 (1960).

van Itterbeek, A., and O. Verbeke, Probl. Low Temp. Phys. Thermodyn. **3**, 179 (1961).

van Itterbeek, A., O. Verbeke, and K. Staes, Physica **29**, 742 (1963).

van Itterbeek, A., and L. Verhaegen, Proc. Phys. Soc. **B62**, 800 (1949).

van Thiel, M., and B. J. Alder, J. Chem. Phys. **44**, 1056 (1966).

van Witzenburg, W., and J. C. Stryland, Can. J. Phys. **46**, 811 (1968).

Vassermann, A. A., Y. Z. Kazavchinskii, and V. A. Rabinovich, Thermophysical properties of air and air components, Israel Program for Scientific Translations, Jerusalem, 1971; *Teplofizicheskie svoistva vozdukha i ego komponentov* (Nauka, Moscow, 1966).

Vassermann, A. A., and V. A. Rabinovich, Thermophysical properties of liquid air and its components, Israel Program for Scientific Translations, Jerusalem, 1970; *Teplofizicheskie svoistva zhidkogo vozdukha i ego komponentov* (GSSD Monograph No. 3, Moscow, 1968).

Verbeke, O. B., V. Jansoone, R. Gielen, and J. de Boelpaep, J. Phys. Chem. **73**, 4076 (1969).

Vidal, D., L. Guengant, and M. Lallemand, Physica **96A**, 545 (1979a).

Vidal, D., R. Tufeu, Y. Garrabos, and B. Le Neindre, *Proceedings of the International Association for Research and Advancement of High Pressure Science and Technology* (AIRAPT, London, 1979b), 7th Conference, Vol. 2, p. 692.

Voronel, A. V., and Y. R. Chashkin, Sov. Phys. JETP **24**, 263 (1967).

Voronel, A. V., V. G. Gorbunova, V. A. Smirnov, N. G. Shmakov, and V. V. Shchekochikhina, Sov. Phys. JETP **36**, 505 (1973).

Voronel, A. V., V. G. Snigirev, and Yu. R. Chashkin, Sov. Phys. JETP **21**, 653 (1965).

Vrabec, J., and J. Fischer, Univ. Bodenkultur, Inst. Land-, Umwelt- und Energietech., Vienna, Austria (private communication, 1996).

Wagner, W., Cryogenics **12**, 214 (1972).

Wagner, W., Cryogenics **13**, 470 (1973).

Wagner, W., Fortschritt-Berichte VDI, Reihe 3, Nr. 39 (VDI, Düsseldorf, Germany, 1974).

Wagner, W., K. Brachthäuser, R. Kleinrahm, and H. W. Lösch, Int. J. Thermophys. **16**, 399 (1995).

Wagner, W., J. Ewers, W. Pentermann, J. Chem. Thermodyn. **8**, 1049 (1976).

Walker, P. A., The equation of state and the specific heat of liquid argon, PhD thesis, Queen Mary College, University of London, 1956.

Waxman, M., and J. R. Hastings, J. Res. Natl. Bur. Stand. (NBS) **75C**, 165 (1971).

Weir, R. D., I. Wynn Jones, J. S. Rowlinson, and G. Saville, Faraday Soc. Trans. **63**, 1320 (1967).

Whalley, E., Y. Lupien, and W. G. Schneider, Can. J. Chem. **31**, 722 (1953).

Wilson, K. G., Phys. Rev. **4**, 3174 (1974).

Yang, Z., Ziran Zazhi **6**, 638 (1983).

Zha, C.-S., R. Boehler, D. A. Young, and M. Ross, J. Chem. Phys. **85**, 1034 (1986).

Zykov, N. A., R. M. Sevast'yanov, and R. A. Chernyavskaya, J. Eng. Phys. **44**, 312 (1983).

10. Appendix: Thermodynamic Properties of Argon

In order to preserve thermodynamic consistency all values presented in Tables 33 and 34 were calculated directly from the new equation of state, Eq. (4.1). In general, entries in the tables are given with five significant digits, which is appropriate with respect to the uncertainties discussed in Sec. 6. But of course, interpolations between entries in the tables may result in uncertainties, which are significantly larger than the uncertainties of Eq. (4.1). This fact has to be considered, especially in the extended critical region. For sophisticated applications, properties should be calculated directly from the new equation of state. Suitable software can be obtained from the authors.

TABLE 33. Thermodynamic properties of saturated argon

Temperature (K)	Pressure (MPa)	Density (kg m^{-3})	Enthalpy (kJ kg^{-1})	Entropy (kJ kg^{-1} K^{-1})	c_v (kJ kg^{-1} K^{-1})	c_p (kJ kg^{-1} K^{-1})	w (m s^{-1})
83.8058[a]	0.068 891	1416.77	−276.56	−2.5440	0.549 60	1.1157	862.43
		4.0546	−112.85	−0.590 44	0.324 71	0.555 03	168.12
84	0.070 447	1415.59	−276.35	−2.5414	0.548 81	1.1157	861.10
		4.1384	−112.77	−0.594 05	0.324 89	0.555 57	168.28
86	0.088 110	1403.40	−274.11	−2.5152	0.540 94	1.1162	847.35
		5.0795	−111.99	−0.630 16	0.326 74	0.561 56	169.87
88	0.109 01	1391.08	−271.86	−2.4896	0.533 62	1.1181	833.47
		6.1737	−111.25	−0.664 49	0.328 76	0.568 24	171.39
90	0.133 51	1378.63	−269.61	−2.4645	0.526 77	1.1212	819.45
		7.4362	−110.55	−0.697 18	0.330 94	0.575 69	172.83
92	0.161 99	1366.01	−267.36	−2.4399	0.520 31	1.1255	805.28
		8.8829	−109.90	−0.728 40	0.333 29	0.583 96	174.20
94	0.194 85	1353.23	−265.09	−2.4158	0.514 20	1.1309	790.95
		10.531	−109.28	−0.758 27	0.335 82	0.593 12	175.49
96	0.232 49	1340.26	−262.80	−2.3920	0.508 40	1.1374	776.45
		12.397	−108.71	−0.786 92	0.338 53	0.603 27	176.71
98	0.275 32	1327.09	−260.50	−2.3687	0.502 87	1.1450	761.78
		14.499	−108.19	−0.814 46	0.341 42	0.614 49	177.85
100	0.323 77	1313.70	−258.19	−2.3456	0.497 60	1.1537	746.91
		16.859	−107.73	−0.841 01	0.344 52	0.626 90	178.91
102	0.378 25	1300.07	−255.85	−2.3229	0.492 57	1.1637	731.83
		19.495	−107.31	−0.866 67	0.347 81	0.640 62	179.89
104	0.439 20	1286.18	−253.49	−2.3005	0.487 77	1.1749	716.54
		22.431	−106.96	−0.891 51	0.351 33	0.655 82	180.80
106	0.507 06	1272.02	−251.11	−2.2783	0.483 19	1.1875	701.02
		25.691	−106.67	−0.915 64	0.355 07	0.672 66	181.62
108	0.582 26	1257.56	−248.70	−2.2563	0.478 82	1.2017	685.24
		29.300	−106.44	−0.939 13	0.359 06	0.691 38	182.37
110	0.665 26	1242.77	−246.26	−2.2345	0.474 68	1.2176	669.20
		33.287	−106.29	−0.962 06	0.363 31	0.712 23	183.03
112	0.756 50	1227.63	−243.78	−2.2129	0.470 76	1.2353	652.87
		37.684	−106.20	−0.98450	0.367 84	0.735 53	183.61
114	0.856 44	1212.10	−241.27	−2.1914	0.467 08	1.2553	636.24
		42.526	−106.20	−1.0065	0.372 67	0.761 68	184.11
116	0.965 53	1196.15	−238.72	−2.1700	0.463 66	1.2779	619.26
		47.853	−106.28	−1.0283	0.377 85	0.791 15	184.52
118	1.0842	1179.74	−236.12	−2.1487	0.460 49	1.3034	601.93
		53.708	−106.45	−1.0497	0.383 39	0.824 55	184.85
120	1.2130	1162.82	−233.48	−2.1274	0.457 63	1.3324	584.19
		60.144	−106.71	−1.0710	0.389 34	0.862 65	185.09
122	1.3524	1145.33	−230.78	−2.1060	0.455 09	1.3656	566.02
		67.221	−107.08	−1.0922	0.395 75	0.906 44	185.23
124	1.5028	1127.20	−228.02	−2.0847	0.452 91	1.4039	547.36
		75.008	−107.57	−1.1133	0.402 69	0.957 20	185.29
126	1.6648	1108.37	−225.19	−2.0632	0.451 16	1.4485	528.16
		83.590	−108.18	−1.1346	0.410 24	1.0166	185.24
128	1.8388	1088.72	−222.28	−2.0416	0.449 89	1.5011	508.36
		93.066	−108.93	−1.1560	0.418 46	1.0871	185.10
130	2.0255	1068.13	−219.29	−2.0197	0.449 20	1.5638	487.88
		103.56	−109.83	−1.1777	0.427 45	1.1717	184.85
132	2.2252	1046.46	−216.19	−1.9975	0.449 21	1.6400	466.63
		115.23	−110.91	−1.1999	0.437 34	1.2751	184.49

TABLE 33. Thermodynamic properties of saturated argon—Continued

Temperature (K)	Pressure (MPa)	Density (kg m^{-3})	Enthalpy (kJ kg^{-1})	Entropy (kJ kg^{-1} K^{-1})	c_v (kJ kg^{-1} K^{-1})	c_p (kJ kg^{-1} K^{-1})	w (m s^{-1})
134	2.4388	1023.50	−212.97	−1.9748	0.450 06	1.7342	444.51
		128.28	−112.19	−1.2227	0.448 35	1.4045	184.02
136	2.6666	999.00	−209.60	−1.9515	0.451 92	1.8539	421.42
		142.96	−113.71	−1.2464	0.460 92	1.5710	183.41
138	2.9096	972.57	−206.06	−1.9275	0.455 04	2.0106	397.21
		159.65	−115.51	−1.2713	0.475 81	1.7932	182.60
140	3.1682	943.71	−202.29	−1.9023	0.459 84	2.2247	371.63
		178.86	−117.65	−1.2978	0.494 04	2.1036	181.50
142	3.4435	911.61	−198.23	−1.8756	0.467 29	2.5349	344.14
		201.37	−120.25	−1.3265	0.517 06	2.5648	180.00
144	3.7363	874.98	−193.76	−1.8467	0.479 72	3.0262	313.80
		228.48	−123.46	−1.3584	0.547 19	3.3149	177.93
146	4.0479	831.38	−188.68	−1.8142	0.502 57	3.9312	278.88
		262.63	−127.57	−1.3956	0.589 23	4.7346	174.89
148	4.3797	775.03	−182.49	−1.7749	0.550 94	6.2097	236.08
		309.60	−133.29	−1.4424	0.656 80	8.3830	169.81
150	4.7346	680.43	−173.01	−1.7145	0.706 03	23.582	174.74
		394.50	−143.60	−1.5185	0.821 82	35.468	157.01
150.687[b]	4.8630	535.60	−159.46	−1.6258			

[a]Triple-point temperature.
[b]Critical temperature.

TABLE 34. Thermodynamic properties of argon

Temperature (K)	Density (kg m^{-3})	Internal energy (kJ kg^{-1})	Enthalpy (kJ kg^{-1})	Entropy (kJ kg^{-1} K^{-1})	c_v (kJ kg^{-1} K^{-1})	c_p (kJ kg^{-1} K^{-1})	w (m s^{-1})
			0.1 MPa isobar				
83.814[a]	1416.80	−276.61	−276.54	−2.5440	0.549 61	1.1156	862.52
85	1409.57	−275.29	−275.22	−2.5283	0.544 83	1.1157	854.35
87.178[b]	1396.16	−272.86	−272.79	−2.5000	0.536 57	1.1171	839.20
87.178[b]	5.7043	−129.08	−111.55	−0.650 58	0.327 91	0.565 41	170.77
90	5.5077	−128.12	−109.97	−0.632 65	0.325 70	0.560 00	173.85
95	5.1933	−126.44	−107.19	−0.602 59	0.322 73	0.552 56	179.11
100	4.9152	−124.78	−104.44	−0.574 39	0.320 58	0.547 02	184.16
105	4.6669	−123.14	−101.71	−0.547 81	0.318 99	0.542 79	189.04
110	4.4436	−121.51	−99.008	−0.522 64	0.317 78	0.539 48	193.76
115	4.2416	−119.89	−96.317	−0.498 72	0.316 85	0.536 85	198.34
120	4.0577	−118.28	−93.639	−0.475 92	0.316 12	0.534 72	202.80
125	3.8896	−116.68	−90.969	−0.454 12	0.315 53	0.532 98	207.15
130	3.7352	−115.08	−88.308	−0.433 25	0.315 06	0.531 53	211.39
135	3.5929	−113.49	−85.654	−0.413 21	0.314 68	0.530 31	215.54
140	3.4613	−111.90	−83.005	−0.393 95	0.314 36	0.529 28	219.60
145	3.3392	−110.31	−80.361	−0.375 39	0.314 10	0.528 40	223.59
150	3.2255	−108.72	−77.721	−0.357 49	0.313 88	0.527 64	227.49
155	3.1194	−107.14	−75.084	−0.340 20	0.313 69	0.526 98	231.33
160	3.0202	−105.56	−72.451	−0.323 48	0.313 53	0.526 41	235.10
165	2.9272	−103.98	−69.820	−0.307 29	0.313 39	0.525 91	238.80
170	2.8398	−102.40	−67.192	−0.291 59	0.313 27	0.525 46	242.45
175	2.7576	−100.83	−64.565	−0.276 37	0.313 17	0.525 07	246.03
180	2.6800	−99.254	−61.941	−0.261 58	0.313 08	0.524 72	249.57
185	2.6067	−97.680	−59.318	−0.247 21	0.313 00	0.524 41	253.05
190	2.5374	−96.108	−56.697	−0.233 23	0.312 94	0.524 12	256.48
195	2.4716	−94.536	−54.077	−0.219 61	0.312 87	0.523 87	259.87
200	2.4093	−92.964	−51.458	−0.206 35	0.312 82	0.523 64	263.21
210	2.2936	−89.824	−46.224	−0.180 82	0.312 73	0.523 24	269.76
220	2.1885	−86.686	−40.993	−0.156 48	0.312 66	0.522 91	276.15
230	2.0927	−83.550	−35.765	−0.133 24	0.312 60	0.522 64	282.40
240	2.0050	−80.415	−30.540	−0.111 01	0.312 55	0.522 40	288.50
250	1.9244	−77.281	−25.317	−0.089 69	0.312 51	0.522 20	294.48
260	1.8500	−74.149	−20.096	−0.069 21	0.312 48	0.522 02	300.33
270	1.7812	−71.018	−14.877	−0.049 51	0.312 45	0.521 87	306.07
280	1.7174	−67.887	−9.6585	−0.030 53	0.312 42	0.521 74	311.70
290	1.6579	−64.757	−4.4417	−0.012 23	0.312 40	0.521 62	317.24
300	1.6025	−61.628	0.774 04	0.005 46	0.312 38	0.521 52	322.67
310	1.5507	−58.499	5.9888	0.022 56	0.312 37	0.521 43	328.02
320	1.5021	−55.371	11.203	0.039 11	0.312 35	0.521 35	333.27
330	1.4565	−52.244	16.416	0.055 15	0.312 34	0.521 28	338.45
340	1.4135	−49.116	21.628	0.070 71	0.312 33	0.521 21	343.55
350	1.3731	−45.990	26.840	0.085 82	0.312 32	0.521 15	348.57
375	1.2814	−38.174	39.867	0.121 77	0.312 30	0.521 03	360.81
400	1.2012	−30.359	52.892	0.155 39	0.312 29	0.520 93	372.65
425	1.1304	−22.546	65.914	0.186 97	0.312 28	0.520 85	384.12
450	1.0676	−14.734	78.935	0.216 74	0.312 27	0.520 79	395.26
475	1.0114	−6.9233	91.954	0.244 90	0.312 26	0.520 73	406.09
500	0.960 76	0.887 14	104.97	0.271 61	0.312 25	0.520 69	416.64
525	0.914 99	8.6970	117.99	0.297 01	0.312 25	0.520 65	426.93
550	0.873 38	16.506	131.00	0.321 23	0.312 24	0.520 62	436.98
575	0.835 40	24.315	144.02	0.344 37	0.312 24	0.520 59	446.79
600	0.800 58	32.124	157.03	0.366 53	0.312 24	0.520 55	465.81
625	0.768 55	39.932	170.05	0.387 78	0.312 24	0.520 53	475.03
650	0.738 98	47.740	183.06	0.408 19	0.312 23	0.520 51	484.07
675	0.711 61	55.548	196.07	0.427 84	0.312 23	0.520 50	492.95
700	0.686 19	63.355	209.09	0.446 77	0.312 23	0.520 50	492.95

TABLE 34. Thermodynamic properties of argon—Continued

Temperature (K)	Density (kg m^{-3})	Internal energy (kJ kg^{-1})	Enthalpy (kJ kg^{-1})	Entropy (kJ kg^{-1} K^{-1})	c_v (kJ kg^{-1} K^{-1})	c_p (kJ kg^{-1} K^{-1})	w (m s^{-1})
			0.5 MPa isobar				
83.914[a]	1417.28	−276.60	−276.25	−2.5438	0.549 69	1.1142	863.76
85	1410.69	−275.39	−275.04	−2.5295	0.545 32	1.1142	856.32
90	1379.78	−269.82	−269.46	−2.4657	0.527 21	1.1194	821.46
95	1347.80	−264.20	−263.83	−2.4049	0.511 60	1.1322	785.49
100	1314.43	−258.50	−258.12	−2.3463	0.497 80	1.1523	748.14
105	1279.27	−252.69	−252.29	−2.2895	0.485 48	1.1807	709.03
105.801[b]	1273.44	−251.74	−251.35	−2.2805	0.483 63	1.1862	702.57
105.801[b]	25.352	−126.42	−106.70	−0.913 27	0.354 69	0.670 91	181.55
110	24.050	−124.72	−103.93	−0.887 68	0.346 59	0.645 36	186.57
115	22.702	−122.79	−100.77	−0.859 51	0.339 67	0.623 24	192.17
120	21.524	−120.92	−97.693	−0.833 35	0.334 64	0.606 84	197.45
125	20.481	−119.10	−94.691	−0.808 84	0.330 84	0.594 26	202.48
130	19.548	−117.32	−91.746	−0.785 73	0.327 91	0.584 35	207.29
135	18.707	−115.57	−88.845	−0.763 83	0.325 59	0.576 38	211.93
140	17.944	−113.84	−85.980	−0.742 99	0.323 73	0.569 85	216.41
145	17.246	−112.14	−83.144	−0.723 09	0.322 22	0.564 43	220.75
150	16.605	−110.45	−80.334	−0.704 04	0.320 98	0.559 87	224.97
155	16.013	−108.77	−77.544	−0.685 75	0.319 94	0.556 00	229.09
160	15.466	−107.10	−74.773	−0.668 15	0.319 07	0.552 68	233.10
165	14.957	−105.45	−72.017	−0.651 19	0.318 33	0.549 81	237.03
170	14.482	−103.80	−69.274	−0.634 81	0.317 70	0.547 31	240.87
175	14.038	−102.16	−66.543	−0.618 98	0.317 16	0.545 11	244.63
180	13.622	−100.53	−63.823	−0.603 65	0.316 69	0.543 18	248.32
185	13.232	−98.899	−61.111	−0.588 79	0.316 28	0.541 47	251.95
190	12.864	−97.277	−58.408	−0.574 37	0.315 92	0.539 94	255.51
195	12.516	−95.659	−55.711	−0.560 36	0.315 61	0.538 57	259.02
200	12.188	−94.046	−53.022	−0.546 74	0.315 33	0.537 34	262.47
210	11.582	−90.829	−47.659	−0.520 58	0.314 87	0.535 23	269.21
220	11.036	−87.623	−42.316	−0.495 72	0.314 50	0.533 49	275.77
230	10.540	−84.428	−36.988	−0.472 04	0.314 19	0.532 04	282.15
240	10.087	−81.241	−31.674	−0.449 42	0.313 95	0.530 81	288.37
250	9.6733	−78.060	−26.372	−0.427 78	0.313 74	0.529 77	294.45
260	9.2924	−74.886	−21.079	−0.407 02	0.313 57	0.528 87	300.40
270	8.9409	−71.716	−15.794	−0.387 07	0.313 43	0.528 09	306.22
280	8.6155	−68.551	−10.516	−0.367 88	0.313 31	0.527 42	311.92
290	8.3133	−65.390	−5.2452	−0.349 38	0.313 20	0.526 83	317.51
300	8.0319	−62.232	0.02041	−0.331 53	0.313 11	0.526 31	323.00
310	7.7691	−59.076	5.2811	−0.314 28	0.313 04	0.525 85	328.39
320	7.5232	−55.924	10.538	−0.297 59	0.312 97	0.525 44	333.69
330	7.2925	−52.773	15.790	−0.281 43	0.312 91	0.525 07	338.90
340	7.0757	−49.625	21.039	−0.265 76	0.312 86	0.524 74	344.03
350	6.8716	−46.478	26.285	−0.250 55	0.312 81	0.524 44	349.08
375	6.4097	−38.619	39.388	−0.214 39	0.312 71	0.523 82	361.38
400	6.0064	−30.767	52.477	−0.180 60	0.312 64	0.523 33	373.27
425	5.6512	−22.922	65.555	−0.148 89	0.312 58	0.522 93	384.78
450	5.3358	−15.082	78.624	−0.119 01	0.312 54	0.522 60	395.94
475	5.0540	−7.2466	91.686	−0.090 76	0.312 50	0.522 34	406.79
500	4.8005	0.58563	104.74	−0.063 97	0.312 47	0.522 11	417.35
525	4.5714	8.4149	117.79	−0.038 50	0.312 45	0.521 92	427.65
550	4.3632	16.242	130.84	−0.014 23	0.312 42	0.521 76	437.70
575	4.1732	24.066	143.88	0.008 96	0.312 41	0.521 62	447.53
600	3.9991	31.889	156.92	0.031 16	0.312 39	0.521 50	457.14
625	3.8389	39.710	169.95	0.052 45	0.312 38	0.521 40	466.54
650	3.6912	47.530	182.99	0.072 89	0.312 37	0.521 30	475.77
675	3.5544	55.349	196.02	0.092 57	0.312 36	0.521 22	484.81
700	3.4274	63.167	209.05	0.111 52	0.312 35	0.521 15	493.69

TABLE 34. Thermodynamic properties of argon—Continued

Temperature (K)	Density (kg m^{-3})	Internal energy (kJ kg^{-1})	Enthalpy (kJ kg^{-1})	Entropy (kJ kg^{-1} K^{-1})	c_v (kJ kg^{-1} K^{-1})	c_p (kJ kg^{-1} K^{-1})	w (m s^{-1})
			1.0 MPa isobar				
84.039[a]	1417.88	−276.59	−275.88	−2.5437	0.549 80	1.1125	865.30
85	1412.07	−275.52	−274.81	−2.5310	0.545 93	1.1124	858.76
90	1381.35	−269.97	−269.24	−2.4674	0.527 81	1.1171	824.17
95	1349.59	−264.37	−263.63	−2.4067	0.512 19	1.1291	788.53
100	1316.48	−258.70	−257.94	−2.3483	0.498 37	1.1483	751.59
105	1281.67	−252.91	−252.13	−2.2917	0.486 01	1.1753	713.01
110	1244.67	−246.97	−246.17	−2.2362	0.475 00	1.2125	672.31
115	1204.80	−240.82	−239.98	−2.1812	0.465 40	1.2643	628.79
116.598[b]	1191.29	−238.79	−237.95	−2.1636	0.462 68	1.2851	614.12
116.598[b]	49.546	−126.50	−106.32	−1.0347	0.379 46	0.800 69	184.63
120	47.202	−124.86	−103.68	−1.0123	0.368 17	0.755 94	189.35
125	44.270	−122.61	−100.02	−0.982 48	0.356 46	0.709 79	195.69
130	41.787	−120.49	−96.555	−0.955 31	0.348 22	0.677 41	201.51
135	39.637	−118.46	−93.231	−0.930 21	0.342 13	0.653 42	206.95
140	37.747	−116.50	−90.012	−0.906 80	0.337 48	0.634 97	212.09
145	36.064	−114.60	−86.875	−0.884 78	0.333 82	0.620 38	216.98
150	34.551	−112.75	−83.804	−0.863 95	0.330 90	0.608 57	221.67
155	33.180	−110.92	−80.786	−0.844 16	0.328 53	0.598 86	226.18
160	31.929	−109.13	−77.812	−0.825 28	0.326 57	0.590 74	230.54
165	30.782	−107.36	−74.876	−0.807 21	0.324 93	0.583 88	234.77
170	29.723	−105.62	−71.972	−0.789 87	0.323 56	0.578 01	238.88
175	28.744	−103.89	−69.095	−0.773 19	0.322 39	0.572 95	242.88
180	27.833	−102.17	−66.241	−0.757 11	0.321 38	0.568 55	246.79
185	26.983	−100.47	−63.408	−0.741 59	0.320 52	0.564 70	250.60
190	26.189	−98.778	−60.594	−0.726 57	0.319 77	0.561 30	254.34
195	25.444	−97.097	−57.795	−0.712 03	0.319 11	0.558 29	258.00
200	24.743	−95.426	−55.010	−0.697 93	0.318 53	0.555 60	261.59
210	23.458	−92.106	−49.478	−0.670 94	0.317 57	0.551 03	268.58
220	22.309	−88.812	−43.987	−0.645 39	0.316 81	0.547 31	275.34
230	21.272	−85.539	−38.530	−0.621 13	0.316 20	0.544 23	281.89
240	20.332	−82.284	−33.100	−0.598 03	0.315 70	0.541 66	288.26
250	19.475	−79.042	−27.695	−0.575 96	0.315 29	0.539 48	294.47
260	18.690	−75.813	−22.310	−0.554 84	0.314 95	0.537 62	300.52
270	17.968	−72.595	−16.942	−0.534 58	0.314 66	0.536 02	306.44
280	17.302	−69.385	−11.589	−0.515 11	0.314 41	0.534 63	312.22
290	16.685	−66.183	−6.2486	−0.496 37	0.314 20	0.533 42	317.88
300	16.111	−62.988	0.919 89	−0.478 31	0.314 02	0.532 35	323.44
310	15.577	−59.799	4.3989	−0.460 87	0.313 87	0.531 41	328.88
320	15.077	−56.615	9.7087	−0.444 01	0.313 73	0.530 58	334.23
330	14.610	−53.436	15.011	−0.427 70	0.313 61	0.529 84	339.49
340	14.171	−50.261	20.306	−0.411 89	0.313 51	0.529 17	344.66
350	13.758	−47.090	25.594	−0.396 56	0.313 41	0.528 57	349.74
375	12.826	−39.175	38.792	−0.360 13	0.313 22	0.527 31	362.12
400	12.014	−31.277	51.962	−0.326 14	0.313 08	0.526 32	374.06
425	11.299	−23.391	65.110	−0.294 25	0.312 97	0.525 52	385.61
450	10.666	−15.516	78.239	−0.264 23	0.312 87	0.524 87	396.80
475	10.101	−7.6498	91.354	−0.235 87	0.312 80	0.524 33	407.67
500	9.5926	0.209 66	104.46	−0.208 99	0.312 74	0.523 88	418.25
525	9.1336	8.0632	117.55	−0.183 44	0.312 69	0.523 50	428.56
550	8.7169	15.912	130.63	−0.159 09	0.312 65	0.523 18	438.62
575	8.3367	23.756	143.71	−0.135 84	0.312 61	0.522 90	448.45
600	7.9885	31.597	156.78	−0.113 59	0.312 58	0.522 66	458.06
625	7.6683	39.434	169.84	−0.092 26	0.312 55	0.522 45	467.47
650	7.3729	47.269	182.90	−0.071 77	0.312 53	0.522 27	476.69
675	7.0996	55.101	195.95	−0.052 07	0.312 51	0.522 11	485.73
700	6.8458	62.931	209.01	−0.033 08	0.312 49	0.521 97	494.61

TABLE 34. Thermodynamic properties of argon—Continued

Temperature (K)	Density (kg m^{-3})	Internal energy (kJ kg^{-1})	Enthalpy (kJ kg^{-1})	Entropy (kJ kg^{-1} K^{-1})	c_v (kJ kg^{-1} K^{-1})	c_p (kJ kg^{-1} K^{-1})	w (m s^{-1})
			1.5 MPa isobar				
84.164[a]	1418.48	−276.57	−275.52	−2.5435	0.549 90	1.1108	866.82
85	1413.45	−275.65	−274.59	−2.5326	0.546 55	1.1107	861.17
90	1382.90	−270.11	−269.03	−2.4690	0.528 41	1.1148	826.85
95	1351.35	−264.54	−263.43	−2.4084	0.512 78	1.1262	791.53
100	1318.51	−258.89	−257.75	−2.3502	0.498 95	1.1443	754.99
105	1284.03	−253.14	−251.97	−2.2938	0.486 56	1.1701	716.91
110	1247.47	−247.24	−246.04	−2.2386	0.475 48	1.2053	676.85
115	1208.19	−241.14	−239.90	−2.1840	0.465 77	1.2539	634.21
120	1165.24	−234.75	−233.46	−2.1293	0.457 71	1.3233	587.99
123.964[b]	1127.54	−229.40	−228.07	−2.0851	0.452 95	1.4031	547.70
123.964[b]	74.861	−127.60	−107.56	−1.1129	0.402 56	0.956 21	185.29
125	73.538	−126.98	−106.58	−1.1051	0.396 88	0.927 80	187.02
130	68.075	−124.25	−102.21	−1.0708	0.376 69	0.829 54	194.58
135	63.690	−121.78	−98.229	−1.0407	0.363 61	0.767 95	201.24
140	60.030	−119.49	−94.502	−1.0136	0.354 40	0.725 40	207.29
145	56.894	−117.32	−90.957	−0.988 71	0.347 56	0.694 18	212.89
150	54.157	−115.25	−87.548	−0.965 60	0.342 30	0.670 30	218.16
155	51.734	−113.24	−84.245	−0.943 94	0.338 15	0.651 46	223.15
160	49.565	−111.29	−81.027	−0.923 50	0.334 82	0.636 26	227.91
165	47.606	−109.39	−77.878	−0.904 12	0.332 08	0.623 75	232.48
170	45.824	−107.52	−74.786	−0.885 66	0.329 82	0.613 30	236.89
175	44.192	−105.69	−71.743	−0.868 01	0.327 92	0.604 45	241.14
180	42.690	−103.88	−68.740	−0.851 09	0.326 30	0.596 88	245.28
185	41.301	−102.09	−65.772	−0.834 83	0.324 93	0.590 34	249.29
190	40.011	−100.32	−62.835	−0.819 16	0.323 74	0.584 64	253.21
195	38.809	−98.575	−59.924	−0.804 04	0.322 71	0.579 64	257.03
200	37.686	−96.841	−57.037	−0.789 43	0.321 81	0.575 23	260.76
210	35.641	−93.410	−51.324	−0.761 55	0.320 32	0.567 80	268.00
220	33.826	−90.021	−45.677	−0.735 28	0.319 15	0.561 83	274.96
230	32.201	−86.666	−40.084	−0.710 41	0.318 21	0.556 94	281.69
240	30.736	−83.338	−34.535	−0.686 80	0.317 45	0.552 88	288.21
250	29.406	−80.033	−29.024	−0.664 30	0.316 83	0.549 47	294.54
260	28.193	−76.748	−23.544	−0.642 81	0.316 31	0.546 58	300.70
270	27.082	−73.479	−18.091	−0.622 23	0.315 88	0.544 10	306.70
280	26.059	−70.223	−12.661	−0.602 48	0.315 51	0.541 96	312.57
290	25.113	−66.980	−7.2507	−0.583 49	0.315 20	0.540 10	318.30
300	24.237	−63.747	−1.8580	−0.565 21	0.314 93	0.538 47	323.91
310	23.422	−60.524	3.5194	−0.547 58	0.314 69	0.537 03	329.42
320	22.662	−57.308	8.8832	−0.530 55	0.314 49	0.535 76	334.81
330	21.951	−54.100	14.235	−0.514 08	0.314 31	0.534 63	340.11
340	21.285	−50.897	19.576	−0.498 14	0.314 15	0.533 62	345.32
350	20.659	−47.701	24.908	−0.482 68	0.314 02	0.532 71	350.43
375	19.248	−39.731	38.201	−0.446 00	0.313 73	0.530 80	362.88
400	18.021	−31.785	51.451	−0.411 79	0.313 51	0.529 30	374.87
425	16.944	−23.859	64.668	−0.379 74	0.313 34	0.528 10	386.45
450	15.990	−15.949	77.858	−0.349 58	0.313 21	0.527 12	397.67
475	15.140	−8.0520	91.026	−0.321 10	0.313 10	0.526 31	408.57
500	14.376	−0.16527	104.17	−0.294 12	0.313 01	0.525 64	419.16
525	13.687	7.7126	117.31	−0.268 49	0.312 94	0.525 07	429.48
550	13.061	15.583	130.43	−0.244 08	0.312 87	0.524 59	439.55
575	12.490	23.447	143.54	−0.220 77	0.312 82	0.524 17	449.38
600	11.968	31.305	156.64	−0.198 47	0.312 77	0.523 81	458.99
625	11.488	39.159	169.73	−0.177 09	0.312 73	0.523 50	468.40
650	11.045	47.008	182.81	−0.156 56	0.312 70	0.523 23	477.62
675	10.635	54.854	195.89	−0.136 82	0.312 66	0.522 99	486.66
700	10.255	62.697	208.96	−0.117 80	0.312 64	0.522 77	495.53

TABLE 34. Thermodynamic properties of argon—Continued

Temperature (K)	Density (kg m⁻³)	Internal energy (kJ kg⁻¹)	Enthalpy (kJ kg⁻¹)	Entropy (kJ kg⁻¹ K⁻¹)	c_v (kJ kg⁻¹ K⁻¹)	c_p (kJ kg⁻¹ K⁻¹)	w (m s⁻¹)
			2.0 MPa isobar				
84.290[a]	1419.07	−276.56	−275.15	−2.5434	0.550 01	1.1092	868.34
85	1414.81	−275.78	−274.36	−2.5341	0.547 16	1.1090	863.56
90	1384.44	−270.26	−268.81	−2.4706	0.529 01	1.1126	829.49
95	1353.09	−264.70	−263.22	−2.4102	0.513 37	1.1233	794.49
100	1320.51	−259.08	−257.57	−2.3522	0.499 53	1.1406	758.33
105	1286.35	−253.36	−251.81	−2.2960	0.487 12	1.1650	720.72
110	1250.21	−247.50	−245.90	−2.2410	0.475 99	1.1984	681.29
115	1211.50	−241.45	−239.80	−2.1868	0.466 18	1.2441	639.46
120	1169.35	−235.14	−233.43	−2.1326	0.457 91	1.3085	594.40
125	1122.34	−228.45	−226.66	−2.0773	0.451 79	1.4048	544.65
129.735[b]	1070.92	−221.56	−219.69	−2.0226	0.449 25	1.5548	490.64
129.735[b]	102.11	−129.29	−109.70	−1.1748	0.426 22	1.1595	184.89
130	101.54	−129.09	−109.40	−1.1725	0.424 03	1.1454	185.42
135	92.589	−125.78	−104.18	−1.1331	0.394 15	0.962 55	194.33
140	85.840	−122.94	−99.640	−1.1000	0.376 35	0.861 77	201.78
145	80.413	−120.38	−95.504	−1.0710	0.364 34	0.796 95	208.38
150	75.879	−118.00	−91.639	−1.0448	0.355 66	0.751 47	214.39
155	71.993	−115.75	−87.970	−1.0207	0.349 09	0.717 74	219.96
160	68.600	−113.60	−84.449	−0.998 36	0.343 97	0.691 71	225.19
165	65.596	−111.53	−81.044	−0.977 40	0.339 87	0.671 04	230.15
170	62.905	−109.53	−77.732	−0.957 63	0.336 53	0.654 24	234.89
175	60.475	−107.57	−74.496	−0.938 87	0.333 78	0.640 35	239.42
180	58.263	−105.65	−71.325	−0.921 00	0.331 47	0.628 68	243.80
185	56.236	−103.77	−68.207	−0.903 91	0.329 51	0.618 75	248.03
190	54.370	−101.92	−65.135	−0.887 53	0.327 84	0.610 22	252.13
195	52.643	−100.09	−62.103	−0.871 77	0.326 40	0.602 83	256.11
200	51.039	−98.291	−59.105	−0.856 59	0.325 15	0.596 36	259.99
210	48.144	−94.740	−53.197	−0.827 77	0.323 10	0.585 61	267.48
220	45.596	−91.249	−47.386	−0.800 73	0.321 50	0.577 08	274.65
230	43.331	−87.807	−41.650	−0.775 24	0.320 23	0.570 17	281.54
240	41.300	−84.404	−35.978	−0.751 09	0.319 21	0.564 49	288.20
250	39.467	−81.033	−30.358	−0.728 15	0.318 37	0.559 75	294.66
260	37.801	−77.689	−24.781	−0.706 28	0.317 67	0.555 75	300.92
270	36.280	−74.367	−19.241	−0.685 37	0.317 09	0.552 34	307.01
280	34.884	−71.065	−13.732	−0.665 33	0.316 60	0.549 41	312.96
290	33.597	−67.780	−8.2510	−0.646 10	0.316 18	0.546 87	318.76
300	32.407	−64.508	−2.7936	−0.627 60	0.315 82	0.544 65	324.43
310	31.303	−61.249	2.6429	−0.609 77	0.315 51	0.542 70	329.98
320	30.274	−58.002	8.0612	−0.592 57	0.315 24	0.540 98	335.42
330	29.314	−54.764	13.463	−0.575 95	0.315 00	0.539 45	340.76
340	28.415	−51.534	18.851	−0.559 86	0.314 80	0.538 08	346.00
350	27.572	−48.312	24.225	−0.544 28	0.314 61	0.536 86	351.15
375	25.674	−40.286	37.613	−0.507 33	0.314 24	0.534 30	363.66
400	24.028	−32.293	50.945	−0.472 92	0.313 95	0.532 29	375.69
425	22.584	−24.327	64.231	−0.440 70	0.313 72	0.530 68	387.31
450	21.308	−16.381	77.481	−0.410 40	0.313 54	0.529 37	398.56
475	20.171	−8.4531	90.701	−0.381 81	0.313 40	0.528 29	409.47
500	19.150	−0.53914	103.90	−0.354 74	0.313 28	0.527 39	420.08
525	18.230	7.3630	117.07	−0.329 03	0.313 18	0.526 63	430.41
550	17.395	15.255	130.23	−0.304 54	0.313 09	0.525 99	440.48
575	16.634	23.139	143.37	−0.281 17	0.313 02	0.525 44	450.32
600	15.938	31.015	156.50	−0.258 82	0.312 96	0.524 96	459.93
625	15.298	38.885	169.62	−0.237 40	0.312 91	0.524 54	469.34
650	14.708	46.749	182.73	−0.216 83	0.312 86	0.524 18	478.56
675	14.162	54.608	195.83	−0.197 06	0.312 82	0.523 86	487.59
700	13.656	62.463	208.92	−0.178 01	0.312 78	0.523 58	496.46

TABLE 34. Thermodynamic properties of argon—Continued

Temperature (K)	Density (kg m^{-3})	Internal energy (kJ kg^{-1})	Enthalpy (kJ kg^{-1})	Entropy (kJ kg^{-1} K^{-1})	c_v (kJ kg^{-1} K^{-1})	c_p (kJ kg^{-1} K^{-1})	w (m s^{-1})
			3.0 MPa isobar				
84.539[a]	1420.24	−276.53	−274.42	−2.5430	0.550 24	1.1059	871.33
85	1417.51	−276.03	−273.91	−2.5370	0.548 39	1.1057	868.28
90	1387.46	−270.54	−268.38	−2.4738	0.530 22	1.1083	834.70
95	1356.52	−265.03	−262.81	−2.4136	0.514 57	1.1177	800.29
100	1324.43	−259.45	−257.19	−2.3559	0.500 70	1.1334	764.85
105	1290.88	−253.79	−251.47	−2.3001	0.488 24	1.1555	728.15
110	1255.53	−248.01	−245.62	−2.2457	0.477 03	1.1856	689.85
115	1217.87	−242.06	−239.60	−2.1922	0.467 06	1.2261	649.52
120	1177.19	−235.88	−233.33	−2.1389	0.458 47	1.2820	606.52
125	1132.38	−229.39	−226.74	−2.0850	0.451 66	1.3623	559.80
130	1081.51	−222.41	−219.64	−2.0293	0.447 54	1.4878	507.52
135	1020.52	−214.63	−211.69	−1.9694	0.448 45	1.7159	445.83
138.714[b]	962.59	−207.86	−204.74	−1.9186	0.456 53	2.0789	388.26
138.714[b]	166.18	−134.28	−116.23	−1.2805	0.481 87	1.8915	182.24
140	159.47	−132.77	−113.96	−1.2642	0.461 95	1.6572	185.90
145	141.19	−128.20	−106.95	−1.2150	0.416 09	1.2209	197.07
150	128.93	−124.64	−101.37	−1.1772	0.392 03	1.0311	205.67
155	119.65	−121.58	−96.508	−1.1453	0.376 69	0.921 56	212.97
160	112.19	−118.83	−92.092	−1.1172	0.365 89	0.849 39	219.47
165	105.97	−116.29	−87.980	−1.0919	0.357 84	0.797 98	225.40
170	100.64	−113.90	−84.091	−1.0687	0.351 61	0.759 40	230.90
175	95.992	−111.62	−80.372	−1.0471	0.346 64	0.729 37	236.08
180	91.878	−109.44	−76.787	−1.0269	0.342 60	0.705 34	240.99
185	88.197	−107.33	−73.311	−1.0079	0.339 26	0.685 68	245.67
190	84.872	−105.27	−69.925	−0.989 81	0.336 46	0.669 32	250.16
195	81.847	−103.27	−66.614	−0.972 61	0.334 09	0.655 51	254.49
200	79.075	−101.30	−63.366	−0.956 17	0.332 06	0.643 70	258.67
210	74.161	−97.482	−57.029	−0.925 24	0.328 77	0.624 61	266.66
220	69.919	−93.767	−50.860	−0.896 54	0.326 26	0.609 91	274.23
230	66.204	−90.135	−44.821	−0.869 70	0.324 29	0.598 28	281.46
240	62.915	−86.570	−38.887	−0.844 44	0.322 71	0.588 88	288.39
250	59.976	−83.058	−33.038	−0.820 56	0.321 43	0.581 16	295.07
260	57.327	−79.591	−27.259	−0.797 90	0.320 38	0.574 72	301.53
270	54.925	−76.160	−21.540	−0.776 31	0.319 50	0.569 28	307.79
280	52.734	−72.760	−15.871	−0.755 69	0.318 76	0.564 65	313.87
290	50.726	−69.387	−10.245	−0.735 95	0.318 13	0.560 66	319.80
300	48.876	−66.036	−4.6561	−0.717 00	0.317 59	0.557 19	325.58
310	47.166	−62.705	0.900 34	−0.698 78	0.317 13	0.554 17	331.23
320	45.579	−59.391	6.4284	−0.681 23	0.316 73	0.551 50	336.75
330	44.102	−56.093	11.931	−0.664 30	0.316 38	0.549 15	342.16
340	42.723	−52.807	17.412	−0.647 94	0.316 07	0.547 05	347.46
350	41.432	−49.534	22.873	−0.632 11	0.315 79	0.545 18	352.67
375	38.537	−41.395	36.452	−0.594 63	0.315 23	0.541 28	365.29
400	36.036	−33.306	49.944	−0.559 80	0.314 80	0.538 23	377.41
425	33.850	−25.258	63.368	−0.527 25	0.314 47	0.535 80	389.09
450	31.922	−17.242	76.738	−0.496 68	0.314 20	0.533 83	400.38
475	30.207	−9.2522	90.063	−0.467 86	0.313 99	0.532 21	411.32
500	28.671	−1.2836	103.35	−0.440 60	0.313 81	0.530 86	421.95
525	27.287	6.6669	116.61	−0.414 72	0.313 66	0.529 73	432.29
550	26.033	14.602	129.84	−0.390 10	0.313 54	0.528 77	442.37
575	24.892	22.525	143.05	−0.366 62	0.313 43	0.527 94	452.21
600	23.847	30.437	156.24	−0.344 16	0.313 34	0.527 23	461.82
625	22.888	38.338	169.41	−0.322 65	0.313 26	0.526 61	471.23
650	22.004	46.232	182.57	−0.302 01	0.313 19	0.526 07	480.44
675	21.187	54.118	195.71	−0.282 17	0.313 13	0.525 59	489.47
700	20.429	61.998	208.85	−0.263 06	0.313 07	0.525 17	498.32

TABLE 34. Thermodynamic properties of argon—Continued

Temperature (K)	Density (kg m^{-3})	Internal energy (kJ kg^{-1})	Enthalpy (kJ kg^{-1})	Entropy (kJ kg^{-1} K^{-1})	c_v (kJ kg^{-1} K^{-1})	c_p (kJ kg^{-1} K^{-1})	w (m s^{-1})
			4.0 MPa isobar				
84.789[a]	1421.41	−276.50	−273.69	−2.5427	0.550 47	1.1027	874.29
85	1420.16	−276.27	−273.45	−2.5400	0.549 62	1.1026	872.90
90	1390.44	−270.82	−267.94	−2.4769	0.531 43	1.1042	839.79
95	1359.88	−265.34	−262.40	−2.4170	0.515 76	1.1125	805.94
100	1328.25	−259.82	−256.80	−2.3596	0.501 88	1.1266	771.18
105	1295.28	−254.21	−251.12	−2.3042	0.489 39	1.1467	735.31
110	1260.66	−248.50	−245.33	−2.2503	0.478 11	1.1738	698.05
115	1223.95	−242.64	−239.37	−2.1973	0.468 01	1.2100	659.06
120	1184.58	−236.58	−233.21	−2.1449	0.459 18	1.2588	617.83
125	1141.65	−230.25	−226.75	−2.0922	0.451 89	1.3270	573.62
130	1093.72	−223.54	−219.88	−2.0383	0.446 71	1.4279	525.19
135	1038.14	−216.22	−212.37	−1.9816	0.444 99	1.5937	470.27
140	968.76	−207.81	−203.68	−1.9185	0.450 35	1.9268	403.80
145	862.44	−196.53	−191.89	−1.8358	0.483 02	3.1513	306.38
145.701[b]	838.50	194.27	−189.49	−1.8193	0.498 10	3.7497	284.49
145.701[b]	256.92	−142.44	−126.88	−1.3896	0.581 84	4.4472	175.43
150	209.45	−134.47	−115.38	−1.3116	0.461 06	1.8982	193.39
155	183.74	−129.23	−107.46	−1.2597	0.418 28	1.3609	204.64
160	166.99	−125.25	−101.30	−1.2205	0.395 18	1.1303	213.25
165	154.53	−121.89	−96.001	−1.1879	0.380 13	0.998 54	220.56
170	144.63	−118.90	−91.238	−1.1595	0.369 38	0.912 27	227.05
175	136.43	−116.16	−86.837	−1.1339	0.361 27	0.851 09	232.98
180	129.46	−113.60	−82.701	−1.1106	0.354 92	0.805 33	238.48
185	123.42	−111.18	−78.767	−1.0891	0.349 83	0.769 79	243.65
190	118.09	−108.86	−74.991	−1.0689	0.345 65	0.741 38	248.55
195	113.33	−106.64	−71.344	−1.0500	0.342 17	0.718 16	253.22
200	109.05	−104.48	−67.803	−1.0321	0.339 23	0.698 84	257.70
210	101.61	−100.34	−60.974	−0.998 74	0.334 57	0.668 58	266.18
220	95.328	−96.366	−54.406	−0.968 18	0.331 07	0.646 03	274.13
230	89.914	−92.523	−48.037	−0.939 86	0.328 35	0.628 62	281.66
240	85.182	−88.780	−41.822	−0.913 41	0.326 20	0.614 83	288.84
250	80.996	−85.116	−35.731	−0.888 54	0.324 47	0.603 67	295.73
260	77.258	−81.517	−29.742	−0.865 05	0.323 05	0.594 47	302.36
270	73.891	−77.970	−23.837	−0.842 77	0.321 87	0.586 79	308.77
280	70.839	−74.468	−18.002	−0.821 55	0.320 89	0.580 29	314.98
290	68.056	−71.003	−12.228	−0.801 28	0.320 05	0.574 74	321.02
300	65.504	−67.570	−6.5049	−0.781 88	0.319 34	0.569 95	326.89
310	63.153	−64.165	−0.826 70	−0.763 26	0.318 72	0.565 78	332.62
320	60.980	−60.783	4.8125	−0.745 36	0.318 19	0.562 13	338.21
330	58.962	−57.423	10.417	−0.728 11	0.317 72	0.558 91	343.69
340	57.084	−54.080	15.992	−0.711 47	0.317 32	0.556 06	349.04
350	55.329	−50.755	21.540	−0.695 39	0.316 95	0.553 52	354.30
375	51.408	−42.500	35.309	−0.657 39	0.316 21	0.548 24	367.01
400	48.032	−34.316	48.961	−0.622 14	0.315 65	0.544 14	379.20
425	45.092	−26.185	62.523	−0.589 25	0.315 21	0.540 89	390.93
450	42.504	−18.099	76.011	−0.558 41	0.314 86	0.538 25	402.25
475	40.207	−10.047	89.439	−0.529 37	0.314 58	0.536 09	413.22
500	38.153	−2.0237	102.82	−0.501 92	0.314 34	0.534 30	423.86
525	36.304	5.9752	116.16	−0.475 89	0.314 14	0.532 79	434.21
550	34.630	13.954	129.46	−0.451 13	0.313 98	0.531 51	444.30
575	33.108	21.915	142.73	−0.427 53	0.313 84	0.530 41	454.13
600	31.716	29.862	155.98	−0.404 98	0.313 72	0.529 47	463.74
625	30.439	37.796	169.21	−0.383 38	0.313 61	0.528 65	473.14
650	29.262	45.719	182.42	−0.362 66	0.313 52	0.527 93	482.34
675	28.174	53.632	195.61	−0.342 75	0.313 44	0.527 30	491.35
700	27.166	61.537	208.78	−0.323 58	0.313 36	0.526 74	500.20

TABLE 34. Thermodynamic properties of argon—Continued

Temperature (K)	Density (kg m^{-3})	Internal energy (kJ kg^{-1})	Enthalpy (kJ kg^{-1})	Entropy (kJ kg^{-1} K^{-1})	c_v (kJ kg^{-1} K^{-1})	c_p (kJ kg^{-1} K^{-1})	w (m s^{-1})
				5.0 MPa isobar			
85.037[a]	1422.56	−276.47	−272.95	−2.5424	0.55070	1.0996	877.21
90	1393.36	−271.09	−267.50	−2.4800	0.53263	1.1003	844.78
95	1363.16	−265.65	−261.98	−2.4204	0.51695	1.1075	811.46
100	1331.98	−260.17	−256.41	−2.3633	0.503 06	1.1202	777.34
105	1299.56	−254.62	−250.77	−2.3082	0.490 55	1.1385	742.24
110	1265.61	−248.97	−245.02	−2.2547	0.479 23	1.1630	705.93
115	1229.78	−243.19	−239.13	−2.2023	0.469 03	1.1954	668.13
120	1191.57	−237.24	−233.05	−2.1506	0.460 01	1.2384	628.46
125	1150.27	−231.07	−226.72	−2.0989	0.452 36	1.2969	586.37
130	1104.78	−224.56	−220.04	−2.0465	0.446 45	1.3801	541.00
135	1053.23	−217.59	−212.85	−1.9922	0.443 11	1.5074	490.95
140	991.96	−209.86	−204.81	−1.9338	0.444 18	1.7280	433.54
145	911.68	−200.63	−195.14	−1.8660	0.455 62	2.2213	362.47
150	765.37	−186.33	−179.79	−1.7622	0.526 22	5.1511	248.19
155	292.81	−141.64	−124.56	−1.3984	0.500 79	3.0736	192.82
160	243.26	−133.87	−113.31	−1.3268	0.438 17	1.7602	206.39
165	216.25	−128.79	−105.66	−1.2797	0.408 73	1.3539	215.83
170	197.63	−124.75	−99.454	−1.2426	0.390 55	1.1490	223.58
175	183.46	−121.30	−94.045	−1.2113	0.377 91	1.0236	230.36
180	172.07	−118.21	−89.152	−1.1837	0.368 50	0.938 49	236.49
185	162.58	−115.38	−84.622	−1.1589	0.361 20	0.876 70	242.15
190	154.47	−112.73	−80.361	−1.1361	0.355 36	0.829 73	247.45
195	147.42	−110.23	−76.308	−1.1151	0.350 60	0.792 81	252.44
200	141.19	−107.84	−72.421	−1.0954	0.346 64	0.763 03	257.20
210	130.60	−103.31	−65.029	−1.0593	0.340 46	0.717 97	266.11
220	121.86	−99.049	−58.020	−1.0267	0.335 89	0.685 57	274.40
230	114.47	−94.970	−51.291	−0.996 79	0.332 39	0.661 22	282.20
240	108.10	−91.033	−44.777	−0.969 07	0.329 66	0.642 30	289.60
250	102.52	−87.205	−38.432	−0.943 16	0.327 46	0.627 22	296.66
260	97.577	−83.465	−32.223	−0.918 81	0.325 68	0.614 96	303.44
270	93.161	−79.796	−26.126	−0.895 80	0.324 21	0.604 81	309.98
280	89.182	−76.187	−20.122	−0.873 96	0.322 98	0.596 29	316.29
290	85.571	−72.627	−14.196	−0.853 17	0.321 94	0.589 07	322.42
300	82.275	−69.109	−8.3370	−0.833 30	0.321 05	0.582 87	328.37
310	79.251	−65.627	−2.5358	−0.814 28	0.320 29	0.577 50	334.17
320	76.463	−62.176	3.2153	−0.796 02	0.319 63	0.572 82	339.82
330	73.883	−58.752	8.9225	−0.778 46	0.319 05	0.568 71	345.34
340	71.487	−55.352	14.591	−0.761 54	0.318 54	0.565 08	350.74
350	69.254	−51.973	20.225	−0.745 20	0.318 10	0.561 85	356.03
375	64.278	−43.603	34.184	−0.706 68	0.317 18	0.555 18	368.82
400	60.011	−35.321	47.997	−0.671 02	0.316 49	0.550 01	381.06
425	56.305	−27.108	61.694	−0.637 80	0.315 94	0.545 93	392.83
450	53.050	−18.950	75.300	−0.606 69	0.315 51	0.542 63	404.18
475	50.167	−10.837	88.831	−0.577 43	0.315 16	0.539 93	415.16
500	47.592	−2.7591	102.30	−0.549 79	0.314 87	0.537 69	425.81
525	45.278	5.2880	115.72	−0.523 61	0.314 62	0.535 81	436.17
550	43.184	13.310	129.09	−0.498 72	0.314 42	0.534 22	446.25
575	41.281	21.310	142.43	−0.475 00	0.314 24	0.532 85	456.08
600	39.543	29.292	155.74	−0.452 35	0.314 09	0.531 68	465.68
625	37.948	37.258	169.02	−0.430 67	0.313 96	0.530 66	475.07
650	36.480	45.209	182.27	−0.409 87	0.313 84	0.529 76	484.26
675	35.123	53.149	195.50	−0.389 89	0.313 74	0.528 98	493.26
700	33.866	61.078	208.72	−0.370 67	0.313 65	0.528 28	502.09

TABLE 34. Thermodynamic properties of argon—Continued

Temperature (K)	Density (kg m⁻³)	Internal energy (kJ kg⁻¹)	Enthalpy (kJ kg⁻¹)	Entropy (kJ kg⁻¹ K⁻¹)	c_v (kJ kg⁻¹ K⁻¹)	c_p (kJ kg⁻¹ K⁻¹)	w (m s⁻¹)
			6.0 MPa isobar				
85.286[a]	1423.70	−276.44	−272.22	−2.5420	0.550 94	1.0965	880.09
90	1396.23	−271.35	−267.06	−2.4831	0.533 83	1.0966	849.67
95	1366.38	−265.95	−261.56	−2.4236	0.518 14	1.1028	816.85
100	1335.62	−260.51	−256.02	−2.3668	0.504 24	1.1142	783.33
105	1303.71	−255.01	−250.41	−2.3121	0.491 71	1.1307	748.98
110	1270.40	−249.43	−244.70	−2.2590	0.480 36	1.1530	713.51
115	1235.38	−243.73	−238.87	−2.2071	0.470 08	1.1820	676.80
120	1198.22	−237.87	−232.87	−2.1560	0.460 92	1.2202	638.51
125	1158.35	−231.83	−226.65	−2.1052	0.452 99	1.2709	598.23
130	1114.91	−225.51	−220.13	−2.0541	0.446 56	1.3408	555.38
135	1066.55	−218.81	−213.19	−2.0017	0.442 15	1.4422	509.04
140	1010.86	−211.54	−205.61	−1.9466	0.440 79	1.6020	457.69
145	942.94	−203.32	−196.96	−1.8859	0.445 02	1.8919	398.54
150	849.71	−193.12	−186.06	−1.8121	0.462 89	2.5932	325.58
155	662.69	−175.62	−166.56	−1.6846	0.540 65	6.7737	222.04
160	376.01	−147.77	−131.81	−1.4635	0.507 51	3.8862	200.04
165	301.84	−137.90	−118.02	−1.3785	0.446 02	2.0826	212.11
170	264.31	−131.86	−109.16	−1.3255	0.415 49	1.5393	221.16
175	239.46	−127.24	−102.18	−1.2851	0.396 46	1.2753	228.72
180	221.03	−123.37	−96.230	−1.2515	0.383 15	1.1179	235.39
185	206.48	−119.98	−90.918	−1.2224	0.373 20	1.0130	241.45
190	194.52	−116.90	−86.051	−1.1964	0.365 46	0.937 85	247.06
195	184.40	−114.05	−81.509	−1.1728	0.359 25	0.881 33	252.32
200	175.67	−111.37	−77.217	−1.1511	0.354 17	0.837 27	257.29
210	161.19	−106.41	−69.186	−1.1119	0.346 37	0.773 04	266.56
220	149.55	−101.81	−61.691	−1.0770	0.340 69	0.728 55	275.11
230	139.87	−97.474	−54.576	−1.0454	0.336 40	0.695 99	283.12
240	131.64	−93.325	−47.745	−1.0163	0.333 06	0.671 19	290.69
250	124.51	−89.322	−41.135	−0.989 33	0.330 41	0.651 72	297.89
260	118.26	−85.433	−34.698	−0.964 09	0.328 26	0.636 07	304.78
270	112.71	−81.636	−28.404	−0.940 33	0.326 50	0.623 26	311.42
280	107.74	−77.915	−22.226	−0.917 86	0.325 03	0.612 58	317.81
290	103.25	−74.257	−16.146	−0.896 52	0.323 78	0.603 58	324.01
300	99.172	−70.651	−10.150	−0.876 20	0.322 73	0.595 91	330.02
310	95.442	−67.090	−4.2247	−0.856 77	0.321 82	0.589 29	335.87
320	92.014	−63.569	1.6389	−0.838 15	0.321 04	0.583 55	341.57
330	88.851	−60.080	7.4487	−0.820 27	0.320 35	0.578 52	347.13
340	85.920	−56.621	13.211	−0.803 07	0.319 75	0.574 09	352.56
350	83.194	−53.188	18.932	−0.786 49	0.319 22	0.570 16	357.88
375	77.140	−44.701	33.080	−0.747 44	0.318 14	0.562 07	370.73
400	71.967	−36.321	47.051	−0.711 37	0.317 31	0.555 83	383.01
425	67.485	−28.026	60.883	−0.677 83	0.316 66	0.550 91	394.80
450	63.558	−19.797	74.605	−0.646 45	0.316 15	0.546 96	406.16
475	60.085	−11.621	88.237	−0.616 97	0.315 73	0.543 72	417.15
500	56.988	−3.4898	101.80	−0.589 15	0.315 39	0.541 04	427.80
525	54.207	4.6054	115.29	−0.562 81	0.315 10	0.538 79	438.15
550	51.694	12.670	128.74	−0.537 79	0.314 85	0.536 89	448.23
575	49.411	20.709	142.14	−0.513 96	0.314 64	0.535 26	458.05
600	47.327	28.725	155.50	−0.491 21	0.314 46	0.533 85	467.64
625	45.417	36.723	168.83	−0.469 44	0.314 31	0.532 64	477.02
650	43.658	44.704	182.14	−0.448 58	0.314 17	0.531 57	486.19
675	42.034	52.670	195.41	−0.428 53	0.314 05	0.530 64	495.18
700	40.528	60.623	208.67	−0.409 25	0.313 94	0.529 81	503.99

TABLE 34. Thermodynamic properties of argon—Continued

Temperature (K)	Density (kg m^{-3})	Internal energy (kJ kg^{-1})	Enthalpy (kJ kg^{-1})	Entropy (kJ kg^{-1} K^{-1})	c_v (kJ kg^{-1} K^{-1})	c_p (kJ kg^{-1} K^{-1})	w (m s^{-1})
			8.0 MPa isobar				
85.781[a]	1425.95	−276.37	−270.76	−2.5413	0.551 42	1.0906	885.77
90	1401.82	−271.87	−266.16	−2.4890	0.536 22	1.0897	859.19
95	1372.64	−266.53	−260.71	−2.4300	0.520 51	1.0940	827.31
100	1342.66	−261.17	−255.21	−2.3737	0.506 60	1.1031	794.88
105	1311.70	−255.77	−249.67	−2.3196	0.494 05	1.1167	761.80
110	1279.55	−250.29	−244.04	−2.2672	0.482 64	1.1350	727.92
115	1245.97	−244.73	−238.31	−2.2162	0.472 27	1.1587	693.11
120	1210.64	−239.05	−232.44	−2.1663	0.462 90	1.1890	657.17
125	1173.19	−233.22	−226.40	−2.1170	0.454 60	1.2281	619.87
130	1133.05	−227.20	−220.14	−2.0679	0.447 48	1.2794	580.93
135	1089.45	−220.92	−213.58	−2.0184	0.441 78	1.3485	539.95
140	1041.20	−214.29	−206.61	−1.9677	0.437 89	1.4456	496.37
145	986.38	−207.16	−199.05	−1.9146	0.436 50	1.5896	449.46
150	921.62	−199.25	−190.57	−1.8572	0.438 88	1.8203	398.37
155	840.50	−190.07	−180.56	−1.7915	0.447 30	2.2279	342.59
160	730.64	−178.63	−167.68	−1.7099	0.464 84	2.9968	284.48
165	585.49	−164.19	−150.53	−1.6044	0.479 01	3.6767	241.35
170	462.68	−151.10	−133.81	−1.5045	0.458 78	2.8723	231.03
175	389.59	−142.12	−121.59	−1.4336	0.432 13	2.0872	233.78
180	343.63	−135.64	−112.36	−1.3815	0.411 88	1.6474	238.94
185	311.47	−130.51	−104.82	−1.3402	0.396 85	1.3872	244.44
190	287.21	−126.19	−98.335	−1.3056	0.385 34	1.2187	249.84
195	267.97	−122.40	−92.550	−1.2756	0.376 26	1.1017	255.04
200	252.14	−118.99	−87.267	−1.2488	0.368 94	1.0159	260.02
210	227.27	−112.94	−77.738	−1.2023	0.357 89	0.899 15	269.41
220	208.27	−107.56	−69.148	−1.1623	0.350 00	0.823 65	278.12
230	193.06	−102.63	−61.189	−1.1269	0.344 14	0.771 04	286.28
240	180.48	−98.009	−53.681	−1.0950	0.339 63	0.732 40	293.98
250	169.81	−93.622	−46.511	−1.0657	0.336 09	0.702 90	301.31
260	160.61	−89.414	−39.603	−1.0386	0.333 24	0.679 70	308.31
270	152.55	−85.345	−32.902	−1.0133	0.330 91	0.661 03	315.04
280	145.41	−81.389	−26.371	−0.989 54	0.328 97	0.645 70	321.52
290	139.02	−77.525	−19.980	−0.967 12	0.327 35	0.632 92	327.78
300	133.26	−73.737	−13.706	−0.945 84	0.325 97	0.622 13	333.85
310	128.03	−70.015	−7.5318	−0.925 60	0.324 79	0.612 91	339.75
320	123.26	−66.347	−1.4434	−0.906 27	0.323 77	0.604 96	345.50
330	118.87	−62.728	4.5708	−0.887 76	0.322 87	0.598 04	351.10
340	114.83	−59.149	10.520	−0.870 00	0.322 09	0.591 97	356.56
350	111.08	−55.607	16.413	−0.852 92	0.321 40	0.586 62	361.91
375	102.81	−46.882	30.935	−0.812 84	0.320 00	0.575 67	374.81
400	95.782	−38.306	45.217	−0.775 96	0.318 92	0.567 29	387.11
425	89.727	−29.845	59.314	−0.741 78	0.318 08	0.560 71	398.92
450	84.444	−21.474	73.263	−0.709 88	0.317 41	0.555 44	410.28
475	79.785	−13.176	87.094	−0.679 97	0.316 87	0.551 14	421.26
500	75.641	−4.9365	100.83	−0.651 79	0.316 41	0.547 59	431.90
525	71.927	3.2542	114.48	−0.625 15	0.316 04	0.544 62	442.23
550	68.577	11.404	128.06	−0.599 87	0.315 72	0.542 11	452.27
575	65.537	19.519	141.59	−0.575 83	0.315 44	0.539 96	462.07
600	62.766	27.605	155.06	−0.552 89	0.315 21	0.538 12	471.63
625	60.227	35.665	168.49	−0.530 95	0.315 00	0.536 51	480.97
650	57.892	43.703	181.89	−0.509 94	0.314 82	0.535 11	490.11
675	55.737	51.721	195.25	−0.489 76	0.314 66	0.533 88	499.06
700	53.741	59.723	208.59	−0.470 37	0.314 51	0.532 80	507.84

TABLE 34. Thermodynamic properties of argon—Continued

Temperature (K)	Density (kg m^{-3})	Internal energy (kJ kg^{-1})	Enthalpy (kJ kg^{-1})	Entropy (kJ kg^{-1} K^{-1})	c_v (kJ kg^{-1} K^{-1})	c_p (kJ kg^{-1} K^{-1})	w (m s^{-1})
			10.0 MPa isobar				
86.275[a]	1428.17	−276.30	−269.30	−2.5406	0.551 91	1.0850	891.32
90	1407.24	−272.37	−265.26	−2.4948	0.538 57	1.0834	868.40
95	1378.68	−267.09	−259.84	−2.4362	0.522 85	1.0860	837.35
100	1349.41	−261.80	−254.39	−2.3803	0.508 93	1.0932	805.91
105	1319.31	−256.48	−248.90	−2.3267	0.496 38	1.1043	773.98
110	1288.18	−251.11	−243.34	−2.2750	0.484 94	1.1193	741.46
115	1255.85	−245.66	−237.70	−2.2249	0.474 50	1.1387	708.26
120	1222.08	−240.13	−231.95	−2.1759	0.465 00	1.1632	674.25
125	1186.59	−234.48	−226.06	−2.1278	0.456 46	1.1941	639.32
130	1149.02	−228.70	−219.99	−2.0802	0.448 93	1.2331	603.33
135	1108.88	−222.72	−213.71	−2.0328	0.442 51	1.2833	566.10
140	1065.51	−216.52	−207.13	−1.9850	0.437 37	1.3491	527.43
145	1017.97	−210.00	−200.18	−1.9362	0.433 76	1.4375	487.14
150	964.88	−203.07	−192.70	−1.8855	0.432 03	1.5594	445.10
155	904.29	−195.56	−184.50	−1.8318	0.432 57	1.7308	401.58
160	833.57	−187.28	−175.28	−1.7732	0.435 63	1.9700	357.76
165	750.34	−178.02	−164.69	−1.7081	0.440 32	2.2700	316.75
170	656.74	−167.92	−152.69	−1.6364	0.442 68	2.4969	284.47
175	565.80	−157.95	−140.27	−1.5644	0.437 28	2.4108	266.06
180	491.85	−149.31	−128.98	−1.5008	0.425 42	2.0914	259.27
185	436.59	−142.25	−119.35	−1.4480	0.412 26	1.7724	258.62
190	395.21	−136.43	−111.13	−1.4041	0.400 30	1.5271	260.68
195	363.25	−131.49	−103.97	−1.3669	0.390 09	1.3477	263.93
200	337.74	−127.18	−97.574	−1.3346	0.381 50	1.2152	267.70
210	299.16	−119.81	−86.387	−1.2799	0.368 15	1.0373	275.72
220	270.90	−113.53	−76.611	−1.2344	0.358 48	0.925 70	283.74
230	248.97	−107.92	−67.754	−1.1951	0.351 26	0.850 14	291.51
240	231.24	−102.78	−59.538	−1.1601	0.345 73	0.795 97	298.98
250	216.50	−97.979	−51.790	−1.1284	0.341 38	0.755 42	306.16
260	203.96	−93.427	−44.399	−1.0995	0.337 90	0.724 04	313.06
270	193.12	−89.070	−37.288	−1.0726	0.335 05	0.699 11	319.72
280	183.60	−84.867	−30.401	−1.0476	0.332 70	0.678 87	326.15
290	175.16	−80.789	−23.699	−1.0240	0.330 72	0.662 16	332.37
300	167.60	−76.814	−17.149	−1.0018	0.329 05	0.648 15	338.42
310	160.78	−72.925	−10.729	−0.980 78	0.327 61	0.636 26	344.29
320	154.58	−69.109	−4.4182	−0.960 75	0.326 37	0.626 05	350.02
330	148.92	−65.355	1.7971	−0.941 62	0.325 29	0.617 22	355.60
340	143.71	−61.655	7.9299	−0.923 31	0.324 34	0.609 51	361.05
350	138.90	−58.002	13.990	−0.905 74	0.323 51	0.602 73	366.38
375	128.34	−49.039	28.878	−0.864 65	0.321 80	0.588 93	379.24
400	119.43	−40.267	43.464	−0.826 99	0.320 49	0.578 43	391.51
425	111.78	−31.641	57.818	−0.792 18	0.319 47	0.570 22	403.28
450	105.13	−23.129	71.989	−0.759 78	0.318 65	0.563 67	414.60
475	99.284	−14.709	86.012	−0.729 45	0.317 98	0.558 35	425.54
500	94.094	−6.3627	99.914	−0.700 93	0.317 43	0.553 95	436.14
525	89.451	1.9223	113.72	−0.673 99	0.316 96	0.550 28	446.42
550	85.268	10.156	127.43	−0.648 47	0.316 57	0.547 18	456.43
575	81.479	18.347	141.08	−0.624 21	0.316 23	0.544 53	466.18
600	78.026	26.500	154.66	−0.601 08	0.315 94	0.542 25	475.69
625	74.866	34.622	168.19	−0.578 99	0.315 68	0.540 28	484.99
650	71.962	42.716	181.68	−0.557 83	0.315 46	0.538 55	494.09
675	69.283	50.786	195.12	−0.537 53	0.315 26	0.537 04	503.00
700	66.802	58.835	208.53	−0.518 03	0.315 08	0.535 70	511.73

TABLE 34. Thermodynamic properties of argon—Continued

Temperature (K)	Density (kg m^{-3})	Internal energy (kJ kg^{-1})	Enthalpy (kJ kg^{-1})	Entropy (kJ kg^{-1} K^{-1})	c_v (kJ kg^{-1} K^{-1})	c_p (kJ kg^{-1} K^{-1})	w (m s^{-1})
				15.0 MPa isobar			
87.501[a]	1433.55	−276.11	−265.64	−2.5388	0.553 13	1.0718	904.80
90	1420.10	−273.53	−262.97	−2.5086	0.544 32	1.0696	890.22
95	1392.88	−268.39	−257.62	−2.4508	0.528 55	1.0690	860.99
100	1365.19	−263.26	−252.27	−2.3959	0.514 62	1.0722	831.63
105	1336.90	−258.12	−246.90	−2.3435	0.502 07	1.0785	802.09
110	1307.91	−252.95	−241.48	−2.2931	0.490 61	1.0877	772.32
115	1278.11	−247.75	−236.01	−2.2445	0.480 09	1.0996	742.28
120	1247.38	−242.51	−230.48	−2.1974	0.470 42	1.1144	711.95
125	1215.59	−237.20	−224.86	−2.1516	0.461 57	1.1325	681.30
130	1182.58	231.83	219.15	2.1067	0.453 51	1.1542	650.35
135	1148.18	−226.38	−213.32	−2.0627	0.446 25	1.1803	619.10
140	1112.18	−220.82	−207.34	−2.0192	0.439 80	1.2117	587.59
145	1074.33	−215.15	−201.19	−1.9761	0.434 15	1.2492	555.90
150	1034.36	−209.34	−194.83	−1.9330	0.429 33	1.2939	524.14
155	991.98	−203.36	−188.24	−1.8897	0.425 30	1.3466	492.55
160	946.91	−197.20	−181.36	−1.8460	0.422 02	1.4070	461.50
165	899.00	−190.84	−174.16	−1.8017	0.419 35	1.4731	431.59
170	848.36	−184.30	−166.62	−1.7568	0.417 05	1.5394	403.63
175	795.54	−177.63	−158.78	−1.7113	0.414 76	1.5965	378.57
180	741.72	−170.92	−150.70	−1.6658	0.412 06	1.6317	357.31
185	688.66	−164.30	−142.52	−1.6209	0.408 62	1.6330	340.45
190	638.31	−157.93	−134.43	−1.5778	0.404 32	1.5965	328.08
195	592.22	−151.93	−126.60	−1.5371	0.399 30	1.5295	319.70
200	551.15	−146.38	−119.16	−1.4995	0.393 86	1.4458	314.53
210	483.76	−136.58	−105.57	−1.4331	0.382 87	1.2741	310.70
220	432.48	−128.26	−93.580	−1.3773	0.372 98	1.1307	311.79
230	392.75	−121.04	−82.846	−1.3296	0.364 66	1.0211	315.29
240	361.11	−114.61	−73.068	−1.2879	0.357 86	0.938 48	319.96
250	335.27	−108.75	−64.012	−1.2510	0.352 31	0.875 42	325.20
260	313.68	−103.33	−55.513	−1.2176	0.347 76	0.826 40	330.71
270	295.31	−98.244	−47.450	−1.1872	0.344 00	0.787 54	336.32
280	279.43	−93.418	−39.737	−1.1591	0.340 86	0.756 16	341.94
290	265.52	−88.801	−32.308	−1.1331	0.338 20	0.730 40	347.53
300	253.20	−84.355	−25.115	−1.1087	0.335 94	0.708 94	353.06
310	242.20	−80.050	−18.118	−1.0857	0.333 99	0.690 84	358.51
320	232.29	−75.863	−11.289	−1.0641	0.332 30	0.675 40	363.87
330	223.30	−71.776	−4.6029	−1.0435	0.330 83	0.662 11	369.15
340	215.10	−67.775	1.9591	−1.0239	0.329 53	0.650 55	374.34
350	207.58	−63.848	8.4130	−1.0052	0.328 38	0.640 44	379.44
375	191.20	−54.297	24.156	−0.961 73	0.326 02	0.619 99	391.83
400	177.52	−45.043	39.454	−0.922 23	0.324 20	0.604 54	403.73
425	165.89	−36.013	54.411	−0.885 95	0.322 77	0.592 54	415.18
450	155.83	−27.157	69.101	−0.852 36	0.321 61	0.583 00	426.25
475	147.04	−18.439	83.576	−0.821 06	0.320 67	0.575 26	436.95
500	139.26	−9.8328	97.876	−0.791 72	0.319 88	0.568 90	447.34
525	132.34	−1.3184	112.03	−0.764 09	0.319 22	0.563 59	457.43
550	126.11	7.1196	126.06	−0.737 98	0.318 65	0.559 11	467.25
575	120.48	15.493	139.99	−0.713 21	0.318 17	0.555 30	476.83
600	115.37	23.812	153.83	−0.689 65	0.317 74	0.552 02	486.19
625	110.69	32.084	167.60	−0.667 18	0.317 37	0.549 17	495.33
650	106.40	40.314	181.29	−0.645 69	0.317 05	0.546 69	504.29
675	102.44	48.510	194.93	−0.625 10	0.316 76	0.544 51	513.06
700	98.783	56.674	208.52	−0.605 33	0.316 50	0.542 58	521.66

TEGELER, SPAN, AND WAGNER

TABLE 3. Thermodynamic properties of argon—Continued

Temperature (K)	Density (kg m^{-3})	Internal energy (kJ kg^{-1})	Enthalpy (kJ kg^{-1})	Entropy (kJ kg^{-1} K^{-1})	c_v (kJ kg^{-1} K^{-1})	c_p (kJ kg^{-1} K^{-1})	w (m s^{-1})
			20.0 MPa isobar				
88.717[a]	1438.74	−275.89	−261.99	−2.5369	0.554 32	1.0599	917.76
90	1432.09	−274.60	−260.63	−2.5216	0.549 85	1.0583	910.63
95	1406.03	−269.57	−255.35	−2.4645	0.534 02	1.0551	882.90
100	1379.63	−264.57	−250.08	−2.4104	0.520 08	1.0554	855.23
105	1352.83	−259.58	−244.79	−2.3589	0.507 52	1.0584	827.58
110	1325.54	−254.58	−239.49	−2.3095	0.496 06	1.0635	799.92
115	1297.70	−249.56	−234.15	−2.2621	0.485 51	1.0707	772.24
120	1269.23	−244.54	−228.78	−2.2163	0.475 78	1.0797	744.54
125	1240.06	−239.48	−223.35	−2.1720	0.466 79	1.0906	716.85
130	1210.13	−234.40	−217.87	−2.1290	0.458 51	1.1035	689.18
135	1179.36	−229.27	−212.31	−2.0871	0.450 90	1.1185	661.58
140	1147.67	−224.11	−206.68	−2.0461	0.443 94	1.1358	634.14
145	1114.98	−218.89	−200.95	−2.0059	0.437 61	1.1555	606.92
150	1081.22	−213.62	−195.12	−1.9664	0.431 88	1.1778	580.04
155	1046.32	−208.29	−189.17	−1.9274	0.426 69	1.2025	553.66
160	1010.24	−202.89	−183.09	−1.8888	0.422 01	1.2292	527.94
165	972.98	−197.43	−176.88	−1.8505	0.417 76	1.2570	503.14
170	934.63	−191.92	−170.52	−1.8126	0.413 87	1.2845	479.54
175	895.36	−186.37	−164.04	−1.7750	0.410 25	1.3095	457.47
180	855.48	−180.81	−157.44	−1.7378	0.406 80	1.3296	437.27
185	815.44	−175.28	−150.75	−1.7012	0.403 44	1.3423	419.21
190	775.74	−169.81	−144.03	−1.6653	0.400 07	1.3454	403.50
195	736.99	−164.45	−137.32	−1.6304	0.396 63	1.3379	390.24
200	699.71	−159.25	−130.67	−1.5968	0.393 11	1.3195	379.38
210	631.35	−149.44	−117.76	−1.5338	0.385 81	1.2562	364.21
220	572.60	−140.54	−105.61	−1.4772	0.378 47	1.1739	355.98
230	523.29	−132.51	−94.289	−1.4269	0.371 50	1.0904	352.48
240	482.15	−125.25	−83.771	−1.3821	0.365 20	1.0151	352.01
250	447.65	−118.63	−73.950	−1.3420	0.359 68	0.950 82	353.46
260	418.42	−112.52	−64.719	−1.3058	0.354 92	0.897 17	356.11
270	393.37	−106.82	−55.977	−1.2728	0.350 83	0.852 63	359.52
280	371.66	−101.45	−47.641	−1.2425	0.347 32	0.815 55	363.42
290	352.65	−96.359	−39.646	−1.2144	0.344 30	0.784 48	367.63
300	335.84	−91.487	−31.936	−1.1883	0.341 69	0.758 24	372.04
310	320.85	−86.802	−24.468	−1.1638	0.339 42	0.735 89	376.56
320	307.38	−82.274	−17.207	−1.1408	0.337 42	0.716 70	381.15
330	295.19	−77.879	−10.125	−1.1190	0.335 67	0.700 09	385.76
340	284.09	−73.597	−3.1984	−1.0983	0.334 12	0.685 60	390.38
350	273.94	−69.415	3.5927	−1.0786	0.332 73	0.672 89	394.99
375	251.92	−59.312	20.077	−1.0331	0.329 87	0.647 10	406.38
400	233.64	−49.604	36.000	−0.991 99	0.327 64	0.627 58	417.53
425	218.14	−40.192	51.492	−0.954 42	0.325 86	0.612 38	428.39
450	204.80	−31.011	66.645	−0.919 77	0.324 42	0.600 29	438.97
475	193.17	−22.011	81.525	−0.887 59	0.323 23	0.590 48	449.27
500	182.91	−13.158	96.183	−0.857 51	0.322 24	0.582 41	459.30
525	173.79	−4.4262	110.66	−0.829 26	0.321 40	0.575 67	469.09
550	165.60	4.2058	124.98	−0.802 62	0.320 68	0.569 98	478.64
575	158.22	12.754	139.16	−0.777 39	0.320 05	0.565 13	487.97
600	151.51	21.229	153.24	−0.753 43	0.319 51	0.560 96	497.10
625	145.38	29.644	167.21	−0.730 61	0.319 03	0.557 34	506.04
650	139.76	38.005	181.11	−0.708 81	0.318 61	0.554 18	514.80
675	134.58	46.320	194.93	−0.687 95	0.318 23	0.551 40	523.39
700	129.80	54.593	208.68	−0.667 94	0.317 89	0.548 95	531.82

TABLE 34. Thermodynamic properties of argon—Continued

Temperature (K)	Density (kg m^{-3})	Internal energy (kJ kg^{-1})	Enthalpy (kJ kg^{-1})	Entropy (kJ kg^{-1} K^{-1})	c_v (kJ kg^{-1} K^{-1})	c_p (kJ kg^{-1} K^{-1})	w (m s^{-1})
			25.0 MPa isobar				
89.922[a]	1443.74	−275.66	−258.34	−2.5349	0.555 45	1.0491	930.31
90	1443.35	−275.58	−258.26	−2.5340	0.555 18	1.0490	929.89
95	1418.28	−270.66	−253.03	−2.4774	0.539 26	1.0436	903.42
100	1393.00	−265.77	−247.82	−2.4239	0.525 28	1.0417	877.15
105	1367.44	−260.89	−242.61	−2.3731	0.512 72	1.0422	851.04
110	1341.54	−256.03	−237.40	−2.3246	0.501 26	1.0445	825.08
115	1315.27	−251.17	−232.16	−2.2781	0.490 70	1.0483	799.25
120	1288.56	−246.31	−226.91	−2.2333	0.480 94	1.0535	773.57
125	1261.40	−241.45	−221.63	−2.1902	0.471 88	1.0600	748.05
130	1233.74	−236.57	−216.31	−2.1485	0.463 49	1.0676	722.75
135	1205.54	−231.69	−210.95	−2.1080	0.455 71	1.0765	697.69
140	1176.78	−226.79	−205.54	−2.0687	0.448 51	1.0865	672.95
145	1147.43	−221.87	−200.08	−2.0304	0.441 87	1.0977	648.60
150	1117.48	−216.94	−194.56	−1.9930	0.435 74	1.1099	624.72
155	1086.91	−211.98	−188.98	−1.9564	0.430 08	1.1232	601.41
160	1055.72	−207.01	−183.33	−1.9205	0.424 85	1.1371	578.78
165	1023.96	−202.03	−177.61	−1.8853	0.420 01	1.1512	556.96
170	991.67	−197.03	−171.82	−1.8507	0.415 50	1.1650	536.08
175	958.96	−192.03	−165.96	−1.8168	0.411 29	1.1777	516.32
180	925.96	−187.05	−160.05	−1.7834	0.407 32	1.1882	497.81
185	892.86	−182.08	−154.09	−1.7508	0.403 57	1.1957	480.71
190	859.88	−177.17	−148.10	−1.7188	0.399 99	1.1993	465.14
195	827.28	−172.32	−142.10	−1.6877	0.396 55	1.1986	451.16
200	795.31	−167.55	−136.12	−1.6574	0.393 23	1.1932	438.81
210	734.22	−158.34	−124.29	−1.5997	0.386 86	1.1687	418.93
220	678.17	−149.66	−112.79	−1.5462	0.380 76	1.1289	404.90
230	628.00	−141.56	−101.75	−1.4971	0.374 95	1.0796	395.73
240	583.83	−134.03	−91.212	−1.4522	0.369 49	1.0273	390.30
250	545.23	−127.05	−81.196	−1.4113	0.364 48	0.976 48	387.63
260	511.55	−120.54	−71.668	−1.3740	0.359 96	0.929 84	386.91
270	482.08	−114.44	−62.582	−1.3397	0.355 93	0.888 32	387.59
280	456.16	−108.69	−53.885	−1.3080	0.352 37	0.851 92	389.26
290	433.23	−103.23	−45.528	−1.2787	0.349 23	0.820 25	391.63
300	412.80	−98.028	−37.466	−1.2514	0.346 46	0.792 71	394.50
310	394.50	−93.033	−29.662	−1.2258	0.344 01	0.768 75	397.74
320	378.00	−88.219	−22.081	−1.2017	0.341 84	0.747 81	401.23
330	363.03	−83.561	−14.697	−1.1790	0.339 90	0.729 45	404.91
340	349.39	−79.038	−7.4848	−1.1574	0.338 17	0.713 28	408.72
350	336.90	−74.632	−0.42508	−1.1370	0.336 62	0.698 96	412.63
375	309.78	−64.038	16.665	−1.0898	0.333 38	0.669 60	422.60
400	287.25	−53.919	33.112	−1.0473	0.330 82	0.647 12	432.68
425	268.18	−44.158	49.061	−1.0087	0.328 76	0.629 49	442.72
450	251.78	−34.676	64.616	−0.973 09	0.327 08	0.615 39	452.62
475	237.49	−25.415	79.852	−0.940 13	0.325 68	0.603 90	462.37
500	224.90	−16.333	94.828	−0.909 40	0.324 50	0.594 42	471.93
525	213.71	−7.3965	109.59	−0.880 60	0.323 50	0.586 48	481.31
550	203.68	1.4178	124.16	−0.853 48	0.322 64	0.579 76	490.51
575	194.62	10.129	138.58	−0.827 84	0.321 89	0.574 02	499.53
600	186.41	18.754	152.87	−0.803 51	0.321 23	0.569 08	508.38
625	178.91	27.303	167.04	−0.780 37	0.320 65	0.564 78	517.06
650	172.03	35.788	181.11	−0.758 29	0.320 14	0.561 03	525.59
675	165.69	44.215	195.10	−0.737 18	0.319 68	0.557 72	533.96
700	159.84	52.594	209.00	−0.716 95	0.319 27	0.554 80	542.19

TEGELER, SPAN, AND WAGNER

TABLE 34. Thermodynamic properties of argon—Continued

Temperature (K)	Density (kg m^{-3})	Internal energy (kJ kg^{-1})	Enthalpy (kJ kg^{-1})	Entropy (kJ kg^{-1} K^{-1})	c_v (kJ kg^{-1} K^{-1})	c_p (kJ kg^{-1} K^{-1})	w (m s^{-1})
			50.0 MPa isobar				
95.804[a]	1466.52	−274.29	−240.19	−2.5244	0.560 38	1.0063	987.92
100	1448.54	−270.50	−235.99	−2.4814	0.548 47	0.999 45	969.74
105	1427.14	−266.04	−231.00	−2.4328	0.535 72	0.993 28	948.53
110	1405.76	−261.62	−226.05	−2.3867	0.524 17	0.988 60	927.77
115	1384.38	−257.23	−221.12	−2.3428	0.513 57	0.984 94	907.45
120	1362.99	−252.88	−216.20	−2.3010	0.503 75	0.981 98	887.55
125	1341.58	−248.57	−211.30	−2.2610	0.494 60	0.979 54	868.07
130	1320.15	−244.28	−206.40	−2.2226	0.486 05	0.977 49	849.02
135	1298.71	−240.02	−201.52	−2.1857	0.478 04	0.975 73	830.42
140	1277.25	−235.79	−196.65	−2.1503	0.470 53	0.974 20	812.28
145	1255.79	−231.59	−191.78	−2.1161	0.463 47	0.972 83	794.61
150	1234.34	−227.43	−186.92	−2.0831	0.456 84	0.971 58	777.44
155	1212.91	−223.29	−182.06	−2.0513	0.450 61	0.970 39	760.78
160	1191.50	−219.18	−177.21	−2.0205	0.444 74	0.969 23	744.66
165	1170.14	−215.10	−172.37	−1.9907	0.439 22	0.968 04	729.09
170	1148.85	−211.06	−167.53	−1.9618	0.434 02	0.966 76	714.08
175	1127.64	−207.04	−162.70	−1.9338	0.429 12	0.965 35	699.65
180	1106.54	−203.07	−157.88	−1.9067	0.424 49	0.963 74	685.82
185	1085.57	−199.13	−153.07	−1.8803	0.420 12	0.961 88	672.59
190	1064.76	−195.22	−148.26	−1.8546	0.415 99	0.959 70	659.98
195	1044.13	−191.36	−143.47	−1.8298	0.412 09	0.957 15	647.99
200	1023.71	−187.53	−138.69	−1.8056	0.408 39	0.954 18	636.63
210	983.63	−180.02	−129.18	−1.7592	0.401 59	0.946 84	615.80
220	944.74	−172.69	−119.76	−1.7153	0.395 48	0.937 53	597.47
230	907.26	−165.55	−110.44	−1.6739	0.389 99	0.926 34	581.56
240	871.36	−158.62	−101.24	−1.6347	0.385 04	0.913 52	567.93
250	837.16	−151.90	−92.174	−1.5977	0.380 55	0.899 42	556.40
260	804.73	−145.39	−83.255	−1.5627	0.376 47	0.884 38	546.77
270	774.10	−139.08	−74.489	−1.5297	0.372 75	0.868 75	538.85
280	745.27	−132.97	−65.881	−1.4983	0.369 33	0.852 84	532.42
290	718.18	−127.05	−57.432	−1.4687	0.366 19	0.836 90	527.30
300	692.78	−121.31	−49.142	−1.4406	0.363 30	0.821 19	523.31
310	668.97	−115.75	−41.007	−1.4139	0.360 63	0.805 88	520.31
320	646.68	−110.34	−33.022	−1.3886	0.358 18	0.791 13	518.16
330	625.79	−105.08	−25.182	−1.3644	0.355 91	0.777 03	516.73
340	606.22	−99.958	−17.479	−1.3414	0.353 82	0.763 65	515.91
350	587.86	−94.962	−9.9067	−1.3195	0.351 89	0.751 02	515.62
375	546.66	−82.959	8.5053	−1.2687	0.347 66	0.722 70	516.72
400	511.19	−71.547	26.264	−1.2228	0.344 14	0.698 69	519.74
425	480.38	−60.614	43.471	−1.1811	0.341 19	0.678 40	524.05
450	453.37	−50.074	60.210	−1.1428	0.338 69	0.661 22	529.26
475	429.51	−39.857	76.553	−1.1075	0.336 55	0.646 61	535.07
500	408.27	−29.910	92.558	−1.0746	0.334 69	0.634 09	541.31
525	389.22	−20.189	108.27	−1.0439	0.333 08	0.623 31	547.83
550	372.04	−10.659	123.74	−1.0152	0.331 66	0.613 96	554.54
575	356.44	−1.2941	138.98	−0.988 06	0.330 41	0.605 81	561.37
600	342.22	7.9297	154.03	−0.962 43	0.329 29	0.598 66	568.28
625	329.19	17.031	168.92	−0.938 13	0.328 29	0.592 35	575.22
650	317.19	26.025	183.66	−0.915 01	0.327 40	0.586 76	582.18
675	306.11	34.924	198.26	−0.892 96	0.326 59	0.581 78	589.14
700	295.84	43.740	212.75	−0.871 88	0.325 85	0.577 33	596.07

TABLE 34. Thermodynamic properties of argon—Continued

Temperature (K)	Density (kg m^{-3})	Internal energy (kJ kg^{-1})	Enthalpy (kJ kg^{-1})	Entropy (kJ kg^{-1} K^{-1})	c_v (kJ kg^{-1} K^{-1})	c_p (kJ kg^{-1} K^{-1})	w (m s^{-1})
			75.0 MPa isobar				
101.472[a]	1486.55	−272.66	−222.20	−2.5136	0.564 53	0.975 93	1038.7
105	1473.22	−269.68	−218.77	−2.4804	0.555 42	0.969 65	1025.7
110	1454.44	−265.51	−213.94	−2.4355	0.543 64	0.962 10	1007.7
115	1435.77	−261.39	−209.15	−2.3928	0.532 89	0.955 66	990.21
120	1417.20	−257.31	−204.39	−2.3523	0.522 98	0.949 97	973.20
125	1398.74	−253.27	−199.65	−2.3136	0.513 77	0.944 81	956.64
130	1380.38	−249.27	−194.94	−2.2767	0.505 16	0.940 04	940.53
135	1362.13	−245.31	−190.25	−2.2413	0.497 08	0.935 54	924.86
140	1343.97	−241.39	−185.58	−2.2073	0.489 48	0.931 26	909.63
145	1325.93	−237.50	−180.93	−2.1747	0.482 33	0.927 15	894.83
150	1307.99	−233.65	−176.31	−2.1434	0.475 58	0.923 16	880.46
155	1290.17	−229.83	−171.70	−2.1131	0.469 21	0.919 28	866.53
160	1272.48	−226.06	−167.12	−2.0840	0.463 20	0.915 47	853.04
165	1254.92	−222.31	−162.55	−2.0559	0.457 51	0.911 72	839.98
170	1237.49	−218.61	−158.00	−2.0287	0.452 13	0.908 01	827.36
175	1220.21	−214.93	−153.47	−2.0025	0.447 05	0.904 32	815.18
180	1203.08	−211.30	−148.96	−1.9771	0.442 23	0.900 65	803.43
185	1186.11	−207.69	−144.46	−1.9524	0.437 67	0.896 96	792.12
190	1169.31	−204.13	−139.99	−1.9286	0.433 35	0.893 25	781.24
195	1152.68	−200.59	−135.53	−1.9054	0.429 25	0.889 50	770.79
200	1136.24	−197.10	−131.09	−1.8829	0.425 36	0.885 71	760.76
210	1103.93	−190.21	−122.27	−1.8399	0.418 16	0.877 94	741.95
220	1072.46	−183.47	−113.53	−1.7992	0.411 65	0.869 86	724.79
230	1041.87	−176.86	−104.88	−1.7608	0.405 76	0.861 44	709.21
240	1012.21	−170.40	−96.305	−1.7243	0.400 42	0.852 67	695.16
250	983.54	−164.08	−87.824	−1.6897	0.395 56	0.843 57	682.55
260	955.88	−157.90	−79.435	−1.6568	0.391 13	0.834 20	671.32
270	929.26	−151.85	−71.141	−1.6255	0.387 08	0.824 63	661.36
280	903.67	−145.94	−62.943	−1.5956	0.383 36	0.814 94	652.59
290	879.12	−140.15	−54.842	−1.5672	0.379 94	0.805 21	644.90
300	855.60	−134.50	−46.839	−1.5401	0.376 79	0.795 49	638.20
310	833.09	−128.96	−38.932	−1.5141	0.373 87	0.785 85	632.40
320	811.56	−123.54	−31.121	−1.4893	0.371 17	0.776 35	627.42
330	790.98	−118.22	−23.404	−1.4656	0.368 66	0.767 03	623.17
340	771.31	−113.02	−15.780	−1.4428	0.366 32	0.757 92	619.59
350	752.53	−107.91	−8.2450	−1.4210	0.364 14	0.749 06	616.60
375	709.16	−95.542	10.216	−1.3700	0.359 29	0.728 13	611.37
400	670.44	−83.689	28.177	−1.3237	0.355 17	0.709 09	608.71
425	635.78	−72.278	45.687	−1.2812	0.351 64	0.691 99	608.01
450	604.64	−61.249	62.792	−1.2421	0.348 58	0.676 73	608.81
475	576.55	−50.547	79.537	−1.2059	0.345 93	0.663 18	610.75
500	551.11	−40.127	95.963	−1.1722	0.343 60	0.651 14	613.56
525	527.96	−29.951	112.11	−1.1407	0.341 54	0.640 45	617.06
550	506.81	−19.988	128.00	−1.1111	0.339 71	0.630 93	621.07
575	487.42	−10.211	143.66	−1.0832	0.338 08	0.622 44	625.50
600	469.57	−0.59627	159.13	−1.0569	0.336 61	0.614 83	630.24
625	453.08	8.8748	174.41	−1.0320	0.335 28	0.608 01	635.22
650	437.80	18.219	189.53	−1.0082	0.334 08	0.601 86	640.40
675	423.59	27.449	204.51	−0.985 62	0.332 99	0.596 31	645.73
700	410.35	36.579	219.35	−0.964 02	0.331 99	0.591 29	651.18

TABLE 34. Thermodynamic properties of argon—Continued

Temperature (K)	Density (kg m^{-3})	Internal energy (kJ kg^{-1})	Enthalpy (kJ kg^{-1})	Entropy (kJ kg^{-1} K^{-1})	c_v (kJ kg^{-1} K^{-1})	c_p (kJ kg^{-1} K^{-1})	w (m s^{-1})
			100.0 MPa isobar				
106.956[a]	1504.62	−270.84	−204.38	−2.5030	0.568 24	0.952 95	1084.1
110	1494.28	−268.41	−201.49	−2.4764	0.561 01	0.947 52	1074.3
115	1477.41	−264.46	−196.77	−2.4344	0.550 03	0.939 59	1058.6
120	1460.70	−260.55	−192.09	−2.3946	0.539 95	0.932 55	1043.4
125	1444.14	−256.69	−187.45	−2.3567	0.530 62	0.926 12	1028.7
130	1427.71	−252.87	−182.83	−2.3204	0.521 92	0.920 14	1014.4
135	1411.43	−249.10	−178.25	−2.2858	0.513 76	0.914 50	1000.5
140	1395.28	−245.36	−173.69	−2.2527	0.506 09	0.909 11	987.00
145	1379.28	−241.66	−169.15	−2.2209	0.498 85	0.903 94	973.91
150	1363.42	−237.99	−164.65	−2.1903	0.492 02	0.898 93	961.21
155	1347.70	−234.36	−160.16	−2.1609	0.485 56	0.894 07	948.89
160	1332.13	−230.77	−155.71	−2.1326	0.479 44	0.889 34	936.96
165	1316.71	−227.22	−151.27	−2.1053	0.473 64	0.884 71	925.39
170	1301.44	−223.70	−146.86	−2.0790	0.468 14	0.880 18	914.20
175	1286.32	−220.21	−142.47	−2.0535	0.462 93	0.875 74	903.37
180	1271.36	−216.76	−138.10	−2.0289	0.457 98	0.871 38	892.89
185	1256.56	−213.34	−133.75	−2.0051	0.453 28	0.867 08	882.77
190	1241.92	−209.95	−129.43	−1.9820	0.448 81	0.862 85	873.00
195	1227.44	−206.60	−125.13	−1.9596	0.444 56	0.858 67	863.57
200	1213.13	−203.27	−120.84	−1.9380	0.440 52	0.854 53	854.48
210	1185.02	−196.73	−112.34	−1.8965	0.433 01	0.846 38	837.28
220	1157.61	−190.30	−103.91	−1.8573	0.426 18	0.838 34	821.35
230	1130.92	−184.00	−95.571	−1.8202	0.419 97	0.830 39	806.65
240	1104.95	−177.81	−87.307	−1.7850	0.414 31	0.822 50	793.12
250	1079.72	−171.74	−79.121	−1.7516	0.409 13	0.814 65	780.71
260	1055.24	−165.78	−71.014	−1.7198	0.404 38	0.806 84	769.35
270	1031.51	−159.93	−62.984	−1.6895	0.400 01	0.799 07	759.00
280	1008.54	−154.19	−55.032	−1.6606	0.395 99	0.791 35	749.60
290	986.31	−148.55	−47.157	−1.6329	0.392 28	0.783 70	741.08
300	964.82	−143.00	−39.358	−1.6065	0.388 85	0.776 13	733.39
310	944.07	−137.56	−31.634	−1.5812	0.385 66	0.768 65	726.46
320	924.03	−132.21	−23.985	−1.5569	0.382 70	0.761 29	720.25
330	904.70	−126.94	−16.408	−1.5336	0.379 95	0.754 07	714.70
340	886.05	−121.76	−8.9027	−1.5112	0.377 37	0.746 99	709.76
350	868.07	−116.67	−1.4675	−1.4896	0.374 96	0.740 07	705.38
375	825.88	−104.26	16.825	−1.4391	0.369 57	0.723 51	696.60
400	787.37	−92.287	34.717	−1.3929	0.364 95	0.708 10	690.42
425	752.20	−80.704	52.239	−1.3504	0.360 94	0.693 86	686.35
450	720.02	−69.465	69.421	−1.3111	0.357 44	0.680 81	683.98
475	690.52	−58.529	86.290	−1.2747	0.354 37	0.668 89	682.97
500	663.41	−47.862	102.87	−1.2406	0.351 65	0.658 05	683.08
525	638.44	−37.433	119.20	−1.2088	0.349 23	0.648 18	684.08
550	615.37	−27.214	135.29	−1.1788	0.347 06	0.639 22	685.80
575	594.00	−17.183	151.17	−1.1506	0.345 11	0.631 08	688.13
600	574.15	−7.3194	166.85	−1.1239	0.343 35	0.623 68	690.94
625	555.67	2.3949	182.36	−1.0986	0.341 75	0.616 93	694.14
650	538.42	11.975	197.70	−1.0745	0.340 30	0.610 78	697.68
675	522.29	21.435	212.90	−1.0516	0.338 96	0.605 15	701.49
700	507.15	30.786	227.96	−1.0296	0.337 74	0.600 00	705.52

TABLE 34. Thermodynamic properties of argon—Continued

Temperature (K)	Density (kg m^{-3})	Internal energy (kJ kg^{-1})	Enthalpy (kJ kg^{-1})	Entropy (kJ kg^{-1} K^{-1})	c_v (kJ kg^{-1} K^{-1})	c_p (kJ kg^{-1} K^{-1})	w (m s^{-1})
			200.0 MPa isobar				
127.440[a]	1564.82	−262.54	−134.73	−2.4643	0.579 82	0.897 21	1231.6
130	1558.46	−260.77	−132.44	−2.4465	0.575 14	0.893 37	1226.2
135	1546.14	−257.35	−127.99	−2.4129	0.566 47	0.886 28	1215.9
140	1533.98	−253.96	−123.58	−2.3808	0.558 36	0.879 61	1205.9
145	1521.96	−250.61	−119.20	−2.3500	0.550 73	0.873 28	1196.2
150	1510.08	−247.29	−114.84	−2.3205	0.543 52	0.867 22	1186.8
155	1498.35	−244.00	−110.52	−2.2922	0.536 69	0.861 40	1177.6
160	1486.75	−240.75	−106.23	−2.2649	0.530 20	0.855 78	1168.8
165	1475.29	−237.53	−101.96	−2.2387	0.524 03	0.850 35	1160.1
170	1463.97	−234.34	−97.726	−2.2134	0.518 15	0.845 09	1151.8
175	1452.78	−231.18	−93.514	−2.1889	0.512 54	0.839 98	1143.6
180	1441.72	−228.05	−89.326	−2.1653	0.507 18	0.835 02	1135.7
185	1430.80	−224.95	−85.163	−2.1425	0.502 06	0.830 20	1128.1
190	1420.00	−221.87	−81.024	−2.1205	0.497 17	0.825 52	1120.6
195	1409.33	−218.82	−76.908	−2.0991	0.492 49	0.820 96	1113.4
200	1398.79	−215.80	−72.814	−2.0783	0.488 01	0.816 52	1106.3
210	1378.08	−209.82	−64.692	−2.0387	0.479 60	0.807 98	1092.9
220	1357.85	−203.94	−56.653	−2.0013	0.471 86	0.799 87	1080.2
230	1338.10	−198.16	−48.693	−1.9659	0.464 73	0.792 15	1068.2
240	1318.82	−192.46	−40.809	−1.9324	0.458 15	0.784 79	1056.9
250	1299.99	−186.84	−32.996	−1.9005	0.452 05	0.777 76	1046.3
260	1281.61	−181.31	−25.253	−1.8701	0.446 40	0.771 03	1036.2
270	1263.67	−175.84	−17.575	−1.8411	0.441 15	0.764 58	1026.8
280	1246.14	−170.46	−9.9603	−1.8134	0.436 26	0.758 39	1017.9
290	1229.04	−165.14	−2.4064	−1.7869	0.431 71	0.752 43	1009.5
300	1212.34	−159.88	5.0890	−1.7615	0.427 45	0.746 70	1001.6
310	1196.03	−154.69	12.528	−1.7371	0.423 46	0.741 16	994.23
320	1180.11	−149.56	19.913	−1.7137	0.419 72	0.735 82	987.27
330	1164.57	−144.49	27.245	−1.6911	0.416 21	0.730 66	980.73
340	1149.39	−139.48	34.527	−1.6694	0.412 91	0.725 67	974.58
350	1134.57	−134.52	41.759	−1.6484	0.409 79	0.720 83	968.82
375	1099.03	−122.34	59.635	−1.5991	0.402 75	0.709 38	955.94
400	1065.54	−110.46	77.235	−1.5536	0.396 60	0.698 76	945.02
425	1033.95	−98.854	94.579	−1.5116	0.391 20	0.688 88	935.81
450	1004.14	−87.490	111.68	−1.4725	0.386 40	0.679 67	928.10
475	975.99	−76.352	128.57	−1.4359	0.382 13	0.671 09	921.70
500	949.38	−65.420	145.24	−1.4017	0.378 29	0.663 07	916.45
525	924.20	−54.677	161.73	−1.3696	0.374 83	0.655 58	912.20
550	900.36	−44.107	178.03	−1.3392	0.371 69	0.648 57	908.82
575	877.75	−33.698	194.16	−1.3105	0.368 83	0.642 02	906.23
600	856.29	−23.435	210.13	−1.2834	0.366 22	0.635 89	904.31
625	835.90	−13.308	225.96	−1.2575	0.363 82	0.630 14	902.99
650	816.50	−3.3061	241.64	−1.2329	0.361 61	0.624 76	902.20
675	798.03	6.5799	257.20	−1.2094	0.359 57	0.619 71	901.88
700	780.42	16.359	272.63	−1.1870	0.357 68	0.614 98	901.97
			400.0 MPa isobar				
163.733[a]	1655.34	−243.54	−1.8964	−2.4038	0.591 90	0.847 80	1449.3
165	1653.18	−242.78	−0.822 93	−2.3973	0.590 24	0.846 43	1447.7
170	1644.71	−239.81	3.3959	−2.3721	0.583 87	0.841 14	1441.7
175	1636.33	−236.86	7.5887	−2.3478	0.577 78	0.836 01	1435.8
180	1628.05	−233.94	11.756	−2.3243	0.571 94	0.831 04	1430.1

TABLE 34. Thermodynamic properties of argon—Continued

Temperature (K)	Density (kg m^{-3})	Internal energy (kJ kg^{-1})	Enthalpy (kJ kg^{-1})	Entropy (kJ kg^{-1} K^{-1})	c_v (kJ kg^{-1} K^{-1})	c_p (kJ kg^{-1} K^{-1})	w (m s^{-1})
			400.0 MPa isobar				
185	1619.87	−231.03	15.899	−2.3016	0.566 34	0.826 21	1424.4
190	1611.77	−228.16	20.019	−2.2796	0.560 95	0.821 51	1419.0
195	1603.77	−225.30	24.115	−2.2584	0.555 77	0.816 94	1413.6
200	1595.85	−222.46	28.188	−2.2377	0.550 79	0.812 49	1408.4
210	1580.28	−216.85	36.270	−2.1983	0.541 36	0.803 95	1398.3
220	1565.05	−211.31	44.269	−2.1611	0.532 60	0.795 85	1388.7
230	1550.14	−205.85	52.188	−2.1259	0.524 43	0.788 16	1379.5
240	1535.54	−200.46	60.033	−2.0925	0.516 81	0.780 87	1370.7
250	1521.25	195.14	67.807	−2.0608	0.509 68	0.773 94	1362.3
260	1507.24	−189.87	75.513	−2.0305	0.503 01	0.767 35	1354.3
270	1493.52	−184.67	83.155	−2.0017	0.496 75	0.761 09	1346.6
280	1480.07	−179.52	90.736	−1.9741	0.490 88	0.755 12	1339.2
290	1466.89	−174.43	98.258	−1.9477	0.485 35	0.749 43	1332.2
300	1453.96	−169.39	105.73	−1.9224	0.480 15	0.744 00	1325.5
310	1441.27	−164.39	113.14	−1.8981	0.475 25	0.738 81	1319.1
320	1428.83	−159.45	120.50	−1.8747	0.470 61	0.733 85	1312.9
330	1416.62	−154.55	127.82	−1.8522	0.466 23	0.729 09	1307.1
340	1404.64	−149.69	135.08	−1.8305	0.462 08	0.724 52	1301.4
350	1392.87	144.87	142.31	−1.8096	0.458 15	0.720 13	1296.0
375	1364.38	−132.99	160.18	−1.7603	0.449 16	0.709 87	1283.5
400	1337.13	−121.34	177.81	−1.7147	0.441 21	0.700 49	1272.2
425	1311.04	−109.89	195.21	−1.6725	0.434 13	0.691 88	1262.1
450	1286.05	−98.623	212.41	−1.6332	0.427 78	0.683 91	1253.0
475	1262.07	−87.528	229.41	−1.5964	0.422 07	0.676 51	1244.9
500	1239.05	−76.589	246.24	−1.5619	0.416 89	0.669 62	1237.5
525	1216.94	−65.795	262.90	−1.5294	0.412 18	0.663 17	1231.0
550	1195.69	−55.137	279.40	−1.4987	0.407 87	0.657 12	1225.1
575	1175.23	−44.603	295.76	−1.4696	0.403 91	0.651 43	1219.8
600	1155.53	34.187	311.97	−1.4420	0.400 26	0.646 06	1215.1
625	1136.55	−23.881	328.06	−1.4157	0.396 89	0.641 00	1210.9
650	1118.25	−13.677	344.03	−1.3907	0.393 77	0.636 22	1207.2
675	1100.58	−3.5696	359.87	−1.3668	0.390 86	0.631 68	1203.9
700	1083.53	6.4472	375.61	−1.3439	0.388 15	0.627 39	1201.0
			600.0 MPa isobar				
196.140[a]	1725.55	−223.25	124.46	−2.3586	0.597 38	0.823 86	1619.9
200	1720.38	−221.12	127.64	−2.3426	0.593 40	0.820 54	1616.6
210	1707.18	−215.66	135.80	−2.3028	0.583 54	0.812 19	1608.3
220	1694.24	−210.26	143.88	−2.2652	0.574 30	0.804 22	1600.3
230	1681.56	−204.93	151.88	−2.2296	0.565 63	0.796 60	1592.6
240	1669.13	−199.66	159.81	−2.1958	0.557 49	0.789 34	1585.2
250	1656.93	−194.44	167.67	−2.1638	0.549 82	0.782 41	1578.1
260	1644.96	−189.29	175.46	−2.1332	0.542 60	0.775 81	1571.2
270	1633.22	−184.18	183.19	−2.1040	0.535 79	0.769 51	1564.6
280	1621.68	−179.13	190.85	−2.0762	0.529 36	0.763 51	1558.3
290	1610.36	−174.13	198.46	−2.0495	0.523 29	0.757 78	1552.1
300	1599.23	−169.17	206.01	−2.0239	0.517 54	0.752 32	1546.3
310	1588.29	−164.26	213.51	−1.9993	0.512 10	0.747 10	1540.6
320	1577.54	−159.39	220.95	−1.9757	0.506 94	0.742 11	1535.1
330	1566.97	−154.55	228.35	−1.9529	0.502 04	0.737 33	1529.8
340	1556.58	−149.76	235.70	−1.9309	0.497 38	0.732 76	1524.7
350	1546.35	−145.00	243.01	−1.9098	0.492 96	0.728 37	1519.8
375	1521.49	−133.26	261.09	−1.8599	0.482 78	0.718 16	1508.3

TABLE 34. Thermodynamic properties of argon—Continued

Temperature (K)	Density (kg m^{-3})	Internal energy (kJ kg^{-1})	Enthalpy (kJ kg^{-1})	Entropy (kJ kg^{-1} K^{-1})	c_v (kJ kg^{-1} K^{-1})	c_p (kJ kg^{-1} K^{-1})	w (m s^{-1})
			600.0 MPa isobar				
400	1497.59	−121.72	278.92	−1.8138	0.473 72	0.708 88	1497.8
425	1474.58	−110.36	296.54	−1.7711	0.465 60	0.700 40	1488.2
450	1452.41	−99.160	313.95	−1.7313	0.458 29	0.692 60	1479.3
475	1431.02	−88.110	331.17	−1.6940	0.451 66	0.685 38	1471.2
500	1410.37	−77.199	348.22	−1.6591	0.445 64	0.678 68	1463.8
525	1390.42	−66.416	365.11	−1.6261	0.440 13	0.672 42	1457.0
550	1371.13	−55.751	381.85	−1.5950	0.435 07	0.666 56	1450.7
575	1352.46	−45.197	398.44	−1.5655	0.430 41	0.661 05	1445.0
600	1334.38	−34.745	414.90	−1.5374	0.426 10	0.655 85	1439.7
625	1316.87	−24.391	431.23	−1.5108	0.422 10	0.650 94	1434.9
650	1299.89	−14.127	447.45	−1.4853	0.418 38	0.646 28	1430.4
675	1283.42	−3.9489	463.55	−1.4610	0.414 91	0.641 86	1426.4
700	1267.44	6.1484	479.54	−1.4377	0.411 66	0.637 66	1422.6
			800.0 MPa isobar				
226.006[a]	1784.00	−202.47	245.96	−2.3227	0.600 62	0.809 24	1763.9
230	1779.52	−200.37	249.19	−2.3086	0.597 14	0.806 29	1761.3
240	1768.42	−195.17	257.22	−2.2744	0.588 76	0.799 12	1754.8
250	1757.53	−190.01	265.17	−2.2419	0.580 82	0.792 23	1748.5
260	1746.83	−184.91	273.06	−2.2110	0.573 30	0.785 63	1742.4
270	1736.32	−179.86	280.89	−2.1814	0.566 17	0.779 31	1736.5
280	1725.98	−174.86	288.65	−2.1532	0.559 41	0.773 26	1730.8
290	1715.82	−169.90	296.35	−2.1262	0.553 00	0.767 47	1725.3
300	1705.83	−164.98	304.00	−2.1003	0.546 90	0.761 93	1720.0
310	1696.00	−160.11	311.59	−2.0754	0.541 11	0.756 64	1714.8
320	1686.32	−155.27	319.13	−2.0514	0.535 60	0.751 57	1709.8
330	1676.80	−150.48	326.62	−2.0284	0.530 36	0.746 71	1704.9
340	1667.42	−145.72	334.07	−2.0061	0.525 36	0.742 06	1700.3
350	1658.19	−140.99	341.46	−1.9847	0.520 60	0.737 61	1695.7
375	1635.69	−129.32	359.77	−1.9342	0.509 60	0.727 24	1685.0
400	1614.00	−117.83	377.83	−1.8875	0.499 76	0.717 84	1675.1
425	1593.04	−106.51	395.67	−1.8443	0.490 91	0.709 28	1665.9
450	1572.79	−95.347	413.30	−1.8040	0.482 90	0.701 44	1657.4
475	1553.18	−84.323	430.75	−1.7662	0.475 62	0.694 21	1649.6
500	1534.19	−73.428	448.02	−1.7308	0.468 98	0.687 52	1642.3
525	1515.78	−62.652	465.13	−1.6974	0.462 89	0.681 29	1635.5
550	1497.92	−51.986	482.09	−1.6659	0.457 29	0.675 47	1629.3
575	1480.58	−41.422	498.91	−1.6360	0.452 11	0.670 00	1623.5
600	1463.74	−30.954	515.59	−1.6075	0.447 31	0.664 86	1618.1
625	1447.37	−20.575	532.15	−1.5805	0.442 85	0.660 00	1613.0
650	1431.45	−10.281	548.59	−1.5547	0.438 69	0.655 40	1608.4
675	1415.96	−0.065 45	564.92	−1.5301	0.434 80	0.651 02	1604.1
700	1400.88	10.075	581.15	−1.5065	0.431 16	0.646 86	1600.0
254.027[a]	1834.58	−181.47	363.61	−2.2930	0.602 96	0.799 12	1889.9
260	1828.75	−178.45	368.37	−2.2744	0.598 43	0.795 23	1886.6
270	1819.10	−173.43	376.30	−2.2445	0.591 13	0.788 91	1881.2
280	1809.62	−168.45	384.15	−2.2159	0.584 18	0.782 83	1876.0
290	1800.29	−163.51	391.95	−2.1886	0.577 55	0.776 99	1870.9
300	1791.11	−158.62	399.69	−2.1623	0.571 23	0.771 39	1866.0
310	1782.07	−153.76	407.38	−2.1371	0.565 21	0.766 01	1861.1
320	1773.16	−148.95	415.02	−2.1129	0.559 46	0.760 86	1856.5

TABLE 34. Thermodynamic properties of argon—Continued

Temperature (K)	Density (kg m^{-3})	Internal energy (kJ kg^{-1})	Enthalpy (kJ kg^{-1})	Entropy (kJ kg^{-1} K^{-1})	c_v (kJ kg^{-1} K^{-1})	c_p (kJ kg^{-1} K^{-1})	w (m s^{-1})
			1000.0 MPa isobar				
330	1764.39	−144.17	422.60	−2.0896	0.553 97	0.755 91	1851.9
340	1755.75	−139.42	430.13	−2.0671	0.548 73	0.751 17	1847.5
350	1747.23	−134.71	437.62	−2.0454	0.543 72	0.746 62	1843.3
375	1726.45	−123.07	456.15	−1.9942	0.532 12	0.736 03	1833.1
400	1706.37	−111.60	474.43	−1.9470	0.521 69	0.726 44	1823.7
425	1686.94	−100.31	492.48	−1.9032	0.512 27	0.717 72	1814.9
450	1668.11	−89.154	510.33	−1.8624	0.503 73	0.709 74	1806.7
475	1649.85	−78.139	527.98	−1.8243	0.495 95	0.702 41	1799.0
500	1632.13	−67.248	545.45	−1.7884	0.488 83	0.695 65	1791.9
525	1614.90	−56.470	562.76	−1.7546	0.482 29	0.689 37	1785.2
550	1598.16	−45.799	579.92	−1.7227	0.476 26	0.683 52	1779.0
575	1581.86	−35.225	596.94	−1.6924	0.470 68	0.678 05	1773.2
600	1566.00	−24.743	613.83	−1.6637	0.465 50	0.672 90	1767.8
625	1550.54	−14.346	630.59	−1.6363	0.460 67	0.668 05	1762.7
650	1535.48	−4.0286	647.23	−1.6102	0.456 16	0.663 47	1757.9
675	1520.79	6.2133	663.76	−1.5852	0.451 95	0.659 12	1753.5
700	1506.46	16.384	680.19	−1.5614	0.447 99	0.654 98	1749.3

^{a}Melting temperature.
^{b}Saturation temperature.